ICMCS-XV

15th International Conference on Mesoscale Convective Systems and High-Impact Weather

22 - 25 May 2023

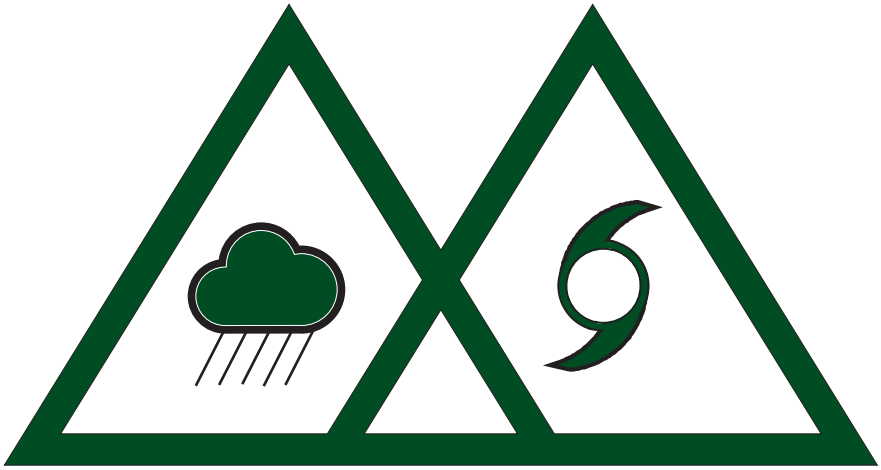

Book of Abstracts

Fort Collins, Colorado

COLORADO STATE UNIVERSITY

What I have learned about MCSs over a 55 year time span

Dr William R Cotton, Emeritus Professor, Dept of Atmospheric Science,
Colorado State University
Corresponding Author: William R. Cotton, william.r.cotton@gmail.com

As a PhD student at Penn State in the late 1960's, I don't recall any lectures on MCSs. Likewise, when working in the NOAA Experimental Meteorology Laboratory from 1970 to 1974, I don't recall any discussion about MCSs. It wasn't until I was a faculty member at CSU during the 1977 South Park Area Cumulus Experiment(SPACE-'77) that I became acquainted with MCS. In all I participated in the writing of 25 reviewed technical publications on MCSs in my career as well as authorship in two books containing reviews of MCSs.

In this talk, I discuss the highlights of what I learned about MCSs. In particular I will focus on the dynamical organization of MCSs, especially the idea they are just a cluster of thunderstorms versus a dynamically-balanced mesoscale system.

Precipitation study in North Korea using South Korean S band dual polarimetric weather radars

Dong-In Lee[1], Hyun-Joon Kim[2] , Jisun Lee[1] and Cheol-Hwan You[1]

[1] *Atmospheric Environmental Research Institute, Pukyong National University, Busan, Korea*

[2] *Department of Civil Environmental & Plant Engineering, Chung Ang University, Seoul, Korea*

Corresponding author: Dong-In Lee, leedi@pknu.ac.kr

ABSTRACT

Hazardous weather that develops in a short period of time, such as localized heavy rain causes many casualties and property damage accompanied by very strong precipitation and strong winds. It has difficulty in disaster prevention due to the low quantitative prediction accuracy due to differences in geographic development when precipitation systems move and differences in microphysical development characteristics according to their types.

Currently, high-resolution precipitation information has been provided in South Korea based on the dual polarization radar that can efficiently monitor the inflowing precipitation system developed within a short time of less than 30 minutes and the AWS observation network of about 600 points. However, in North Korea, it is difficult to respond to disasters in areas where landslides, floods, and river flooding are expected due to the provision of ground observation data with low spatial resolution.

In this study, we investigated the developmental characteristics of the rainfall system in North Korea and improved the accuracy of quantitative rainfall estimation by South Korean S band dual-polarized radars for the rainfall system in North Korea based on the observation data of the rain gauge. In addition, the rainfall distribution characteristics of North Korea are analyzed by the rainfall field data obtained through the optimal rainfall estimation method and calculated a short-term prediction field of precipitation in North Korea.

Outbreak Mechanism Identification of Line-Shaped Convective Rainbands Based on Large Eddy Simulation

Kosei Yamaguchi [a], Yoshiyuki Kawatani [b], and Eiichi Nakakita [a]

[a] *Disaster Prevention Research Institute, Kyoto University, Uji, Kyoto, Japan*

[b] *Graduate School of Engineering, Kyoto University, Kyoto, Kyoto, Japan*

Corresponding author: Kosei Yamaguchi, yamaguchi.kosei.5r@kyoto-u.ac.jp

Line-shaped rainbands with self-organization due to back-building phenomena are called line-shaped convective systems, and which stagnate in the same location for a long time, causing flooding and inundation. Predicting their occurrence is extremely difficult because of the mixture of factors derived from necessity, such as topography, and factors derived from contingency, such as natural fluctuations, which are currently expressed by stochastic processes.

Therefore, this study aims to understand the outbreak mechanism of line-shaped convective systems using the LES (Large-Eddy Simulation) model developed by Yamaguchi et al. (2016). Moreover, the influence of necessity and contingency, which cannot be evaluated by RANS (Reynolds-Averaged Navier-Stokes equation), is evaluated.

First, mountain waves generated by topography on the upstream of the area where the line-shaped convective systems occurred transported a low-potential temperature air mass to the initiation area, which generated a local front and triggered the outbreak of the line-shaped convective systems. Another mountain wave transported a high-potential temperature air mass to the area where the heavy rainfall developed, which caused atmospheric instability and expanded the rainfall area. These are the factors derived from necessity brought about by the topography. But in this case, the wind direction and topographic undulations were considered to have combined well to cause the outbreak.

Next, regarding factors derived from contingency, when an ensemble experiment was conducted with a very small random noise of variance 0.1 K of potential temperature in order to represent natural fluctuations, the line-shaped convective systems ceased to occur in about half of the members. This suggested the importance of small-scale phenomena. Therefore, we changed the SGS (Sub-Grid Scale) model to the Bardina model to represent the inverse cascade of energy transport. This resulted in a stronger back-building structure of the line-shaped convective systems as shown in figure 1. This suggests that small-scale turbulence (i.e., natural fluctuations) may order large-scale phenomena.

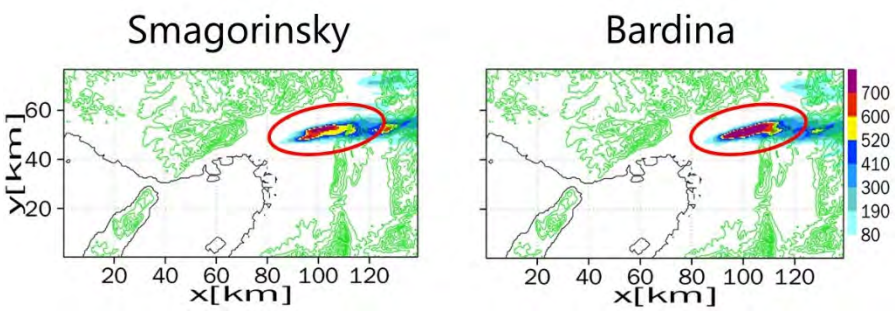

Figure 1 Total precipitation difference between SGS model

Low Level Jets and Heavy Rainfall Events Over Taiwan Revealed from Wind Profiler Radars

Pay-Liam Lin, Yen-Ling Liou
National Central University, Taoyuan, Taiwan

Corresponding author: Pay-Liam Lin, tliam@atm.ncu.edu.tw

The 499 MHz wind profiler is used to study the relationship between low-level jet (LLJ) and heavy rainfall over Taiwan and Dongsha island during the mei-yu season of 2018~2020. The LLJ day is defined as LLJ that occurs more than 6 hours in a day. On the LLJ day of northern Taiwan, the low layer wind speed extreme appears on the northwest side of Taiwan, and Taiwan locates at the front edge of the frontal system. On the LLJ day of Dongsha island, the extreme low layer wind speed appears on the southeast side of Taiwan and the South China Sea, and the frontal system locates over Taiwan. The boundary layer jet (BLJ) is defined as LLJ occurs below 1000 m, and the synoptic system-related low-level jet (SLLJ) is defined as LLJ occurs above 1000 m. On the SLLJ day of northern Taiwan and SLLJ day of Dongsha island, water vapor transportation mainly comes from the coastal South China to the South China Sea in the boundary layer. On the BLJ day of northern Taiwan and BLJ day of Dongsha island, water vapor transportation mainly comes from the coastal South China and the South China Sea in the boundary layer, respectively. When the strong BLJ events occurred in northern Taiwan, the average hourly extreme rainfall happened in the southern mountains and the northwest coast from Hsinchu to Taichung. When the strong SLLJ events occurred in northern Taiwan, the average hourly extreme rainfall happened on the northwest coast from Taoyuan to Hsinchu. When the strong BLJ events occurred on Dongsha island, the average hourly extreme rainfall happened on the southwest coast to the mountains and the northwest coast of Miaoli to the mountains. When the strong SLLJ events occurred on Dongsha island, there was no significant precipitation in Taiwan.

Dynamics of two episodes of high winds produced by an unusually long-lived quasi-linear convective system in South China

Xin Xu[a,b,*], Yuanyuan Ju[a,b], Qiqing Liu[a,b], Kun Zhao[a,b], Ming Xue[a,c], Shushi Zhang[d], Ang Zhou[a,b], Yuan Wang[a], Ying Tang[e]

[a]*Key Laboratory of Mesoscale Severe Weather/Ministry of Education, and School of Atmospheric Sciences, Nanjing University, Nanjing 210023, Jiangsu, China*

[b]*Key Laboratory of Radar Meteorology, China Meteorology Administration, Nanjing 210023, Jiangsu, China*

[c]*Center for Analysis and Prediction of Storms, University of Oklahoma, Norman 73072, OK, US*

[d]*Key Laboratory of Transportation Meteorology of China Meteorological Administration, Nanjing Joint Institute for Atmospheric Sciences, Nanjing 210000, Jiangsu, China*

[e]*Nanjing Marine Radar Institute, Nanjing 210000, Jiangsu, China*

Corresponding author: Xin Xu, xinxu@nju.edu.cn

Abstract

Based on radar observation and convection-permitting numerical simulation, this work investigates the storm-scale dynamics governing the generation of two episodes of high winds by an unusually long-lived quasi-linear convective system (QLCS) in South China on 21 April 2017. The first episode of high winds occurred at the apex of a bow segment embedded in the southern QLCS, due to the downward transport of high momentum by the descending rear-inflow jet (RIJ) behind the apex. The jet was initially elevated, forming as the thermal contrast between the cold pool and tilted front-to-rear flow induced a midlevel pressure minimum. The descent of the RIJ was initiated by the negative buoyancy of cold pool but was mainly strengthened by hydrometeor loading. The second episode of high winds occurred as the QLCS evolved into a large bow echo and merged with another mesoscale convective system (MCS) at its northern end where a meso-β-scale cyclonic vortex was present in the middle level. During the merger, the line-end vortex experienced a downward development, because of the enhancement of low-level convergence which increased the vertical vorticity through vertical stretching. The high winds were generated by the superposition of ambient flow with the low-level

rotational flow of line-end vortex which contributed up to 30%. The findings suggest the complexity in the generation of high winds by QLCSs and highlight the importance of merger which can produce more damaging winds than the well-recognized RIJ at the bow apex.

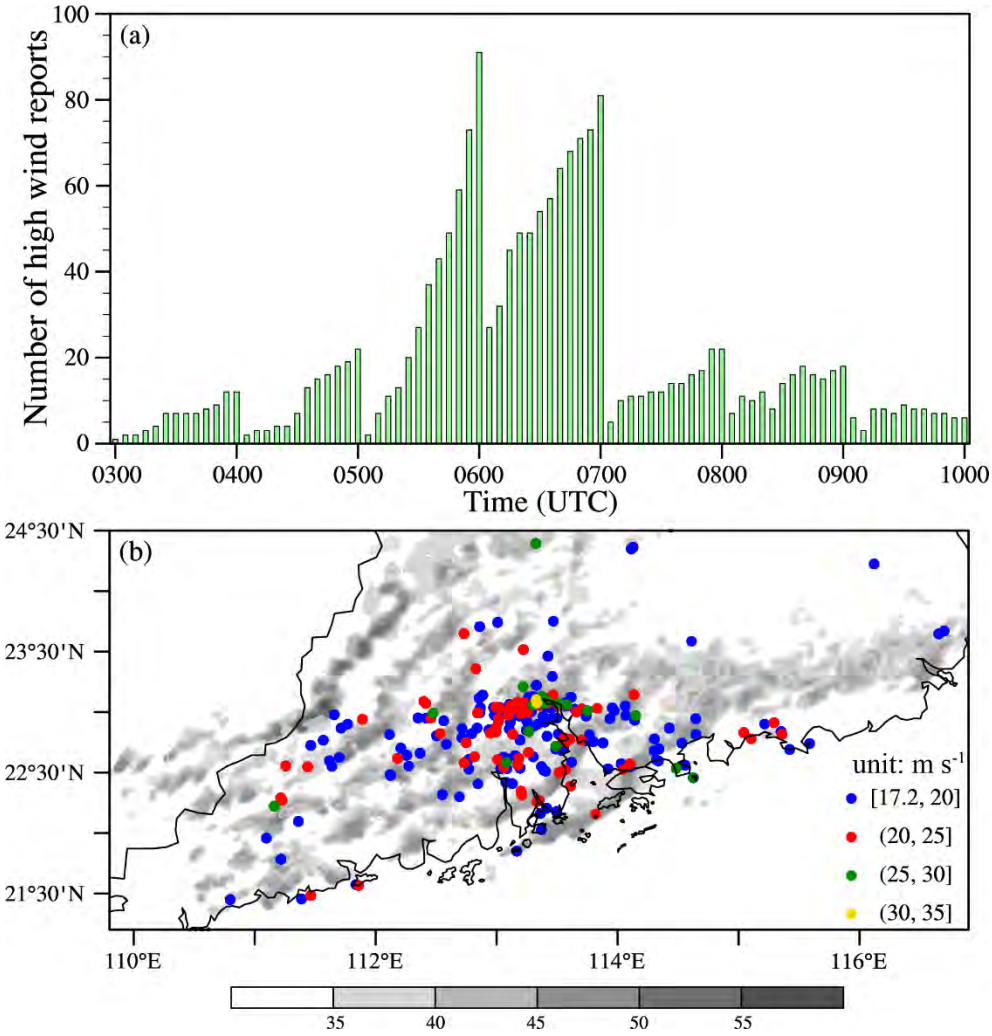

Fig 1. (a) Number of high wind (≥17.2 m s^{-1}) reports and (b) their locations (color dots) between 0300 and 0800 UTC of 21 April 2017 recorded by automatic weather stations in Guangdong province. The grey shading in (b) designates the hourly composite reflectivity (unit: dBZ) from the four *S*-band operational radars in South China.

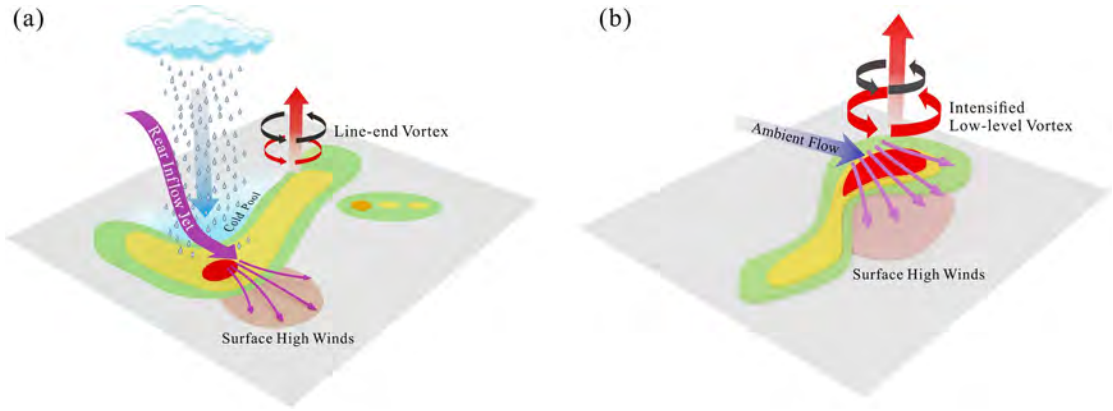

Fig 2. A conceptual model for the generation of near-surface high winds in the different stages of the QLCS. (a)Surface high winds occurred in the early stage of the QLCS, due to the downward transport of high momentum by the descending rear-inflow jet (RIJ) behind the apex. The RIJ resulted from the thermal contrast between cold pool and front-to-rear flow and descended due in large part to hydrometeor loading. (b)Surface high winds occurred in the merger stage of the QLCS. The QLCS merged with another mesoscale convective system at its northern in (a) led to a downward development of line-end vortex which produced stronger high winds than RIJ via superposition with ambient flow.

MCSs in Australia: Recent Findings

Stacey M. Hitchcock [a,b], Todd P. Lane [a,b], Ewan Short [a,b]

[a] *School of Geography, Earth and Atmospheric Sciences, The University of Melbourne, Melbourne, Australia*

[b] ARC *Centre of Excellence for Climate Extremes, The University of Melbourne, Melbourne, Australia*

Corresponding author: Stacey Hitchcock, Stacey.Hitchcock@unimelb.edu.au

Mesoscale convective systems are common in parts Australia, from the tropics to mid-latitudes, yet they have been the subject of very few studies in this region in the past. Several recent and on-going studies at the University of Melbourne have explored aspects of MCSs in Australia. Hitchcock et al. 2021 used 15 years of Melbourne radar observations to explore the relationship between linearly organized precipitation systems and regional rainfall. We showed that those systems associated with heavy rainfall events were often larger, slower, and longer-lived, and that more extreme events tended towards more north south orientation, more southward propagation, and deeper convection. In a follow-up study using two consecutive QLCSs, we found that systems with seemingly similar reflectivity had different flow structures, and suggest a link to the strength of the synoptic forcing (Hitchcock and Lane 2023). Meanwhile, Short et al. 2023 used objective methods to both track and diagnose the structure of tropical MCSs using 15 years of radar data in the Darwin region. They found that 65-80% of MCS observations were consistent with the classical leading-line trailing-stratiform model. However, during the humid, active monsoon phase, most systems were inconsistent with the classical model, and instead propagated upshear. Using different approaches, this set of studies adds to our understanding of Australian MCSs and provides explanation for observed structural differences that reflect key aspects of the study regions.

Airborne Phased Array Radar (APAR): The Next Generation of Airborne Polarimetric Doppler Weather Radar

Everette Joseph, Wen-Chau Lee, Scott McIntosh, Krista Laursen, Angela Richardson

National Center for Atmospheric Research
Boulder, CO 80307-3000

Corresponding author: Everette Joseph, ejoseph@ucar.edu

Abstract

This paper presents a configuration of a novel, airborne phased array radar (APAR) designed by NCAR to be installed on the National Science Foundation (NSF)/NCAR C-130 aircraft to address scientific frontiers. APAR is enabled owing to major advances in cellular technology, component miniaturization, and radar antenna simulation software, The APAR system will consist of four removable C-band active electronically scanned arrays (AESA) strategically placed on the fuselage of the aircraft. Each AESA measures approximately 1.5 x 1.5 m and is composed of 2368 active radiating elements arranged in a total of 37 line replaceable units (LRU). Each LRU is composed of 64 radiating elements that are the building block of the APAR system.

Polarimetric measurements are not available from current airborne tail Doppler radars. However, APAR, with dual-Doppler and dual polarization diversity at a lesser attenuating C-band wavelength, will further advance the understanding of the microphysical processes within a variety of high-impact weather systems, especially over the ocean and complex terrain where ground-based radars are not effective. Such unprecedented observations, in conjunction with the advanced radar data assimilation schema, will be able to address the key science questions to improve understanding and predictability of significant weather.

A Mid-Scale Research Infrastructure proposal is submitted to the NSF to request the implementation cost. The development is expected to take ~5 years after the funding is in place. It adopts a phased approach as an active risk assessment and mitigation strategy. At the present time, both the NSF and the National Oceanic and Atmospheric Administration are funding the APAR project for risk reduction activities. An APAR science and engineering advisory panel has been organized.

The authors will review the scientific motivation, overall engineering design and current progress of APAR and outline ambitious future development work needed to bring this exceptional tool into full operation.

Temporal Resolution and Variance of Airborne Phased Array Radar Estimates

Greg Meymaris, Jothiram Vivekanandan, Michael Dixon, and Eric Loew
National Center for Atmospheric Research (NCAR)
Boulder, CO, USA
Email:vivek@ucar.edu

Abstract

Phased array radar (PAR) has the potential mapping of storms and precipitation at unprecedented temporal and spatial resolution in a relatively short duration than a mechanically scanning radar. Weather radar signal from precipitation is a random variable due to hydrometeors' random location and size distribution. The temporal averaging of weather radar signals reduces statistical fluctuation in weather radar signals. PAR uses Active Electronic Scanning Array (AESA) technology for several scanning and customized beam shapes that were not possible with a mechanically scanning antenna: (i) rapid electronic scanning, (ii) beam multiplexing, (iii) formation of customized beams for transmit and receive, and (iv) fan and pencil beams for imaging.

For a mechanically scanning radar, the dwell time required for acquiring samples of backscattered signals at each beam position for estimating reflectivity and Doppler wind measurements with acceptable accuracy limits the scan rate. This type of sampling is known as contiguous-pair sampling (CPS). One key advantage of PAR is it enables beam multiplexing (BMX). This is called independent-pair sampling (IPS). Statistical independent signals are recorded by rapidly steering the beam to a different position after every pulse pair. Then, selecting the revisit time of the beam such that it samples the same pulse volume after the weather signals are de-correlated and before the clouds and precipitations have advected from the sample volume, statistically independent radar signals are measured. Steering the beam to different directions for collecting independent signals during the periods when backscattered signals are correlated is defined as beam multiplexing. IPS reduces errors in reflectivity measurements while providing rapid updates of scan volumes in less time than a mechanically scanning radar. However, CPS is preferred for estimating Doppler and polarimetric radar observations that depend on the temporal correlation of received signals.

A typical scan sequence for airborne phased array radar (APAR) consists of three types of scans: (i) dual-Doppler, (ii) dual-Doppler and dual-polarization, and (iii) surveillance. Dual-Doppler (DD) mode will be the primary mode of operation. This paper describes the time requirements of APAR scan sequences to achieve reasonable along-track resolution and expected standard errors of Doppler and polarimetric measurements.

In this study, we introduce a newly-developed upper-air observational instrument for atmospheric research. The “Storm Tracker” (or “NTU mini-Radiosonde”), is an ultra-lightweight (about 20g including battery), multi-channel simultaneous capable radiosonde designed by the Department of Atmospheric Sciences at National Taiwan University. Developed since 2016, the Storm Tracker aims to provide an alternative for observation of atmospheric vertical profiles with a high temporal resolution, especially lower-level atmosphere under severe weather such as extreme thunderstorms and tropical cyclones.

Several field experiments were conducted as trial runs from 2017 to 2020 at Wu-Chi, Taichung, and Taipei Taiwan, to compare the Strom Tracker with the widely used Vaisala RS41 radiosonde. Among 1200 co-launches of the Storm Tracker and Vaisala RS41 radiosondes, the raw measurements of pressure, wind speed, and wind direction are highly consistent between the Strom Tracker and Vaisala RS41. However, a significant daytime warm bias was found due to solar heating. A metal shield specifically for the Storm Tracker was thus installed and shows good mitigation for the warm biases.

With the much lower costs of the sondes and the simultaneous multi-channel receiver, the Storm Tracker system has been proved to be beneficial for high-frequency observational needs in atmospheric research under expensive trend of Helium gas market.

Introduction of KMA/NIMS atmospheric research aircraft and characteristic of airborne measurement for 2018-2022

Tae-Young GOO*[1], Sueng-Pil JUNG[1], Dong-Hyeun Cha[2], Min-Seong KIM[1], Deok-Du Kang[1], Seung-Beom HAN[1], Kwang-Jae LEE[1], Jong-Hoon Shin[1]
*gooty@korea.kr

[1]National Institute of Atmospheric Sciences, KMA, Republic of KOREA
[2]UNIST, Republic of KOREA

The National Institute of Atmospheric Sciences (NIMS) has operated a research aircraft since 2018 in order to investigate the features of severe weathers and cloud physics and to monitor atmospheric compounds such as aerosols, reactive gases and greenhouse gases as well as weather modification. The NIMS research aircraft is a modified KingAir 350H manufactured by the Beechcraft Inc. Its maximum altitude and flight hours are up to 10.7 km and 5.5 hours. Crew and instrument capacities are two pilots, two operators, and one scientist with 25 instruments and devices. Annual total flight time is about 400 hours and it is equivalent to about 100 ~ 120 observation days per year.

In order to observe the severe weather (SW) such as heavy rainfall and snowfall, and typhoon, dropsonde (RD-94/AVAPS II, Vaisala), AIMMS-20 (Aventech), and two radiometers (GVR and SFMR, Prosensing) are employed. The main purpose of SW observation is not only to give the observation of atmospheric structure to KMA weather forecasters but also to provide input with operational weather prediction model. It is found that 15% improvement on wind speed prediction of typhoon as well as 5 ~ 10% improvement on rainfall prediction. In terms of the sensitivity of data assimilation with dropsonde observation, preliminary research on typhoon founds a significant improvement on track errors. On AIMMS-20 which provides T, P, RH, and 3D winds along the flight route, sensitivity test of data assimilation based on the WRF is also on-going work.

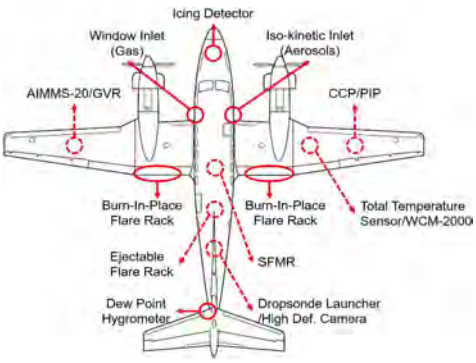

Fig.1 Instruments of the NIMS research aircraft (solid line: top, broken line: bottom, Kim et al., Geosci. Data J. 2022)

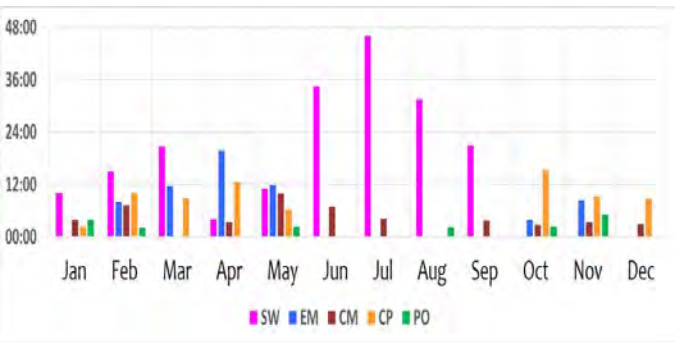

Fig. 2 Monthly flight time of science missions in 2022.

Evaluation and Assimilation of Low-Level Moisture from the MPD during the "PRE"-CIP Experiment

Yunji Zhang[1, 2, 3], Xingchao Chen[1, 3]

[1]Center for Advanced Data Assimilation and Predictability Techniques, The Pennsylvania State University

[2]Alliance for Education, Science, Engineering & Design with Africa, The Pennsylvania State University

[3]Department of Meteorology and Atmospheric Science, The Pennsylvania State University

The MicroPulse DIAL (MPD) is a new type of differential absorption lidar (DIAL) that can monitor the moisture in the lower troposphere under clear-sky conditions continuously with high temporal and vertical spatial resolutions. Three MPDs were deployed during the “PRE”-CIP2021 experiment in Colorado in the 2021 summer and the PRECIP2022 campaign in Taiwan in the 2022 summer. Verifications during the “PRE”-CIP2021 experiment suggest that the real-time forecasts with the assimilation of all-sky infrared radiances match the MPD observations reasonably good, although notable discrepancies exist, since all-sky infrared radiances are unable to observe moisture near the surface. The assimilation of the MPD observations lead to improved match between the data assimilation analyses and the observations – as well as during the subsequent forecasts, although the improvements after assimilating MPD observations only last for a limited time during the forecasts. On the other hand, rainfall forecasts are only slightly improved, likely due to the fact that the majority of the rainfall systems during “PRE”-CIP experiment are localized thunderstorms; while low-level moisture conditions are important for the formation and development of thunderstorms, many other factors also contributed to their forecasts. However, MPD is proved to be a reliable, stable, and relatively economical instrument that can provide critical, high-resolution lower-tropospheric moisture observations that compliments the current observing system.

Analysis of the Back-building Mesoscale Convective Systems from NOCOVID-2021/TAHOPE-2022

Wei-Yu Chang [a], Yu-Shuang Tang [b], and Yu-Chieng Liou[a]

[a] *National Central University, Taoyuan City, Taiwan*

[b] *Central Weather Bureau, Taipei City, Taiwan*

Corresponding author: Wei-Yu. Chang, author@address.com

Multiple radars, wind profilers and sounding data from the pre-TAHOPE (NOrthern Coast Observation Validation and Investigation of Dynamics 2021, NOCOVID-2021) and TAHOPE (Taiwan-Area Heavy rain Observation and Prediction Experiment) were apply to investigate the back-building mesoscale convective systems. The kinematic fields of an eastward-moving mesoscale convective system (MCS) from NOCOVID-2021 was derived by variational wind retrieval technique (WISSDOM). The vertical cross-section profile reveals the easterly leading-edge inflow with the depth about 1.5 km. The echo top of the convection was up to 12 km. The vorticity budget analysis was performed to understand the development and maintenance mechanism. The analysis results reveal the features of back-building MCS. The positive vertical vorticity extended from surface up to 6 km at the leading edge of the MCS. The tilting term dominate the vorticity tendency. It's postulated that the horizontal vorticity of vertical shear due to terrain effect and the vertical motion were responsible for the tilting effect. The vertical motion in the convective region stretched up to 12 km. A meso-vortex was also found embedded within the back-building MCS. Further analysis of the interaction between microphysical and kinematical processes will be performed.

Impact of sea surface temperature warming by anthropogenic forcing on the extreme East Asian Summer Monsoon in 2020

Dong-Hyun Cha [a], Taeho Mun[a], and Dong-Kyou Lee [b]

[a] *Department of Urban and Environmental Engineering, Ulsan National Institute of Science and Technology, Ulsan, Republic of Korea*

[b] *School of Earth and Environmental Sciences, Seoul National University, Seoul, Republic of Korea*

Corresponding author: Dong-Hyun Cha, dhcha@unist.ac.kr

In 2020, the East Asian summer monsoon (EASM) produced a record-breaking amount of precipitation, which significantly damaged Korea, China, and Japan's people and property. It is crucial to investigate the possible mechanisms which caused extreme EASM in 2020. This study analyzed the effects of global warming on synoptic-scale circulation, which is the cause of the extraordinary EASM in 2020, using regional climate model experiments. The control experiment reasonably reproduced precipitation patterns such as those of the EASM and the Western North Pacific summer monsoon during summer. In sea surface temperature (SST) sensitivity experiments, which added or subtracted the trend of increasing SST due to global warming, a positive correlation was found between SST and precipitation change in the tropics, but a slight negative correlation was observed in the EASM region. Increasing SST due to global warming provided moisture to the tropics, strengthening convection, and increasing the SST gradient between the Indian Ocean and western North Pacific. This enhanced westerly wind in the tropics and convection activity in the South China Sea, which dynamically inhibited convection in East Asia through the strengthening of the local Hadley cell. Meanwhile, there was a positive correlation between changes in SST and the frequency of extreme precipitation in both tropic and extratropic regions. Through this study, it is feasible to examine the regional and local effects of increasing SST by global warming that may have an impact on the EASM.

Future projections in rainfall and frontal structure during the Baiu season in Japan using 150-year continuous simulations

Yukari Naka [a], Machi Harada[b], and Eiichi Nakakita[a]

[a] *Disaster Prevention Research Institute, Kyoto University, Uji, Kyoto, Japan*

[b] *Nomura Real Estate Development, Shinjuku, Tokyo, Japan*

Corresponding author: Yukari Naka, naka.yukari.2z@kyoto-u.ac.jp

We investigated the gradual future changes in rainfall and frontal structure during the Baiu season (mainly June to July) in Japan using 150-year (1950–2099) continuous climate simulations by 20-km atmospheric general circulation model. Rainfall over the land of Japan gradually increase in the future climate, and in particular, early July shows a significant large increase in rainfall at the end of the century. This increase was caused by the Baiu front that covered the entire Japan, increasing rainfall not only in western Japan but also in eastern and northern Japan, resulting in an increase in rainfall over the whole of Japan at the same time. Figure 1 shows the cloud water content at 500-hPa and cloud-top height in Early July in period 1–4 (1: 1960–1994, 2: 1995–2029, 3: 2030–2064, 4: 2065–2099). The cloud water content and the cloud height will increase markedly especially in period 4, and the Baiu front will cover the whole of Japan.

Figure 2 shows the water vapor flux (arrow), updraft at 500-hPa (shaded) and west-east component of wind at 200-hPa (contour) which is corresponding to jet stream in (A) period 1 and (B) period 4, and (C) represents the change in the jet stream. The jet stream meanders southward to form a trough near the Korean Peninsula and the meandering (trough) will become stronger in the future. This strengthening of the trough will have resulted in enhanced upwelling around the Northern Japan which is in the front (east side) of the trough, contributing to the development of the Baiu front as shown in Figure 1. In addition, the temperature increase is relatively larger over land than over sea (figure omitted). The increase in the continental-ocean temperature difference will enhance the Asian monsoon flowing from the South China Sea to the East China Sea and western Japan, and contribute to increased water vapor transport to the Japan. In addition, the convective intensification around the tropical area will enhance the anticyclonic circulation of Pacific High. The enhanced anticyclonic circulation has also enhanced the southerly wind near eastern and northern Japan, and this change contributes to the transport of water vapor to the northern and eastern Japan. Moreover, the increase in water vapor, combined with the enhancement of southwesterly winds due to the monsoon and the enhancement of anticyclonic circulation due to the strong Pacific High, greatly increased the water vapor flux from the southwesterly direction into the entire Japan.

The increased water vapor transport due to monsoon and Pacific High intensification and meandering of the jet stream confirmed in this study are very similar to the characteristics of the atmospheric field of the recent heavy rainfall associated

with the Baiu front. It is suggested that cases affected by global warming have already begun to occur in Japan.

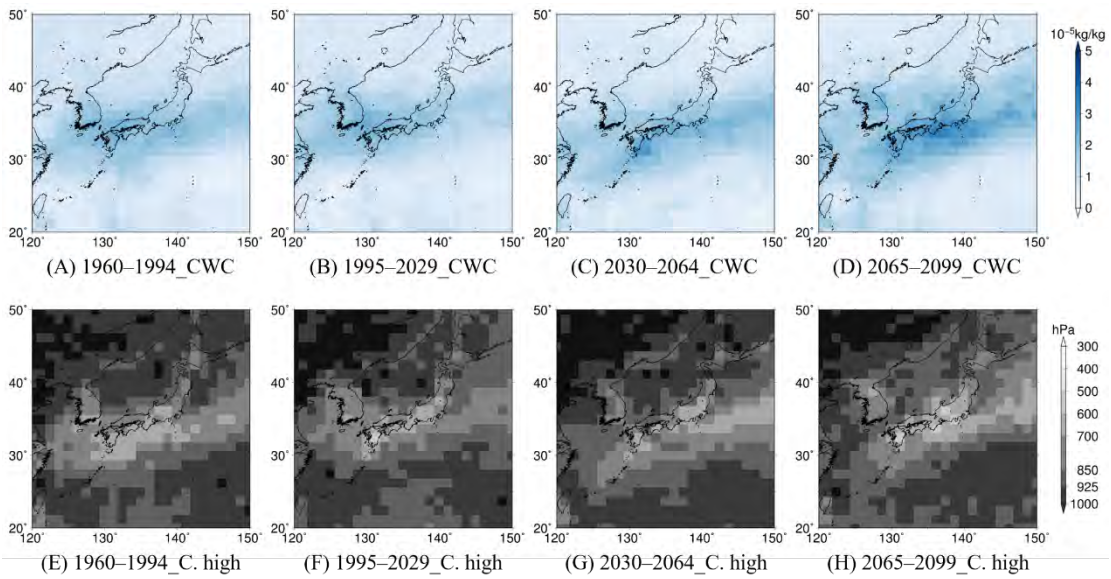

Figure 1: The spatial distribution of (A–D) the cloud water content at 500-hPa and (E–H) the cloud top height in 1960–1994, 1995–2029, 2030–2064, 2065–2099.

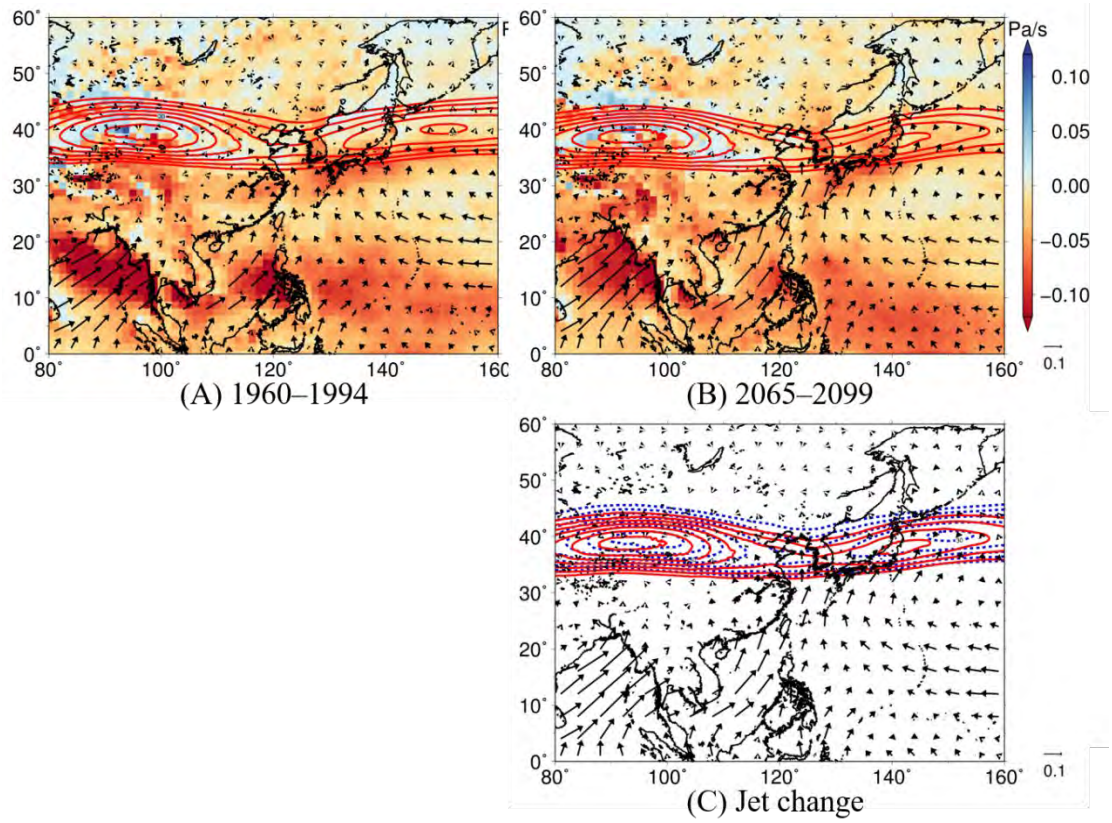

Figure 2: The spatial distribution of updraft at 500-hPa (shade), surface water vapor flux (arrow) and west-east wind component at 200-hPa (contour; corresponding to jet stream). The lower figure shows the change of the jet stream from 1960–1994 to 2065–2099.

Effect of a scale-aware convective parameterization scheme on the simulation of heavy rainfall events in South Korea

Haerin Park[a] and Dong-Hyun Cha[a]

[a] *Department of Urban & Environmental Engineering, Ulsan National Institute of Science and Technology, 50 UNIST-gil, Ulju-gun, Ulsan 689-798, South Korea*

Corresponding author: Dong-Hyun Cha, dhcha@unist.ac.kr

We investigated the predictability of precipitation in the non-scale-aware and scale-aware cumulus parameterization scheme (CPS) to generalize the necessity of the CPSs within the gray zone. The sensitivity of heavy rainfall simulations over the Korean Peninsula during 10 years (i.e., 2010-2020) to the CPS was examined using the Weather Research and Forecasting (WRF) model. We selected the Kain–Fritsch (KF) scheme and Multiscale Kain–Fritsch (MSKF) scheme as non-scale-aware and scale-aware CPSs, respectively. In general, the MSKF scheme showed improved precipitation simulation performance compared with the KF scheme. The results showed that the sensitivity to CPSs depended on the type (characteristics) of heavy rainfall events (HREs) in the Korean Peninsula. A scale-aware CPS might be less necessary for HREs characterized by significant vapor transport resulting from strong winds across the Korean Peninsula. These events could be explicitly resolved, allowing for accurate predictions of both CPSs. Nevertheless, in cases of HREs with weak environmental conditions, the MSKF scheme could improve the overall simulated precipitation by explicitly increasing the resolved precipitation and reducing the overprediction of subgrid-scale precipitation simulated in the KF scheme. In particular, the results showed that the MSKF scheme significantly improved light precipitation (<10 mm). Therefore, during localized HREs, we found that the scale-aware CPS could improve the prediction of light precipitation in the gray zone. This finding supports the thesis that selecting an appropriate parametrization scheme for specific meteorological conditions can lead to more accurate weather forecasting.

IMPACT OF ENSEMBLE DATA ASSIMILATION WITH SURFACE MOISTURE AND RADAR DATA ON HEAVY RAINFALL FORECAST: A CASE STUDY OF TAHOPE–2022

Kao-Shen Chung, Phuong-Nghi Do,
Jui Le Loh, Pei-Jung Tsai, Yu-Chieng Liou, Shu-Chih Yang

Department of Atmospheric Sciences, National Central University, Taoyuan City, Taiwan

ABSTRACT

In this study, the moisture information of surface stations was assimilated with the radar reflectivity and radial velocity by using the WRF local ensemble transform Kalman filter data assimilation system. A heavy rainfall case of the Taiwan-Area Heavy rain Observation and Prediction Experiment–2022 (TAHOPE–2022) caused by the quasi-stationary Mei-Yu front was examined. The results revealed that assimilating reflectivity and radial velocity from three radars (S-Pol, TEAM-R, and RCWF) improved quantitative precipitation forecasting but may not optimize the correction of moisture to forecast well heavy rainfall. With the assimilation of additional moisture near the surface, the more precise humidity and temperature correction at the low level was presented with a more noteworthy impact on the humidity field. Additionally, the wind convergence was enhanced. Therefore, a better short-term forecast was achieved, particularly for heavy rain. The preliminary results of this study proved the critical role of moisture information in improving quantitative precipitation forecasting. During the TAHOPE–2022 campaign, besides the surface observation, moisture information was obtained using various types of equipment, such as radar-derived refractivity and MicroPulse DIAL (MPD). The S-Pol radar in Hsinchu can obtain refractivity, which provides information regarding two-dimensional near-surface moisture. The MPDs deployed in National Central University, Hsinchu, and Yilan can provide vertical water vapor information in the lower troposphere. Further and ongoing studies will be conducted to investigate (1) the added value of assimilating MPD, (2) the benefit of assimilating N and how it compared with assimilating moisture from surface observation, and (3) how the impact on QPF would be if all data was assimilated.

Keywords: surface moisture data; radar observations, data assimilation

Exploring the relationship of QPE/QPF exceedances of precipitation thresholds with observed flash floods

Eric P. James [a,b,c], and Russ S. Schumacher[a]

[a] *Colorado State University, Fort Collins, Colorado, USA*

[b] *University of Colorado, Boulder, Colorado, USA*

[c] *NOAA Global Systems Lab, Boulder, Colorado, USA*

Corresponding author: Eric James, eric.james@noaa.gov

Rainfall from mesoscale convective systems (MCSs) provides a large portion of the average annual precipitation for central portions of the United States, while extreme precipitation from MCSs poses a significant hazard for life and property, as well as a forecasting challenge. However, existing quantitative precipitation estimate (QPE) datasets have varying degrees of skill and realism in depicting heavy rainfall from MCSs. In this study, we examine the relationship between QPE exceedances of various precipitation thresholds (fixed thresholds, average recurrence intervals, and ratios of Flash Flood Guidance) and flash flood reports over a seven year period.

It is found that the spatial pattern of exceedances varies across threshold datasets, with average recurrence intervals approximately normalizing the frequency of events across the CONUS, while fixed threshold and Flash Flood Guidance exceedances maximize in the eastern CONUS. The number of events also varies by QPE dataset, with the climatology corrected precipitation analysis substantially reducing the frequency of heavy precipitation events seen in Stage IV QPE in the high plains region from New Mexico to Montana, and the multi-radar multi-sensor (MRMS) gauge correction more slightly reducing the number of events seen in the radar-only MRMS QPE dataset. In terms of equitable threat score, correspondence with flash flood reports is highest in the eastern CONUS and lowest in the interior northwestern CONUS. We conclude by evaluating all the QPE datasets, as well as forecasts from an operational convection-allowing model (the High-Resolution Rapid Refresh, HRRR), against flash flood report occurrences using performance diagrams. We demonstrate that HRRR QPF exceedances of average recurrence intervals and Flash Flood Guidance have comparable skill to QPE datasets in depicting the location of flash flood reports in the southwestern CONUS.

Impact of Assimilating Radar Refractivity in the Context of Ensemble Kalman Filter: Cases Study of the SoWMEX

Phuong-Nghi Do[1], Kao-Shen Chung[1], Ya-Chien Feng[2],

Pay-Liam Lin[1], Bo-An Tsai[1]

[1]*Department of Atmospheric Sciences, National Central University, Taoyuan City, Taiwan.*

[2]*Pacific Northwest National Laboratory, Washington.*

ABSTRACT

In this study, the high-resolution *Weather Research and Forecasting* local ensemble transform Kalman filter data assimilation system was employed for two cases in the Southwest Monsoon Experiment to conduct two experimental sets. The first set was applied in both cases to investigate the effects of assimilating radar-retrieved refractivity along with reflectivity and radial wind. The second set was conducted in the second case to examine the benefit of increasing the frequency of refractivity assimilation and investigate the optimal strategy to assimilate refractivity. Results of the two cases revealed that assimilating reflectivity and radial velocity modified near-surface humidity on the basis of the flow-dependent back ground error covairance estimated by the ensemble, but the spatial distribution may not be proper, causing underestimation of quantitative precipitation forecast (QPF). With additional refractivity assimilation, stronger convergence and more accurate low-level moisture, temperature, and wind field corrections were obtained, leading to improved QPF for both light and heavy rainfall during 6 h. The results of the second set indicated that increasing the frequency of assimilating radar refractivity enabled capturing the moisture variation and enhancing wind convergence, resulting in short-term forecast improvement. Furthermore, assimilating refractivity information before the weather system was approached quaranteed that it was capable of optimizing the correction of environmental moisture, then accurately representing the humidity and strengthening the wind convergence when precipitation occurred. Therefore, the most noteworthy improvement of the short-term forecast was achieved, particularly for heavy rain

Keywords: radar refractivity, data assimilation, QPF

Impact of GNSS radio occultation data on the prediction of a pre-frontal squall line associated with a Mei-Yu front

Ying-Hwa (Bill) Kuo[1], Jenny Sun[2], Ying Zhang[2], I-Han Chen[1,2], Yuan Ho[1]
[1]University Corporation for Atmospheric Research, Boulder, CO, U.S.A.
[2]National Center for Atmospheric Research, Boulder, CO, U.S.A.

Jing-Shan Hong
Central Weather Bureau, Taipei, Taiwan

On 21-22 May 2020, a strong squall line developed over the Taiwan Strait, ahead of a surface Mei-Yu front. The squall line made landfall over southern Taiwan, interacted with the steep topography of Taiwan's Central Mountain Range and produced severe flooding in southwestern Taiwan. The maximum 24-h rainfall recorded at the Da-Han-Shan station was 723 mm. The prediction of such a strong convective system is a significant challenge due to the lack of observations over the ocean. Often these convective systems form over the Taiwan Strait, and make landfall over Taiwan in 6 hours or less, which does not allow much time for warning.

Since the launch in June 2019, the FORMOSAT-7/COSMIC-2 has been providing ~6,000 GNSS (Global Navigation Satellite Systems) radio occultation (RO) data from 40S to 40N, which can be very valuable for the prediction of severe weather systems. In particular, the RO measurement technique can provide valuable information on the moisture and temperature in the tropical lower troposphere. In this paper we examine the impact of COSMIC-2 GNSS RO data on the prediction of this heavy rainfall event. Using a configuration of the Weather Research and Forecasting (WRF) Model similar to the operational system of Taiwan's Central Weather Bureau with 15/3 km nested grids, we performed continuous assimilation of conventional observations and RO data, with 3-h cycling starting from 0000 UTC 18 May 2020 to 0000 UTC 22 May 2020 and conducted short-range (12-h) forecasts at the end of each data assimilation cycle. Our results showed that the assimilation of COSMIC-2 RO data using a nonlocal excess phase operator significantly improved the moisture analysis over the South China Sea, the structure and movement of the Mei-Yu front over the Taiwan Strait, and the development of the pre-frontal squall line ahead of the Mei-Yu front. Although the timing for the development of the squall line was off by about 3 hours (ahead of the actual event), the model was able to accurately capture the landfall of the squall line and its interaction with the Central Mountain Range, and the subsequent heavy rainfall over southern Taiwan on the windward side of the mountain. The prediction was not successful when RO data were not assimilated, or when RO data below 2.5 km were excluded from assimilation. The structure of the squall line and its movement are very sensitive to the movement of the Mei-Yu front over the Taiwan Strait and the moisture transport associated with the southwesterly monsoon flow, which could only be accurately simulated with the assimilation of the full GNSS RO data, including the tropical lower troposphere. These

results suggest that the COSMIC-2 GNSS RO data have the potential to improve the prediction of mesoscale convective systems associated with the Mei-Yu front. It also highlights the importance of observing the tropical lower troposphere using an advanced GNSS receiver. Detailed analysis will be presented to illustrate how GNSS RO improves the prediction of the prefrontal squall line associated with the Mei-Yu front.

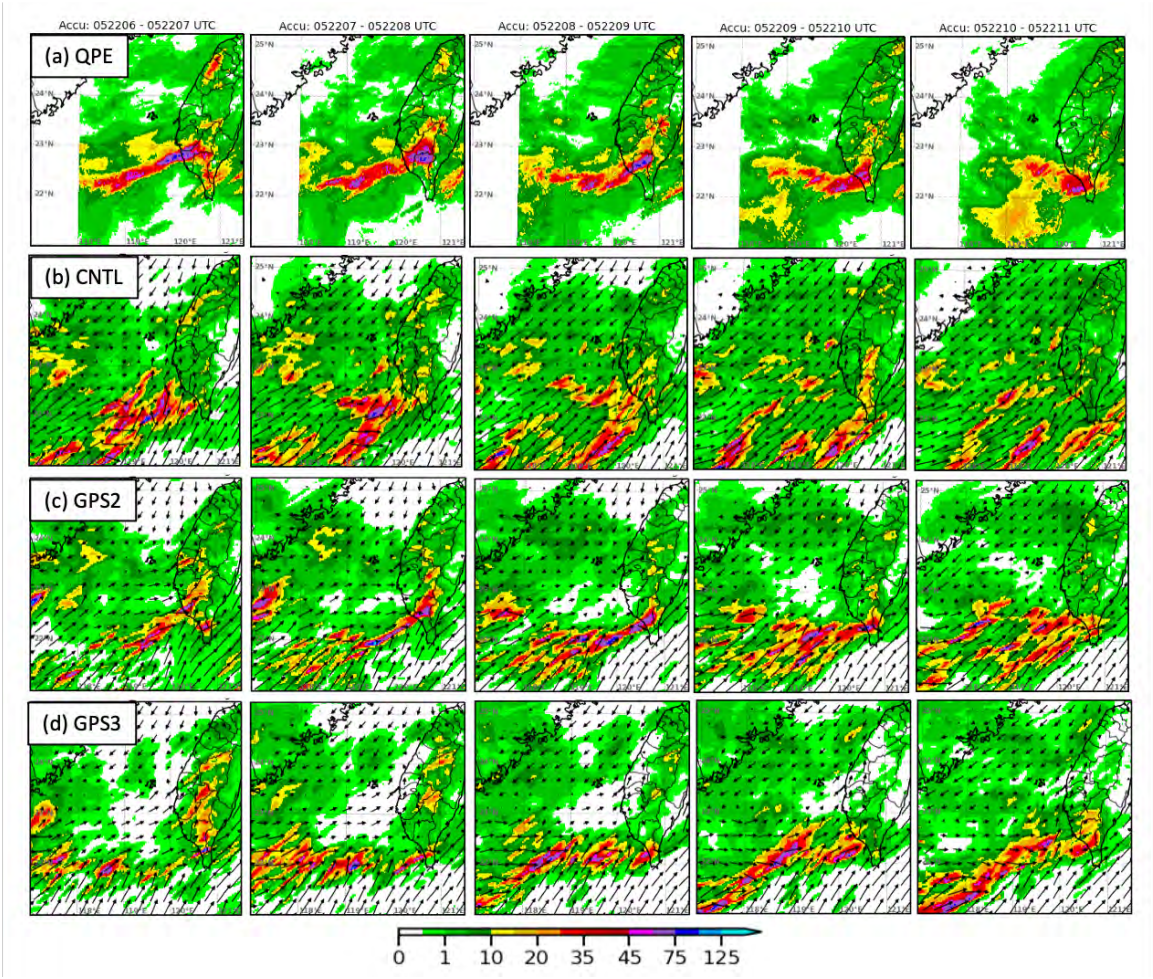

Fig. 1. Comparison of hourly rainfall from (a) QPE (quantitative precipitation estimate), (b) CNTL (Control, which does not assimilation RO data), (c) GPS2 experiment (which assimilates GNSS RO data using nonlocal excess phase operator, (d) GPS3 experiment (which is the same as GPS2 experiment, except that the RO data below 2.5 km were excluded from assimilation). The QPE is shown from 06 UTC to 11 UTC 22 May, and model precipitation from 03 UTC to 08 UTC May. There is a 3-hr time shift between observed and model precipitation. Only the GPS2 experiment developed the squall line, with a structure and orientation similar to the observation, and made landfall over southern Taiwan to produce heavy rainfall.

Hourly and Sub-hourly Rainfall under Synoptic Patterns during the Meiyu Anomaly in 2020

Liye Li [a b] and Fan Zhang [a]

[a] *State Key Laboratory of Severe Weather, Chinese Academy of Meteorological Sciences, Beijing China*

[b] *College of Earth and Planetary Sciences, University of Chinese Academy of Sciences, Beijing, China*

Corresponding author: Fan Zhang, zhang_fan@cma.gov.cn

The Meiyu season of 2020 has drawn extensive attention due to its record-breaking rainfall at Yangtze Huai River Basin (YHRB) region of China. Although its rainfall features from various time scale have been well studied, the sub-hourly/hourly rainfall feature are unknown. In this paper, wavelet analysis is applied on 1-min rainfall data from 480 national rain gauges over YHRB. Results suggest that variances at sub-hourly and hourly scale contribute 63.4% of Meiyu rainfall 2020, and distinct rainfall feature at short-duration is associated with hourly synoptic variations. By method of PCT, hour synoptic variations in Meiyu season are summarized as three major patterns, characterized by weak synoptic forcing (P1, Fig.1a), a convergence line (P2, Fig.1b) and a vortex (P3, Fig.1c).

When YHRB is largely under steady southwesterlies without strong synoptic disturbance (trough/vortex), circulation patterns tend to be sorted as P1 (Fig 1a). Under P1, Meiyu front is around 31-32° N, WPSH extends northwestward and sufficient moisture is conveyed into YHRB by low-level wind. The relatively uniformed dynamic and thermal-dynamic environment produces short-term and dispersed rainfall within YHRB, and rainfall episodes under P1 have the shortest time scale with 70.4% expectation from sub-hourly to hourly scale than others (Fig 2). Accumulated rainfall and hourly rainfall frequency are widely distributed in the warm-sector, enhanced near the dense isotherm line of equivalent potential temperature and terrain. With the highest frequency of P1 of 56.3%, accumulation of short-term rainfall contributes significantly to the total rainfall in Meiyu season 2020.

YHRB is frequently affected by sets of east-ward moving disturbance in mid-latitude and southwest during Meiyu season of 2020, summarized as P2 with occurrence of 30.6% (Fig 1b). If the approaching trough/vortexes is to the north of YHRB, dry northerly will converge with moist southwesterly converge near 31° N in average. Meiyu front is intensified with stronger horizontal gradient of equivalent potential temperature. Strong synoptic forcing under P2 favor the upward motion and bring concentrated rainfall clusters along convergence line. Duration of rainfall episodes is extended compared to P1, and percentage of sub-hourly and hourly rainfall in energy analysis reduces to 59.8% (Fig 2), with most rainfall expectation from time scale of ~30 min - 1 hour.

Once the east-ward moving southwest vortexes with its center right entering YHRB, the area will be occupied by quasi-stationary cyclonic wind flow at low level and significant vertical lifting (Fig 1c). It is classified as P3 with the less frequency (7.5%) among the major patterns. But it generates intense and localized rainfall in the southern quadrant of horizontal shear line, where the moisture is strongly confined to. In terms of duration, rainfall episodes under P3 is elongated with maximum variance on 1-4 hours, distinctively longer than that under P1 or P2 (Fig 2).

Compared with climate mean, hourly rainfall frequency are indispensable factors to the accumulated Meiyu rainfall anomaly 2020. This research highlights the dominant role of synoptic pattern in temporal and spatial features of Meiyu rainfall.

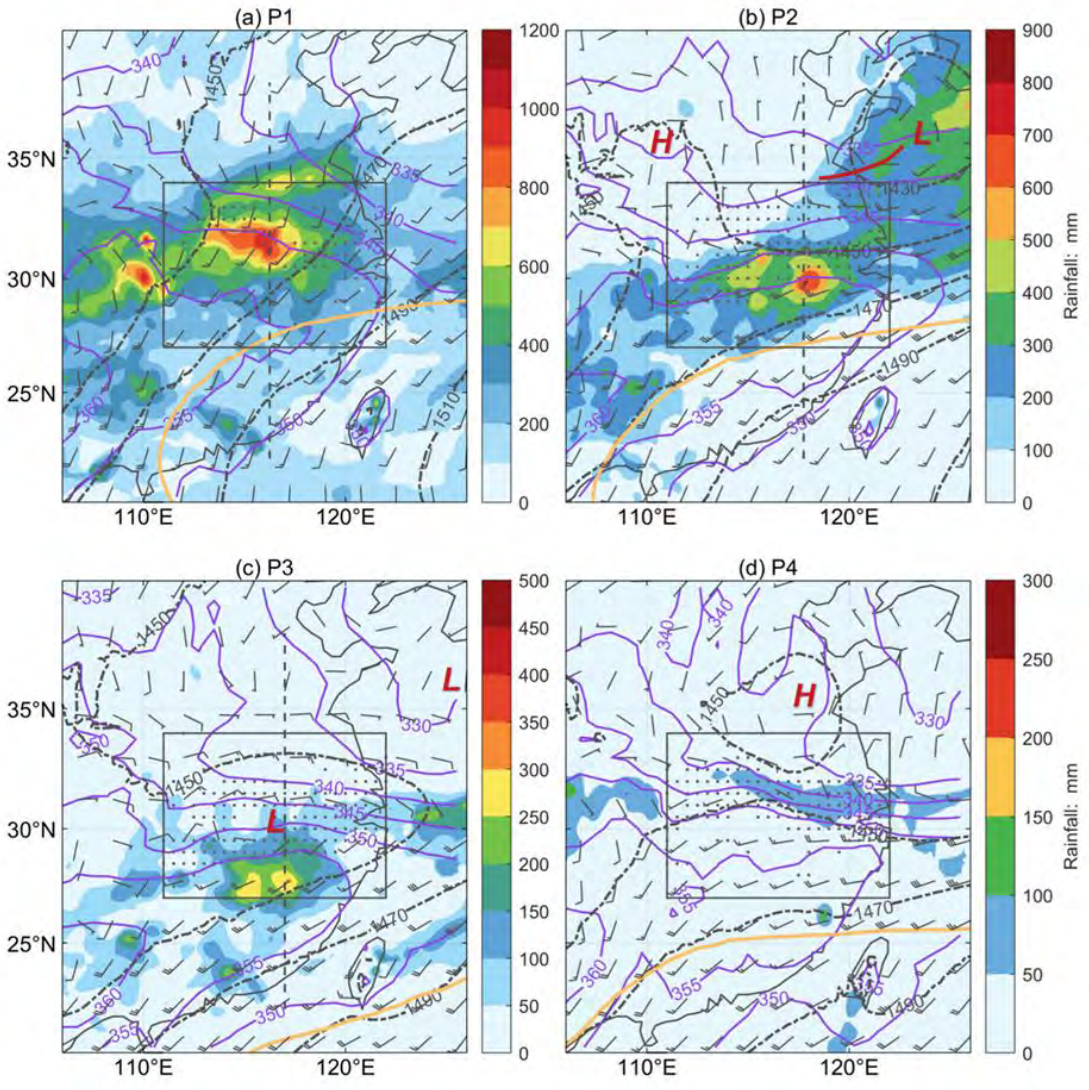

Figure 1. Composite synoptic patterns under PCT classifications (P1-P4), including accumulated rainfall (shading, unit: mm) interpolated from dateset of R1m, mean equivalent potential temperature (purple contours), mean geopotential height (black dashed contours) and mean horizontal wind vectors at 850 hPa (a full barb is 4 m s^{-1} and a triangle is 20 m s^{-1}). Yellow lines denote the ridge axis of a subtropical high, defined by 5880-gpm at 500 hPa. Black dots denote the area with maximum gradient of equivalent potential temperature at 850 hPa greater than 3 K (deg lat^{-1}). A black rectangular represents the study area used for this study, similar to that in Figure 2. Centers of high- and low- pressure centers in mid-latitudes are marked by red letters H and L. Axis of trough is drawn by red solid-line. Black dash line along N-S in (a, b, c) are cross lines for Figure 5. Frequencies of P1-P4 during Meiyu seasons in 2018-2021 are 1873, 781, 449, 174 in number of hours and 52.39%, 21.85%, 12.56%, 4.84% in percentage, respectively.

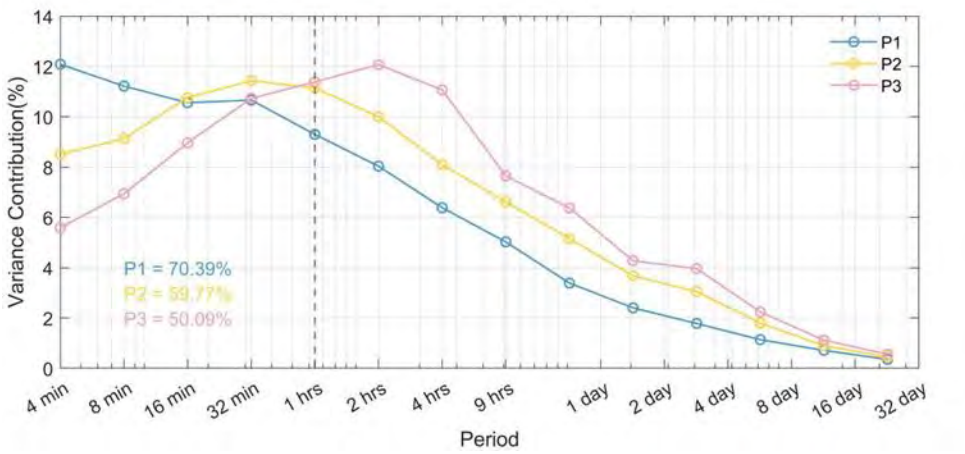

Figure 2. Wavelet spectrum by method of DWT on 1-min Meiyu rainfall in June-July 2020 under synoptic patterns f P1, P2 and P3. The accumulated contribution from wavelet variance at sub-hourly and hourly period (2 min to 1 hour) is 70.39%, 59.77% and 50.09% under P1, P2 and P3 respectively.

An Overview of Low-Level Jets (LLJs) and Their Roles in Heavy Rainfall over the Taiwan Area during the Early Summer Rainy Season

Abstract

During the early summer rainy season over Taiwan, three types of low-level jets are observed, including a synoptic low-level jet (SLLJ) situated in the 850–700 hPa layer in the frontal zone, a marine boundary layer jet (MBLJ) embedded within the southwesterly monsoon flow over the northern South China Sea at approximately the 925 hPa level, and an orographically induced jet at approximately the 1 km level off the northwestern Taiwan coast (e.g., barrier jet (BJ)). The characteristics and physical processes of the formation of these three types of low-level jets are reviewed, and their roles in the development of heavy rainfall are discussed.

Collaborators: Chuan-Chi Tu, Feng Hsiao, Ching-Sen Chen, Pay-Liam Lin, Po-Hsiung Lin

Keywords: low-level jets; Mei-Yu; heavy rainfall

Factors Leading to Heavy Rainfall in Southern Taiwan in the Early Mei-yu Season of 2020

Fang-Ching Chien, and Yen-Chao Chiu

Department of Earth Sciences, National Taiwan Normal University, Taipei, Taiwan

Corresponding author: Fang-Ching Chien, jfj@ntnu.edu.tw

This study examines the meteorological factors that led to the record-breaking heavy precipitation event in Taiwan in the early 2020 mei-yu season (May 15–31). The extreme amount of rainfall (135.9 mm per station) during the 36-h period around May 22 (hereafter Y20R) also set a record (Fig. 1). Compared to climatology, the Pacific subtropical high was stronger and the southwesterly monsoonal flow was more intense during the first half of the 2020 mei-yu season, resulting in a stronger moisture conveyor belt over the northern Indo-China Peninsula. The record-breaking precipitation in Y20R was mainly caused by the eastward movement of a southwest vortex (SWV) generated in southwestern China. When the eastern portion of the SWV touched the northern side of Taiwan, its associated west-southwesterly winds and the large-scale southwesterly monsoonal flow transported moisture toward the Taiwan Strait. The moisture-laden southwesterly flow was lifted by the stationary mei-yu front, leading to the heavy rainfall in southern Taiwan. When the SWV passed through the north side of Taiwan, it became the dominant weather system that enhanced the west-southwesterly winds and transported moisture from South China to Taiwan. The front moved southward through the Taiwan Strait during this period, with its location greatly determining the rainfall in southern Taiwan. In summary, the most critical factors leading to heavy rainfall in southern Taiwan are the strong 850-hPa southwesterly winds and moisture fluxes associated with the SWV. The other key factors include, in order of sensitivity to rainfall, the distance of the front, the distance of the SWV, the frontal speed, and the intensity of the SWV.

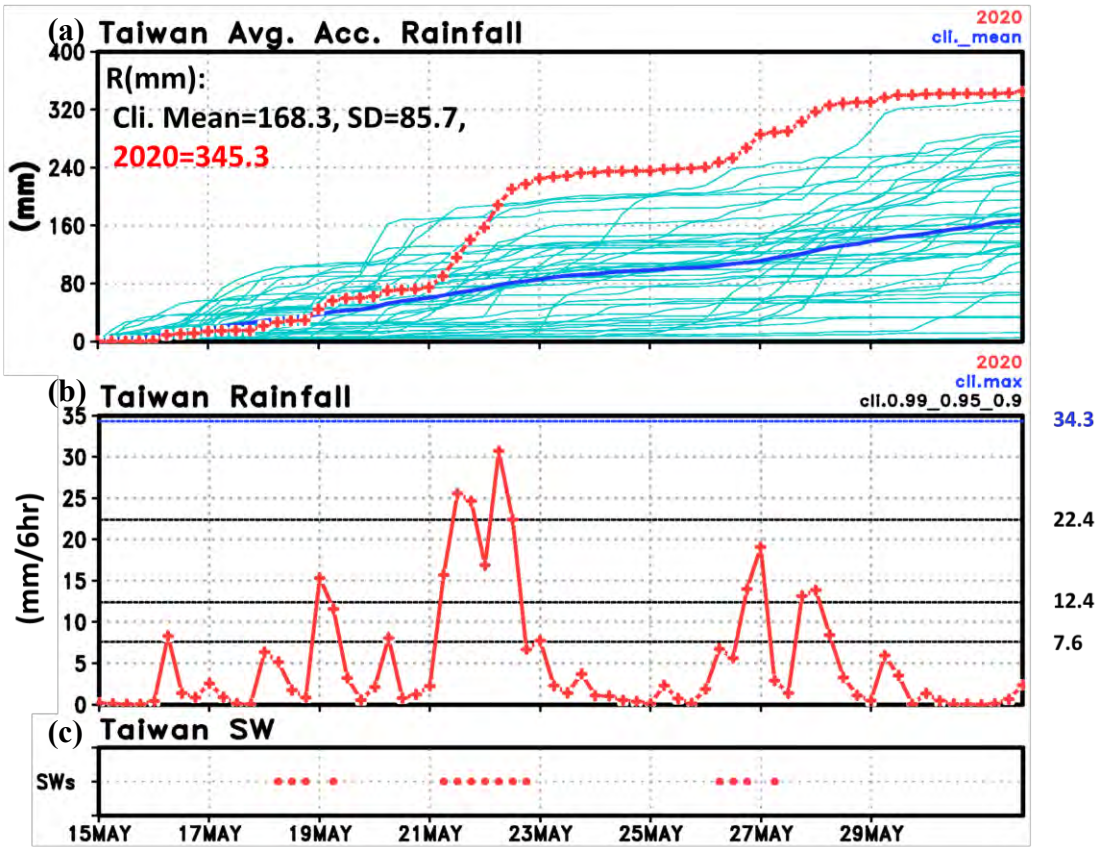

Figure 1: (a) The accumulated average rainfall (mm) of the 28 surface stations of the CWB (see Fig. 4a for locations) during FHMY (May 15–31) in 2020 (red) and 1979–2019 (green), with the climatological mean from 1979 to 2020 shown in blue. The total rainfall amounts during FHMY (with standard deviation) are denoted on the top left of the diagram. (b) The average 6-h rainfall intensity in Taiwan [unit: mm (6 h)$^{-1}$] for the same period in 2020 (red), with a blue line showing the maximum and 3 black lines from top to bottom representing the 99th, 95th, and 90th percentiles of the climatological rain intensity. (c) Red dots denote the occurrence of the SW flow event in southern Taiwan (SWs; see Chien et al. 2021 for definition) during FHMY in 2020.

Contribution of Thunderstorms to Frequency Changes in Hourly Extreme Precipitation Over China

Chan-Pang Ng [a], Qinghong Zhang [a,b], Wenhong Li [c] and Ziwei Zhou[a]

[a] *Department of Atmospheric and Oceanic Sciences, School of Physics, Peking University, Beijing, China*

[b] *HIWeather International Coordination Office, Chinese Academy of Meteorological Sciences, Beijing, China*

[c] *Earth and Ocean Sciences, Nicholas School of the Environment, Duke University, Durham, North Carolina*

Corresponding author: Chan-Pang Ng, cpng@pku.edu.cn

Abstract

The changes in extreme precipitation, particularly hourly extreme precipitation (HEP), under warmer climates have drawn much attention from academic and public bodies. Though **thunderstorms (TDs) are the primary contributor to extreme precipitation**, the prior studies have shown that the number of TDs decreased steadily while HEP has increased significantly in several areas over the past half-century in China. The role of TDs in changes in HEP remains largely unknown in China. Therefore, **the changes in extreme precipitation associated with TDs (TD-HEP) and the reasons behind them were explored.**

Based on the continuous records of hourly rainfall and thunder data sets, as well as the reanalysis data. **We found that the decreasing TDs trend was mainly caused by a decrease in nonextreme precipitation TDs and TDs without precipitation.** We analyze thunderstorm changes under various vertical wind shear (VWS) environments and their contribution to HEP occurrence for the first time in China. **The number of HEP events associated with thunderstorms (TD-HEP) increased significantly in southern China (SC) but decreased significantly in northeastern China (NEC) and east of the Tibetan Plateau (ETP).** Weak VWS thunderstorms accounted for 69.1% of TD-HEP in SC. Changes in the most unstable convective available potential energy and precipitable water (PW) in SC favored an increase in weak-VWS thunderstorms, which resulted in a rise of 2.35 h per warm season in overall "station-mean" TD-HEP events. As the primary contributor to HEP in NEC, moderate VWS thunderstorms decreased by 0.37 h per warm season due mainly to a reduction in PW, leading to a negative trend in TD-HEP events. Similarly, the decreasing TD-HEP occurrence on the ETP was due to a decrease of 1.12 h per warm season of moderate VWS thunderstorms. Studying the VWS environments of thunderstorms and changes therein under a warming climate can improve understanding of the changes in HEP in China.

Moreover, we discussed the different spatial scales of precipitation and found that the **HEP events' frequency changes were dominated by synoptic-scale precipitation**. **The results show here for the first time that changes in the HEP occurrence are dominated by changes in the duration of the Meiyu front system.** Further analyses reveal that the greater occurrence of HEP in northeastern China, the lower reach of the Yangtze River, and southern China during the warm season is largely due to a longer duration of the post-Meiyu I stage when Meiyu front stays in northern China, and meridional circulation dominates the eastern coastal area of China. These results improve our understanding of the changing behavior of extreme rainfall in China and shed light on preventing flash floods.

Three-dimensional Fujiwhara Effect

Kosuke Ito[a,†], Jae-Deok Lee[a,b], Soichiro Hirano[a], and Johnny C. L. Chan[c]

[a] *University of the Ryukyuys, Nishihara, Okinawa, Japan*

[b] *Kyungpook National University, Kongju, Korea*

[c] *City University of Hong Kong, Hong Kong, China*

Corresponding author: Kosuke Ito, itokosk@gmail.com

† Current affiliation: *Kyoto University*

When two or more tropical cyclones (TCs) coexist within a certain area, they directly or indirectly interact with each other depending on the separation distances, TC sizes, or the radii of gale-force winds. This effect was first documented by Fujiwhara (1921) and is generally referred to as the Fujiwhara effect or binary interaction. So far, many studies have been carried out using two-dimensional barotropic models showing binary TCs rotate and get closer around the center of the "mass" of the two vortices. However, they lack diabatic heating, which is important for the TC track in some cases (Yamada et al. 2016; Ito and Ichikawa 2021). In this study, we hypothesize that the motion of binary TCs can be modified by diabatic heating (DH) asymmetry associated with self-induced vertical wind. To demonstrate this hypothesis, a set of the idealized *f*-plane numerical experiments in the quiescent environment were conducted. Results show that the binary TC tracks are affected by the initial separation distance. When the separation distance of binary TCs is less than approximately 1000 km, a TC rotated counterclockwise about the binary center and finally merged as in the conventional study. However, when the separation distance is more than approximately 1000 km, binary TCs gradually repel each other. PV budget analysis shows that the horizontal advection vector appears to be greater than the diabatic heating contribution in the merging cases. On the other hand, the diabatic heating contribution served to separate binary TCs in the repulsion case. It is explained by the fact that the large-scale upper-level anticyclonic (due to outflows) and lower-level cyclonic circulations serve as the vertical wind shear for each TC, and the vertical wind shear tends to be directed to the rear-left quadrant from the direction of the counterpart TC, where the maxima of rainfall and diabatic heating are seen. This three-dimensional Fujiwhara effect was shown to be effective in the western North Pacific using the ERA5 reanalysis. It reveals the interaction can be seen for binary TCs separated by more than 1500 km.

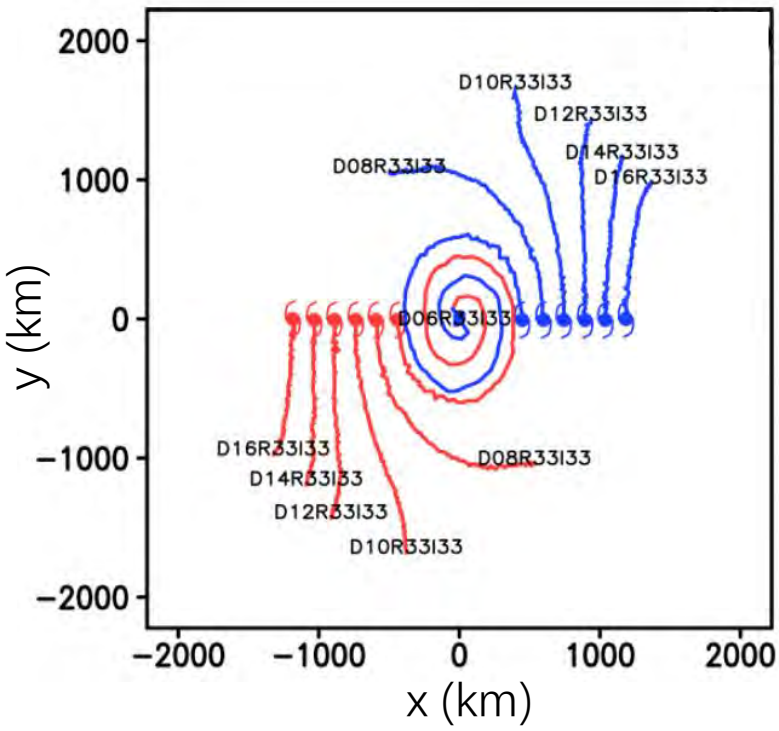

Fig. 1. The track of binary TCs in the idealized simulations. DXX means the initial separation distance of XX hundreds kilometers.

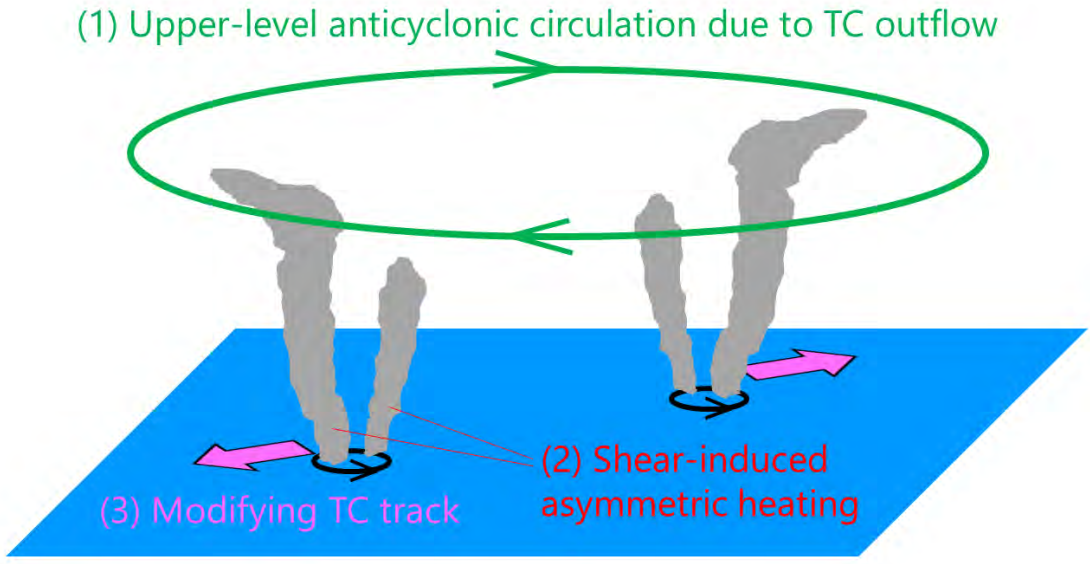

Fig. 2. Conceptual diagram of three-dimensional Fujiwhara effect.

A Tale of Two Rapidly-Intensifying Super Typhoons: Hagibis (2019) and Haiyan (2013)

I.-I. Lin[1*], Robert F. Rogers[2], Hsiao-Ching Huang[1], Yi-Chun Liao[1], Derrick Herndon[3], Jin-Yi Yu[4], Ya-Ting Chang[1], Jun A. Zhang[2, 5], Christina M. Patricola[6, 7], Iam-Fei Pun[8], and Chun-Chi Lien[1]

[1] *Dept. of Atmospheric Sciences, National Taiwan University, Taipei, Taiwan*

[2]*NOAA/AOML Hurricane Research Division, USA*

[3]*Cooperative Institute for Meteorological Satellite Studies, University of Wisconsin, USA*

[4]*Dept. Of Earth System Science, UC Irvine, USA*

[5]*Cooperative Institute for Marine and Atmospheric Studies, University of Miami, USA*

[6]*Department of Geological and Atmospheric Sciences, Iowa State University, USA*

[7]*Climate and Ecosystem Sciences Division, Lawrence Berkeley National Laboratory, USA*

[8]*Inst. of Hydrological and Ocean Sciences, National Central University, Taiwan*

*Corresponding to: Dr. I-I Lin (iilin@as.ntu.edu.tw)

Abstract

Devastating Japan in October 2019, Supertyphoon (STY) Hagibis was an important typhoon in the history of the Pacific. A striking feature of Hagibis was its explosive RI (rapid intensification). In 24 h, Hagibis intensified by 100 kt, making it one of the fastest-intensifying typhoons ever observed. After RI, Hagibis's intensification stalled. Using the current typhoon intensity record holder, i.e., STY Haiyan (2013), as a benchmark, this work explores the intensity evolution differences of these 2

high-impact STYs.

We found that the extremely high pre-storm sea surface temperature reaching 30.5° C, deep/warm pre-storm ocean heat content reaching 160 kJ cm^{-2}, fast forward storm motion of ~8 m s^{-1}, small during-storm ocean cooling effect of ~ 0.5° C, significant thunderstorm activity at its center, and rapid eyewall contraction were all important contributors to Hagibis's impressive intensification. There was 36% more air-sea flux for Hagibis's RI than for Haiyan's.

After its spectacular RI, Hagibis's intensification stopped, despite favorable environments. Haiyan, by contrast, continued to intensify, reaching its record-breaking intensity of 170 kt. A key finding here is the multiple pathways that storm size affected the intensity evolution for both typhoons. After RI, Hagibis experienced a major size expansion, becoming the largest typhoon on record in the Pacific. This size enlargement, combined with a reduction in storm translational speed, induced stronger ocean cooling that reduced ocean flux and hindered intensification. The large storm size also contributed to slower eyewall replacement cycles (ERCs), which prolonged the negative impact of the ERC on intensification.

Reference:

Lin, I-I*, Robert F. Rogers*, Hsiao-Ching Huang, Yi-Chun Liao, Derrick Herndon, Jin-Yi Yu, Ya-Ting Chang, Jun A. Zhang, Christina M. Patricola, Iam-Fei Pun, Chun-Chi Lien, A Tale of Two Rapidly-Intensifying Supertyphoons: Hagibis (2019) and Haiyan (2013), Bulletin of the American Meteorological Society, doi: 10.1175/BAMS-D-20-0223.1, 2021.

Exploring the dynamics of TC's inner core with the 30-second imagery of Himawari-8: mean circulation shift and wavenumber-1 disturbance that affect the rotation in the eye

Takeshi Horinouchi,[a] Satoki Tsujino,[b] Masahiro Hayashi, [b] Udai Shimada,[b] Wataru Yanase,[b] Akiyoshi Wada,[b] and Hiroyuki Yamada[c]

[a] *Faculty of Environmental Earth Science, Hokkaido University, Sapporo, Hokkaido, Japan*

[b] *Meteorological Research Institute, Tsukuba, Ibaraki, Japan*

[c] *University of Ryukuus, Naha, Okinawa, Japan*

Corresponding author: Takeshi Horinouchi, horinout@ees.hokudai.ac.jp

Dynamics of low-level flows in the eye of Typhoon Haishen (2020) in its late phase of intensification are investigated with a special rapid-scan observation of the Himawari-8 geosynchronous satellite conducted every 30 seconds. This is accomplished by deriving storm-relative atmospheric motion vectors at an unprecedentedly high spatiotemporal resolution by tracking clouds across five consecutive visible-light reflectivity. The overall low-level circulation center was situated several kilometers away from the storm center defined in terms of the inner edge of the lower part of eyewall clouds. The shift direction is rearward the storm translation, consistently with a numerical study of tropical cyclone (TC) boundary layer. Over the analysis period of 10 hours, azimuthal-mean tangential wind around this center was increased at each radius within the eye, and the rotational angular velocity was nearly homogenized. The instantaneous low-level circulation center is found to orbit around the overall circulation center at distances around 5 km. Its orbital angular speed was close to the maximum angular speed of azimuthal-mean tangential winds. This rotating transient disturbance is found to transport angular momentum inward, which explains the tangential wind increase and the angular velocity homogenization in the eye. These features are consistent with an algebraically growing wavenumber-1 barotropic instability proposed by Nolan and Montgomery (2000), whose impact on TC structures has not been explored. This instability enhances wavenuber-1 asymmetry in ring shaped vorticity, which can be induced by various processes such as translation, environmental shear, and exponential barotropic instability. Therefore, it may appear broadly in TCs to affect wind distribution in their eyes.

Publication: Horinouchi et al. 2023, Monthly Weather Review, 151(1), DOI: https://doi.org/10.1175/MWR-D-22-0179.1

Reference: Nolan and Montgomery (2000): https://doi.org/10.1175/1520-0469(2001)058<3243:TWOIAT>2.0.CO;2

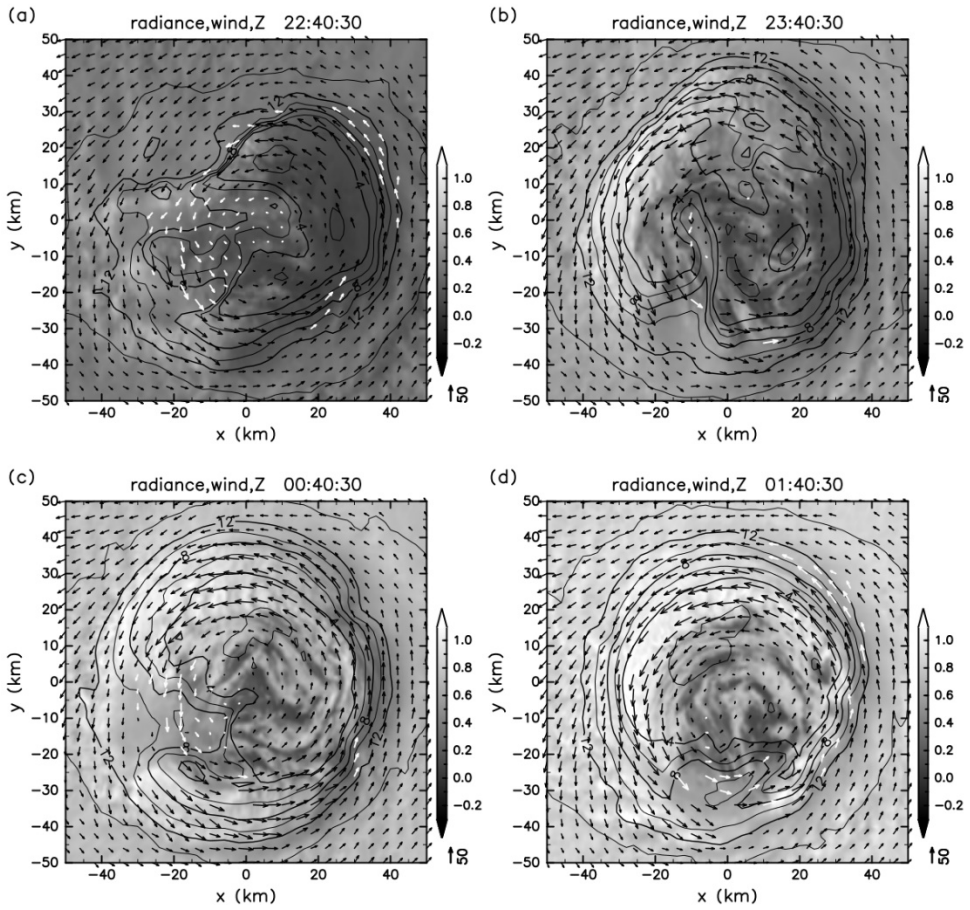

Fig. 1. Example of AMVs obtained at the Cartesian grid (vectors) overlayed on the reflectivity at the reference (central) time of tracking (gray shading), (a) 22:40, (b) 23:40, (c) 00:40, and (d) 01:40 UTC. The arrow on the lower-right corner of each panel indicates the length corresponding to 50 $\mathrm{m\ s^{-1}}$. Black arrows are AMVs used in this study, and white arrows are AMVs rejected by the post-processing in Appendix Db. Contours shows the cloud-top height obtained from Band-13 brightness temperature and the JRA-55 reanalysis (interval: 2 km). The coordinate origin is eyewall relative.

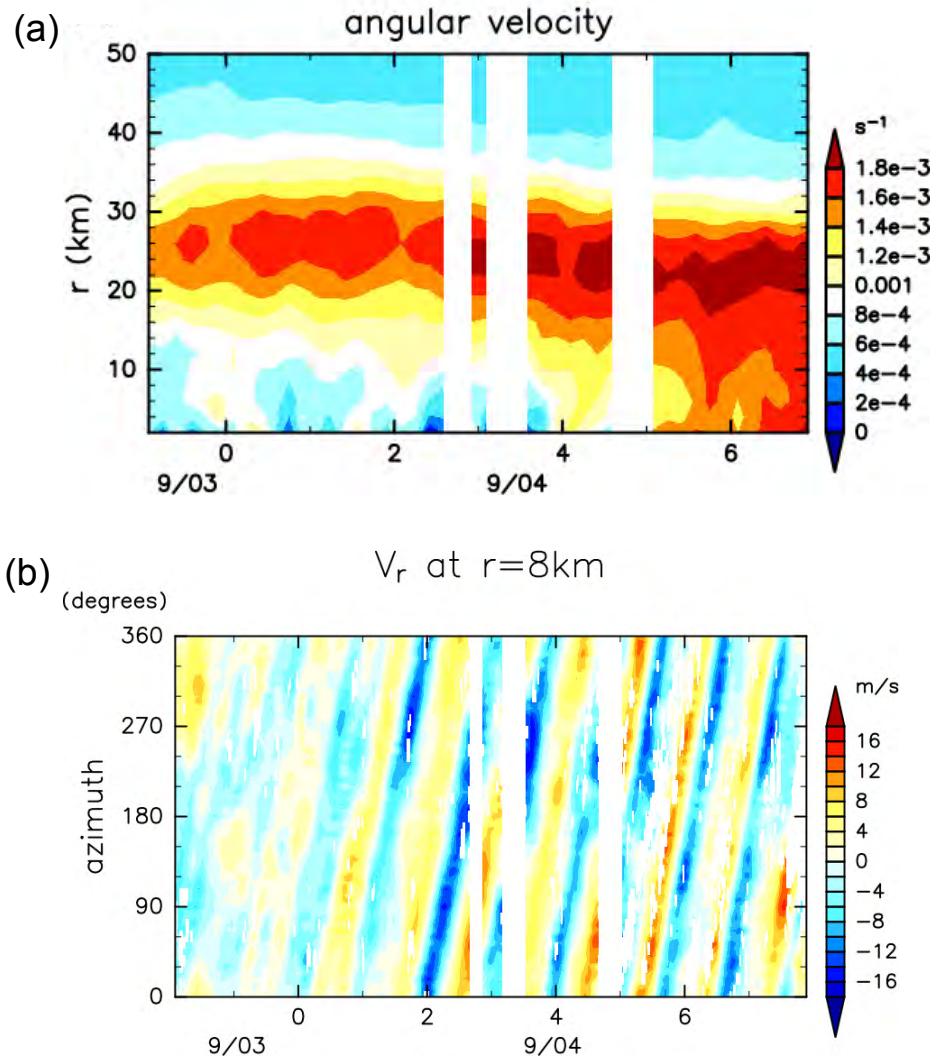

Fig. 2. (a) Azimuthal-mean and 10-minute running-mean angular velocity with respect to the circulation relative origin. The abscissa is date and time in UTC. (b) 10-minute running-mean radial wind u at the radius of 8 km with respect to the low-level circulation (circulation relative coordinate). Values are shown where AMVs are obtained originally (before running mean). The ordinate is the azimuth θ (counterclockwise from the east).

Multiscale Characteristics of the Development of Weak Tropical Cyclones

Robert Rogers[1], Michael Fischer[1,2], Trey Alvey[1,2]

[1]NOAA/AOML Hurricane Research Division, Miami, FL
[2]Cooperative Institute for Marine and Atmospheric Studies, University of Miami, Miami, FL

Characterizing the inner core structure of weak tropical cyclones (weak TCs; defined here as ranging in intensity from pre-tropical depressions to tropical storms), at the onset of genesis or intensification (termed "development" here) is an important factor in identifying whether development is likely to occur. The formation of a deep cyclonic circulation that reaches the surface is a key step in this development process. Such a circulation can form either locally, in the case of genesis, or through the alignment of a low- and mid-level circulation, in the case of intensification of a tropical depression or storm. Understanding how this circulation forms is challenging, however, since weak TCs have a weak rotational constraint, are dominated by divergent flow, and are more vulnerable to hostile environments (e.g., dry air, vertical shear) than stronger TCs. For these reasons weak TCs occupy a different parameter space of intensification processes than stronger TCs.

This work will present aircraft observations of the structural characteristics of weak TCs that undergo development and compare them with those that do not. Emphasis will be placed on the structures of cyclonic circulations; the distribution of thermodynamic parameters and their variation on the mesoscale; and the resultant precipitation structure, divergence, and mass flux profiles. Notable differences in these structures will point toward physical hypotheses that explain why some weak TCs develop while others do not.

Impact of Soil Moisture Initialization on Poleward-moving Tropical Cyclone Forecasts

Jinyoung Park and Dong-Hyun Cha

Ulsan National Institute of Science and Technology, Ulsan, South Korea

Corresponding author: Dong-Hyun Cha, dhcha@unist.ac.kr

Tropical cyclones (TCs) moving poleward to mid-latitudes in the western North Pacific (WNP) basin are complex to forecast in terms of their track since their paths are largely influenced by the upper-level synoptic fields in subtropical and mid-latitude regions (i.e., western North Pacific subtropical high; WNPSH, mid-latitude trough, and jet stream). Therefore, forecast performances are especially poor when TCs approach the East Asian region. It is known that soil moisture (SM) modulates the total available energy into sensible heat fluxes (SHF) and latent heat fluxes (LHF) at the land surface, which play key roles in land-atmospheric feedback. This land surface process is necessary for accurate weather forecasts or climate predictions because soil moisture can affect atmospheric temperature, clouds, and even precipitation through the land-atmosphere interaction (e.g., evapotranspiration; ET). Therefore, we used two types of SM data for the initial condition of the Weather Research and Forecasting (WRF) model to investigate the sensitivity of the TC forecasts to the SM initialization. The Global Land Data Assimilation System (GLDAS) Version 2.1 and the European Centre for Medium-Range Weather Forecasts (ECMWF) Reanalysis v5 (ERA5) were selected in this study, and we examined the effect of different SM initial data on forecast performances for three recent TC cases that made landfall in South Korea. The results showed that ERA5 data had wetter SM contents than GLDAS data over the entire simulations except for some areas located south of Mongolia. Also, TC intensity forecast performances were similar in both runs, while TC track forecast performances were improved in the experiments with GLDAS data. The differences in track forecasts between the two runs were more significant during the landfall period. In addition, in the experiments with ERA5 data, simulated TCs tended to move westward compared to the experiments with GLDAS data due to the strengthened interaction between simulated TCs and the mid-latitude trough. Therefore, this study showed the notable impact of initial SM data on short- to mid-term poleward-moving TC forecasts.

Typhoon Rapid Intensification with 200 PVU Convective Potential Vorticity Tower in Numerically Simulated Supertyphoon Haiyan (2013)

Hung-Chi Kuo[a] and Satoki Tsujino[b]

[a] *Department of Atmospheric Sciences, National Taiwan University, Taipei, Taiwan*

[b] *Meteorological Research Institute, Tsukuba, Japan*

Corresponding author: Hung-Chi Kuo, kuo@as.ntu.edu.tw

The present study examines the inner core dynamics of Supertyphoon Haiyan (2013) undergoing rapid intensification (RI) with a 2-km resolution cloud-resolving model simulation from the non-hydrostatic Cloud-Resolving Storm Simulator (CReSS). The results highlight the important roles of the potential vorticity (PV) tower and PV-mixing processes around the inner core on RI through a boundary layer (BL) linkage. At the low level in the simulated storm, the PV field reveals an elliptical and polygonal-shaped eyewall during RI onset. Then, the PV changes to a more monopole shape in the lower troposphere during the later period of RI. The PV budget analysis confirms the importance of PV mixing at this stage, i.e., the asymmetric transport of diabatically generated PV to the storm center from the eyewall and the ejection of PV filaments outside the eyewall. The piecewise PV inversion (PPVI) further indicates that PV mixing accounts for about 50% of the central pressure fall during RI onset. The decrease of central pressure enhances the symmetric BL radial inflow. The radial inflow increases tangential wind speed through the inward advection of absolute angular momentum. The enhanced radial inflow leads to the contraction of the radius of maximum wind (RMW). The nonlinearity of the BL inflow forms a near shock structure, i.e., the dramatic decrease of radial inflow in a short distance forms a strong BL updraft up to 20 m s^{-1} strength. Moreover, the dramatic decrease of the radial inflow leads to a significant decrease in the tangential wind with very large shear vorticity. The shock formation region is thus with a strong updraft and large vorticity coupled together to form the convective PV tower inside the RMW. Our simulation with 500 m resolution produces a PV tower of 200 PVU. The simulation highlights the importance of PV mixing to enhance the nonlinear BL inflow to form the near shock structure in radial flow and the associated 200 PVU convective PV tower. The results also highlight the symmetric structure during the RI. The simulation is also in general agreement with the aircraft observations of the axisymmetric PV evolution of Hurricane Patricia (2015).

Aircraft observation of the inner core of rapidly intensifying Typhoon Nanmadol (2022)

Kazuhisa Tsuboki[a,b], Hiroyuki Yamada[c,b], Kosuke Ito[c,b], Soichiro Hirano[c], Tadayasu Ohigashi[d], Satoki Tsujino[e], Takeshi Horinouchi[f,b], Taiga Tsukada[f], Masashi Minamide[g], Takeshi Enomoto[h], Masaya Kato[a], Sachie Kanada[a], Kensaku Shimizu[i], and Norio Nagahama[i],

[a]*Institute for Space-Earth Environmental Research, Nagoya University, Nagoya, Japan*
[b]*Typhoon Science and Technology Research Center, Yokohama National University, Yokohama, Japan*
[c] *Faculty of Science, University of the Ryukyus, Nishihara, Okinawa, Japan*
[d]*National Research Institute for Earth Science and Disaster Resilience, Tsukuba, Japan*
[e]*Meteorological Research Institute, Japan Meteorological Agency, Tsukuba, Japan*
[f]*Graduate School of Environmental Science, Hokkaido University, Sapporo, Japan*
[g]*Department of Civil Engineering, The University of Tokyo, Tokyo, Japan*
[h]*Disaster Prevention Research Institute, Kyoto University, Kyoto, Japan*
[i]*Meisei Electric CO., LTD., Isezaki, Japan*

Corresponding author: Kazuhisa Tsuboki, tsuboki@nagoya-u.jp

Typhoons cause severe disasters in East Asian countries including Japan. Accurate estimation of intensity and quantitative forecast of typhoon are the most important for disaster mitigation. However, a significant uncertainty is present in intensity estimation and almost no improvement of intensity forecast has been made in the last decades. In the intensity forecast, rapid intensification is a big problem. Concentric eyewall structure of inner core is a problem in intensity estimation. To solve these problems, in situ observation using an aircraft is indispensable. T-PARCII (Tropical cyclone-Pacific Asian Research Campaign for Improvement of Intensity estimations/forecasts) project has been performing in situ aircraft observations of typhoons since 2017. The first phase of T-PARCII ended in 2021 and the second phase that is supported by Grant-in-Aid for Scientific Research (S) has started in July 2021. The objective of the second phase is a mechanism of rapid intensification and thermodynamic structure of concentric eyewalls in addition to accurate measurements and predictions of typhoon intensity.

Using the dropsonde system on the Gulfstream IV (G-IV) jet, the T-PARCII team performed dropsonde observations of Supertyphoon Nanmadol (2022) on September 16 and 17, 2022. In each day, 25 dropsondes were launched in the eye and the surrounding regions of the typhoon. All dropsonde data were transmitted to the Japan Meteorological Agency from the aircraft in real time.

The characteristics of Nanmadol are as follows. Genesis of the storm occurred at a high latitude of 22.4 °N. Nanmadol reached the supertyphoon intensity at a high latitude after rapid intensification. Its inner core showed a concentric eyewall structure. Nanmadol made landfall over southern Kyushu with the fourth lowest central pressure since 1951 and caused severe flooding in Kyushu. Satellite observations showed the concentric eyewall structure over the Pacific Ocean and the ground-based radars also showed that the structure was maintained until the storm approached lands.

The radar of G-IV (Fig. 1) showed that the diameter of the eye was approximately 20 km and the inner eyewall surrounded the eye. The outer eyewall is relatively obscure,

but it may be present outside of the moat. Figure 2 shows wind speed profiles observed at the maximum wind region in the inner eyewall on the two days. The wind speeds are almost uniformly strong up to around 300 hPa. This may correspond to almost upright structure of the inner eyewall indicated by visual observations. An increase in wind speed of more than 15 m/s occurred below a height of 300 hPa during 20 h, indicating that the typhoon was intensified rapidly during the two days.

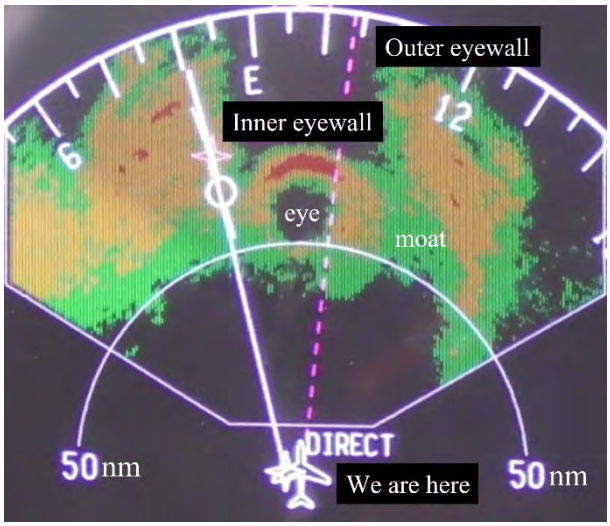

Figure 1: Eye of Nanmadol and the concentric eyewall structure observed by the radar of G-IV at 01:35 UTC on September 17, 2022.

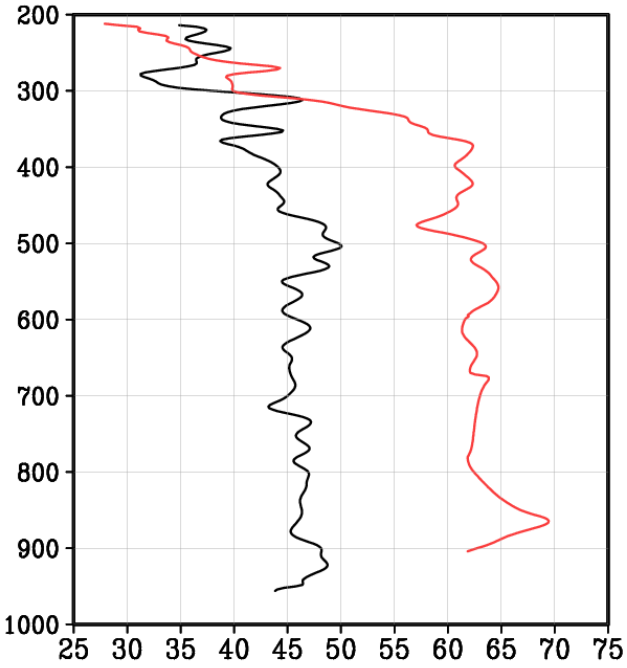

Figure 2: Profiles of wind speed (m/s) in pressure coordinates (hPa) at 04:54 UTC on September 16, 2022 (black solid line) and 00:48 UTC on September 17, 2022 (red solid line).

Tropical Cyclone Forecast Error Statistics Stratified by Environmental and Structural Metrics

Authors: Alvey, Hazelton, Alaka, Gramer

It is well established that the interplay between internal tropical cyclone (TC) characteristics and the external environment can modulate TC intensity and track evolution. Previous studies have demonstrated that different environmental conditions like moderate vertical wind shear (5–10 m/s) can also affect the predictability of tropical cyclone track and intensity resulting in larger forecast errors on average. The potential linkage between varying environmental and storm-scale characteristics on TC forecast errors, however, has only been quantified in a limited number of studies typically focusing on individual cases.

In this study, 3-year model retrospectives from the Hurricane Weather Research and Forecasting (HWRF) model and its successive counterpart, the Hurricane Analysis and Forecast System (HAFS), a high-resolution nested-FV3 modeling system, are used to provide an extensive dataset of real TCs in different modeling systems. Track and intensity forecast errors are stratified by environmental conditions like vertical wind shear and mid-tropospheric humidity. Additional stratifications of forecast errors by internal storm dynamic metrics like vortex tilt direction and magnitude reveal that misaligned storms have greater forecast errors biased spatially in the direction of the shear vector.

How does cloud–radiation feedback promote convective upscale development?

James Ruppert[a] and Emily Luschen[a]

[a] *School of Meteorology, University of Oklahoma, Norman, Oklahoma, USA*

Corresponding author: James Ruppert, jruppert@ou.edu

Mounting evidence underscores the critical role of cloud–radiation feedback in promoting the upscale development of tropical convection, which manifests itself in the maintenance of the Madden–Julian Oscillation and in the genesis of tropical cyclones (TCs). While moist static energy budgets and balanced circulation frameworks have helped advance this story, we still have yet to understand how this feedback acts in the context of convective-scale behavior. Furthermore, we have yet to link this feedback to extant theoretical frameworks for moist convection, including those for TCs in particular. Here we share our efforts to address these questions by leveraging a series of convection-resolving model simulations, including two tropical cyclone case studies (Typhoon Haiyan, 2013; Hurricane Maria, 2017) and a series of non-rotating self-aggregation simulations. We've leveraged these two distinct frameworks to probe the response of convective behavior to the switch-off/switch-on of cloud–radiation interaction. Our results suggest a novel finding: the longwave feedback due to widespread areas of stratiform precipitation is especially important, which acts to suppress the formation of downdrafts and midlevel dry-air import (more on this in Emily Luschen's presentation). This kinematic response provides a potential link to extant TC genesis theories, given that downdrafts are linked to *ventilation* of the column. It also links to Neelin and Held (1987)'s gross moist stability (GMS) concept, which is a quantity originating from theoretical frameworks that characterizes the tendency of moist convective systems to intensify (or not) via their own thermodynamically coupled circulation. We discuss some of these interpretations and their implications here.

The Stratiform Radiation Effect on Tropical Cyclone Genesis

Emily Luschen [a], James Ruppert [a], Shun-Nan Wu[a], and Yunji Zhang[b]

[a] *University of Oklahoma, Norman, OK, USA*

[b] *Penn State University, State College, PA, USA*

Corresponding author: Emily Luschen, Emily.W.Luschen-1@ou.com

Moistening the environment of a precursor storm is a necessary step for tropical cyclone (TC) genesis. Cloud-radiative forcing has been implicated in accelerating this process, but we do not fully understand how. Downdrafts in developing TCs are directly associated with midlevel ventilation, which opposes the column moistening process. There is a growing consensus from observations that the areal growth of stratiform precipitation is a key precursor to TC genesis and intensification. This observational finding presents a conundrum, given that stratiform precipitation is directly tied to downdrafts, and hence ventilation. Therefore, we hypothesize that the cloud-radiative effect within stratiform cloud regions weakens downdrafts, allowing the environment to moisten more easily. To test this hypothesis, we analyzed output from Weather Research and Forecasting (WRF) model simulations of Super Typhoon Haiyan. Two tests were run with one including cloud-radiative feedback (CTL) and the second without it (NCRF). Precipitation categorization indicates that stratiform cloud-radiative heating dominates that of deep convective regions in terms of areal coverage. The analysis further shows CTL tests have less downward vertical mass flux in the mid to lower troposphere, indicating weaker (and/or fewer) downdrafts, than that of the NCRF tests, with the greatest differences being in stratiform regions. These findings support our hypothesis that cloud-radiative effects in the stratiform regions weaken downdrafts in developing TCs, in turn allowing the environment to moisten more easily. Future work will conduct new experiments to isolate the specific role of (or impact of excluding) the radiative forcing due to stratiform clouds. Understanding the importance of the stratiform radiation effect on TC genesis could provide insight into why some precursor storms develop and intensify while others do not.

Role of Advection of Parameterized Turbulence Kinetic Energy in Idealized Tropical Cyclone Simulations

Xiaomin Chen[a, b†] and George H. Bryan[c]

[a]*University of Alabama in Huntsville, Huntsville, AL*

[b]*NOAA/AOML Hurricane Research Division, Miami, FL*

[c]*National Center for Atmospheric Research, Boulder, CO*

Corresponding author: Xiaomin Chen, xc0011@uah.edu

†Current address: University of Alabama in Huntsville.

Accurately parameterizing turbulent processes in numerical weather prediction models is crucial for advancing the tropical cyclone forecast skill. One important assumption in the design of planetary boundary layer (PBL) parameterizations is horizontal homogeneity. Consistent with this assumption, PBL schemes with predictive equations for subgrid turbulence kinetic energy (TKE) typically neglect advection of TKE. However, tropical cyclone boundary layers are inhomogeneous, particularly in the eyewall. To gain further insight, this study examines the effect of advection of TKE using a modified Mellor-Yamada-Nakanishi-Niino (MYNN) PBL scheme in idealized tropical cyclone simulations. The analysis focuses on two simulations, one that includes TKE advection (CTL) and one that does not (NoADV). Results show that with the inclusion of TKE advection, the simulated tropical cyclone is stronger and more compact. Interestingly, the relatively large TKE in the eyewall above 2 km in CTL (Fig. 1a), a structure observed in previous airborne Doppler radars, is found predominantly attributable to vertical advection of TKE. In comparison, buoyancy production of TKE is negative in this region in both simulations; thus, buoyancy effects cannot explain observed columns of TKE in tropical cyclone eyewalls. Both horizontal and vertical advection of TKE tends to reduce TKE and vertical viscosity in the near-surface inflow layer, particularly in the eyewall of tropical cyclones (Fig. 1f). Importance of eyewall turbulent mixing in TC intensification and recommendations for improvements of TKE-based PBL schemes in hurricane conditions will be discussed.

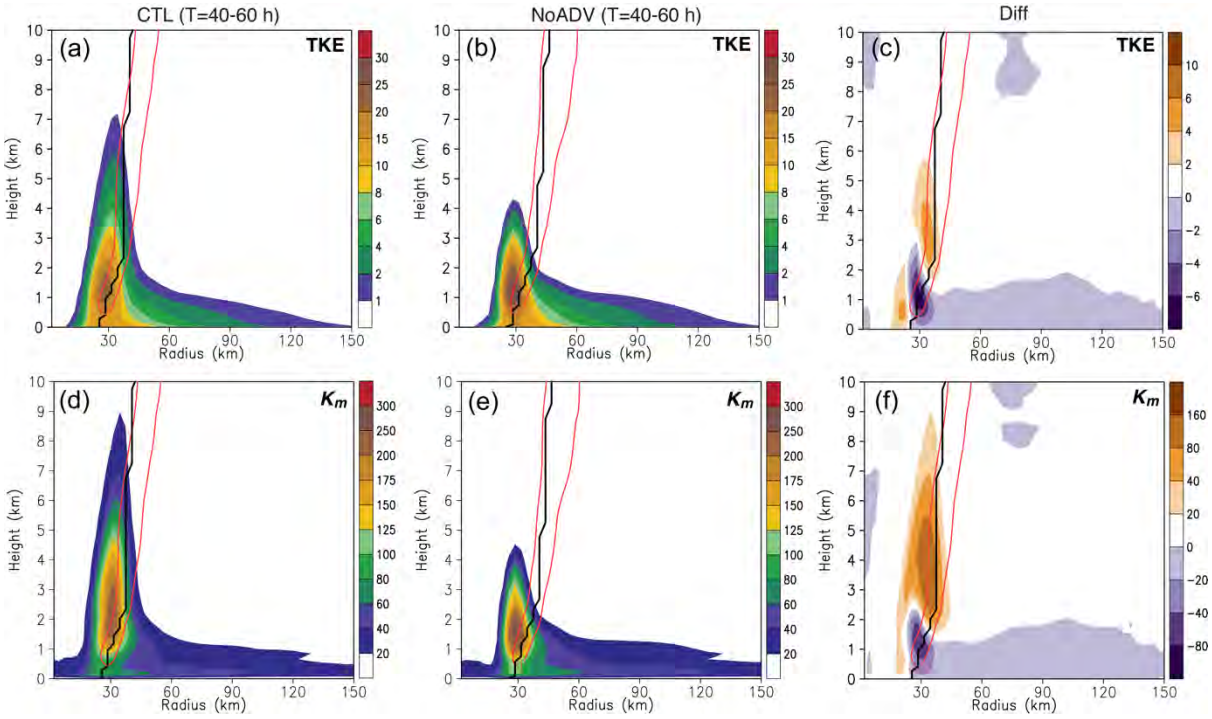

Fig. 1. (a), (b) Radius–height distribution of azimuthally averaged subgrid TKE (shading, m^2 s^{-2}) over t = 40–60 h for the CTL and NoADV experiments, respectively. (c) The difference in the distribution of TKE between the two experiments (i.e., CTL – NoADV). (d)–(f) As in (a)–(c), but for eddy viscosity K_m (shading, m^2 s^{-1}). In each panel, the red contour denotes w =1 m s^{-1} and the black line denotes the radius of maximum wind (RMW). In (c) and (f), the RMW and w contours are from CTL.

Evaluation of Vortex Structure and Near-surface Winds in WRF Simulations of Typhoon Faxai (2019)

Takuya Takahashi[a,b], David S. Nolan[a], and Brian McNoldy[a]

[a] *Univ. of Miami Rosenstiel School, Miami, Florida, United States*

[b] Japan Meteorological Agency*, Minato City, Tokyo, Japan*

Corresponding author: Takuya Takahashi, ttakahashi@earth.miami.edu

The accuracy of numerical tropical cyclone (TC) forecasts has improved significantly with increasing spatial resolution and the improved representation of model physics. In particular, previous studies have confirmed that strong TCs can be represented much more accurately with the grid spacings as fine as ~ 1 km. However, point-by-point forecasts of strong surface winds of landfalling TCs based on numerical models have not yet been realized. Several issues need to be addressed for such point-by-point forecasts, especially for hurricane-force winds. One such issue is the limited number of ground-based validations of numerical expressions for TCs making landfall with hurricane-force winds.

Recent studies have evaluated the accuracy of near-surface wind fields in Weather Research and Forecasting (WRF) model simulations for landfalling hurricanes with different planetary boundary layer (PBL) parameterizations, and have shown that the simulated near-surface wind fields are quantitatively consistent with observations. However, the accuracy of simulated surface winds directly caused by eyewalls during typhoons or hurricanes has not been evaluated comprehensively. In addition, it is not clear which dynamical components in TCs are crucial for accurate surface wind forecasts during such “direct hit” events. To address the above two points, we conducted a detailed comparative analysis between WRF simulations and observations of Typhoon Faxai (2019). It was the strongest typhoon that made landfall over the Kanto region in Japan in recorded history. With a highly symmetric inner core structure during landfall, Faxai set records for the highest winds at many stations. We will present the result of the observational analysis of the dynamical decay of the vortex over the PBL, the PBL wind profile, and the surface winds based on the combination of C-band radar dual-doppler analysis and spatially dense surface wind observations, and compare it with WRF simulations. We show how different surface roughness lengths affect the simulated vortex structure over the PBL (Fig. 1), and the surface winds (Fig. 2). In addition, we discuss the dynamical characteristics of the inner core PBL jet that are key for accurate simulation of surface winds, and compare the WRF simulations with different PBL parameterizations.

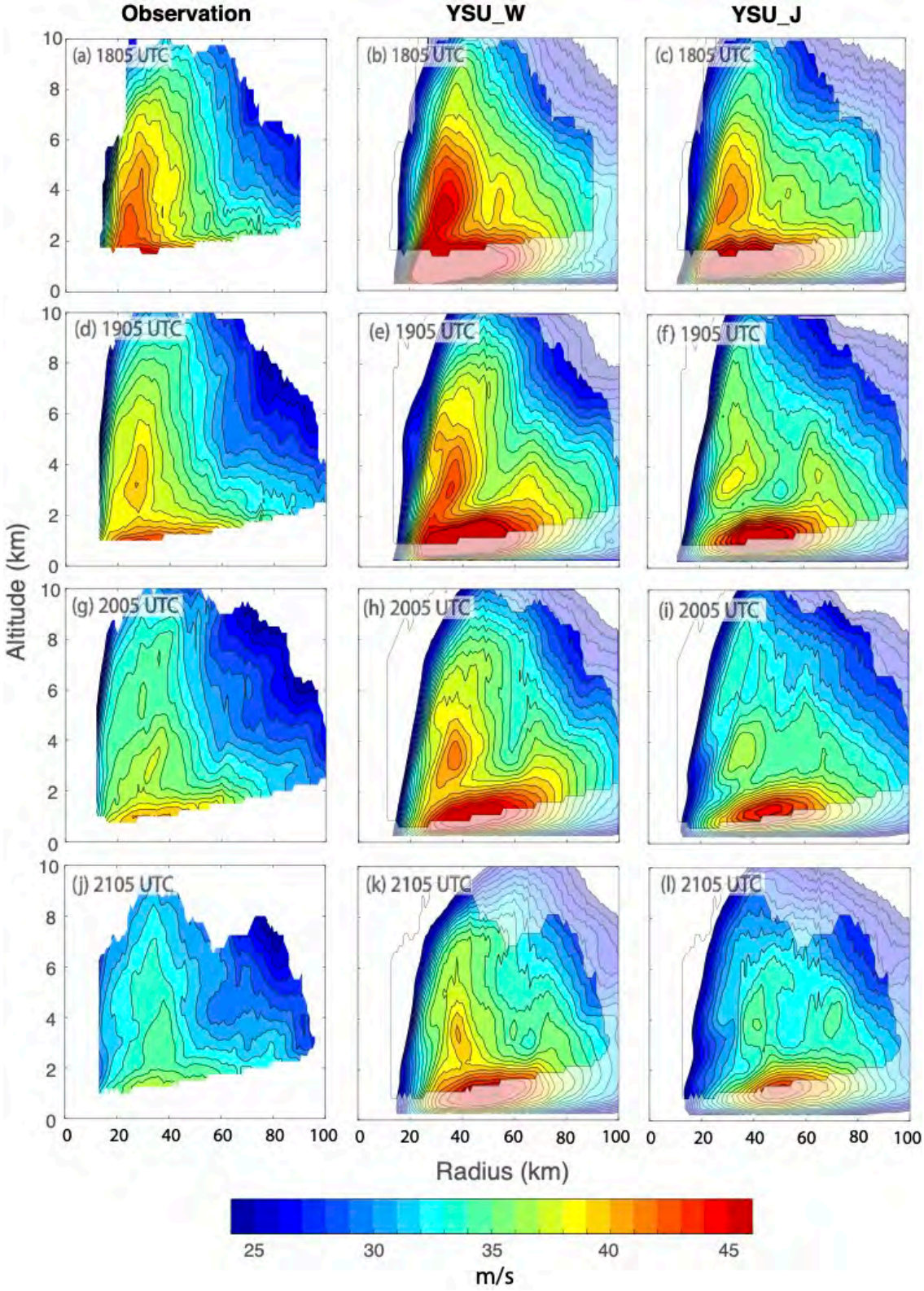

Fig. 1 The dynamical decay of the vortex during landfall over the PBL. The colored shadings show axisymmetric tangential winds. The left, middle, and right columns show the observation (dual-doppler analysis), the WRF simulation with the default surface roughness length, and the WRF simulation with enhanced surface roughness length, respectively.

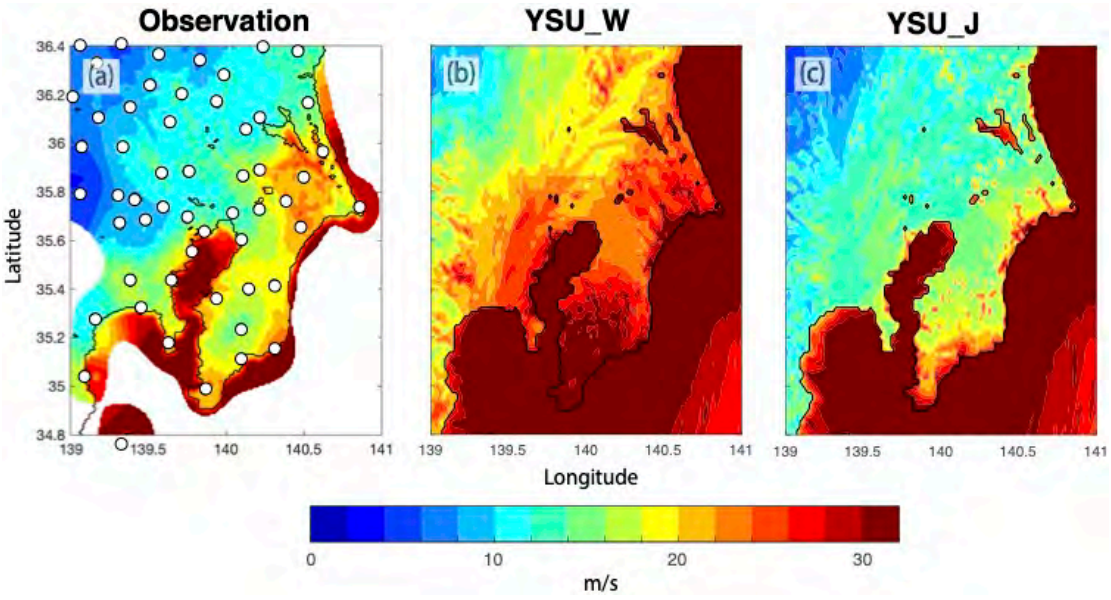

Fig. 2 The wind swath (map of the maximum 10-minute sustained wind) during Faxai. (a) is the analysis based on surface observation (station locations are shown as black circles). (b) and (c) are the results of WRF simulation with original, and enhanced surface roughness length, respectively.

Tropical Cyclone Precipitation Structure Response to Sea Surface Temperature Warming in Idealized WRF

Alyssa M. Stansfield[1] and Kristen L. Rasmussen[1]

[1] *Department of Atmospheric Science, Colorado State University, Fort Collins ,CO, USA*

Corresponding author: Alyssa M. Stansfield, alyssa.stansfield@colostate.edu

Extreme precipitation from tropical cyclones (TCs) often results in fatalities and expensive property damage in both coastal locations and hundreds of miles inland. Climate models project that TC precipitation rates will increase in the future due to climate change, but little is known about how the precipitation structures within TCs may be impacted. TC precipitation comes from the inner core and outer rainbands, and changes in these precipitation structures may shift the distribution of precipitation within TCs, which in turn could impact flooding patterns. Recent observational studies found a decreasing trend in TC inner core precipitation and an increasing trend in TC outer rainband precipitation; however, previous modeling studies on TC precipitation and climate change have used coarse resolution models that cannot resolve TC precipitation structures. This work uses idealized Weather Research and Forecasting (WRF) simulations with an inner nest with 1.67 km grid spacing to explore how three-dimensional TC precipitation structures change with sea surface temperature (SST) warming. An analysis of storm modes, which was originally developed for mesoscale convective systems, will be applied on TCs for the first time.

Effects of low salinity water on air-sea interaction under typhoon Chaba (2016)

Woojin Cho [a], Jinyoung Park [a,], and Donghyun Cha[a]

[a] *Department of Urban and Environment, Ulsan National Institute of Science and Technology, Ulsan, Republic of Korea*

Corresponding author: Donghyun Cha, dhcha@unist.ac.kr

One of the causes of the weakening of typhoons moving into mid-latitudes is the decrease in sea surface temperatures (SSTs) at high latitudes. In 2016, the track of Typhoon Chaba passed over the East China Sea where the SST was abnormally high; hence, Chaba maintained a relatively high intensity. The Changiang River discharge peaked in early July and gradually decreased before typhoon Chaba approached. Conversely, the salinity in the East China Sea was minimal in early August and then increased. Moreover, the positive anomaly area of SST in the East China Sea matched the negative anomaly area of sea surface salinity related to Changiang river discharge. Changiang freshwater inflow and SST in the East China Sea had 30 days lagged positive correlation. Therefore, based on these, we determined that the increase in the East China Sea's SST was associated with the outflow of the Changiang River. In this study, we investigated the SST warming due to ocean stratification caused by Changiang diluted water and analyzed the following typhoon-ocean interaction after the warming using a coupled atmosphere-ocean modeling system. The freshwater inflow caused ocean stratification in the East China Sea and formed a barrier layer, and this barrier layer inhibited the vertical mixing and energy transport between the surface and the thermocline and led to sea surface warming. As a result, the stabilized ocean structure restricted sea surface cooling induced by typhoon-forced upwelling and turbulent mixing. In conclusion, this study discovered the physical mechanism that maintains the intensity of TCs moving northward using ocean-atmosphere couple modeling, which may be used to improve the performance of ocean-atmosphere couple modeling in predicting the intensity of TCs.

An Insight Into the Microphysical Attributes of Northwest Pacific Tropical Cyclones

Balaji Kumar Seela[1,2], Jayalakshmi Janapati[1], Pay-Liam Lin[1], Meng-Tze Lee[3]

[1]*National Central University, Taoyuan,Taiwan*,

[2]*Academia Sinica,Taipei, Taiwan*,

[3]*McGill University, Canada*

Corresponding author: Pay-Liam Lin, tliam@atm.ncu.edu.tw

Northwestern Pacific (NWP) tropical cyclones (TCs) impose a severe threat to the life and economy of the people living in East Asian countries. The microphysical features, mainly the raindrop size distributions (RSD) of TCs that improve the modeling simulation and rainfall estimation algorithms, are limited to case studies, and an extensive understanding of TCs' RSD is still scarce over the northwest Pacific. Here, we examine a comprehensive outlook on disparities in microphysical attributes of NWP TCs with radial distance and storm type, using sixteen years of disdrometer, ground-based radar, and reanalysis datasets in north Taiwan. We find that dominant stratiform precipitation in the inner rainbands leads to the occurrence of more bigger drops in the inner rainbands than the inner core and outer rainbands. Moreover, a decrease in mass-weighted mean diameter and rainfall rate with radial distance is associated with a reduction in moisture availability for various circumstances, and this association is deceptive in intense storms. Our findings give an insight into crucial processes governing microphysical inequalities in different regions of NWP TCs, with implications for the ground-based and remote-sensing rainfall estimation algorithms.

Observed Relationships between Tropical Cyclone Vortex Height, Intensity, and Intensification Rate

Alexander J. DesRosiers, Michael M. Bell, Philip J. Klotzbach, Michael S. Fischer, Paul D. Reasor

As a tropical cyclone (TC) intensifies, the tangential wind field expands vertically and increases in magnitude. Observations and modeling support vortex height as an important TC structural characteristic. The TC-RADAR dataset provides kinematic analyses for calculation of the height of the vortex (HOV) in observed storms. Analyses are azimuthally-averaged with tangential wind values taken along the radius of maximum winds. A threshold-based technique is used to determine the HOV. A fixed threshold HOV strongly correlates with current intensity. A dynamic HOV metric quantifies vertical decay of tangential wind with reduced dependency on intensity. Statistically significant differences are present between dynamic HOV values in groups of steady-state, intensifying, and rapidly-intensifying cases categorized by subsequent changes in pressure. A tall vortex is always observed in cases meeting a pressure-based rapid intensification definition. Taller vortices are also evident with slower intensification. Results suggest HOV may be a helpful predictor for TC intensification.

Tropical Storm Aere (2022) Intensification and Decaying Under Upper-Level Cut-off Low Forcing

Tamon Watanabe [a] and Hiroyuki Yamada [a]

[a] *University of the Ryukyus, Nishihara, Okinawa, Japan*

Corresponding author: Tamon Watanabe, k228343@eve.u-ryukyu.ac.jp

The intensification and decaying of Tropical Storm Aere (2022) in the western North Pacific under the forcing of an upper-level cut-off low (COL) is investigated. Aere formed to the east of Philippines at 1800 UTC 30 June, moved northward, and passed over the Okinawa Island around 1200 UTC 02 July. During this period, this COL moved from northwest to southeast around Aere anticlockwise and was weakened by diabatic heating. We carried out radiosonde observations every 3 hours for thirty-six hours during the passage of the storm in collaboration with the Meteorological research Institute of the Japan Meteorological Agency. We succussed in observing the vertical structure in and around the storm. The tropical cyclone (TC)-COL interaction is investigated using ECMWF reanalysis (ERA-5) and radiosonde data. First, we calculated a vorticity budget to estimate the vortex evolution and found that vorticity between lower and middle troposphere increased until 1800 UTC 01 July due to stretching and vertical advection in the lower to middle troposphere. This suggests that the vortex enhanced by deep convection that was identified in Himawari-8 infrared images. Next, to investigate TC-COL interaction, we calculated eddy momentum flux convergence (EFC, Molinari and Vollaro 1990) at 200 hPa (i.e., a TC outflow layer). Time series of EFC (Fig.1) shows a peak of convergence greater than 30 m s^{-1} day^{-1} during intensification, suggesting cyclonic spin-up in the TC's outflow layer. In fact, the radial-vertical distribution of the radial wind speed (Fig. 2) shows the enhancement of the mid-level inflow, which led the deep-layer spin-up due to the radial advection of angular momentum. 9 Finally, the decaying process of this storm is discussed using radiosonde data. The sounding profile at 1200 UTC 02 July, near the time of peak storm intensity, shows a clear subsidence inversion layer around 600 hPa. This suggests the penetration of a dry air brought by COL from the western quadrant of storm. The presence of such dry air may have suppressed convective heating and thus prevented the further development of the storm.

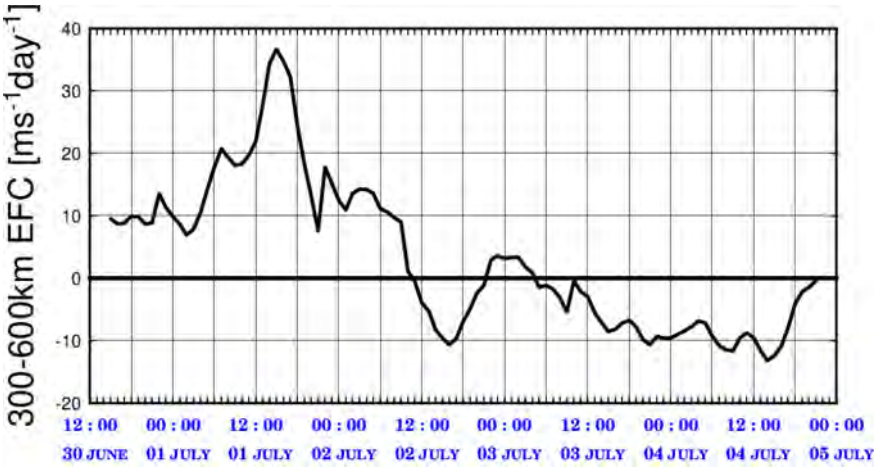

Fig.1 Time series of the EFC averaged between 300 and 600 km from the storm center.

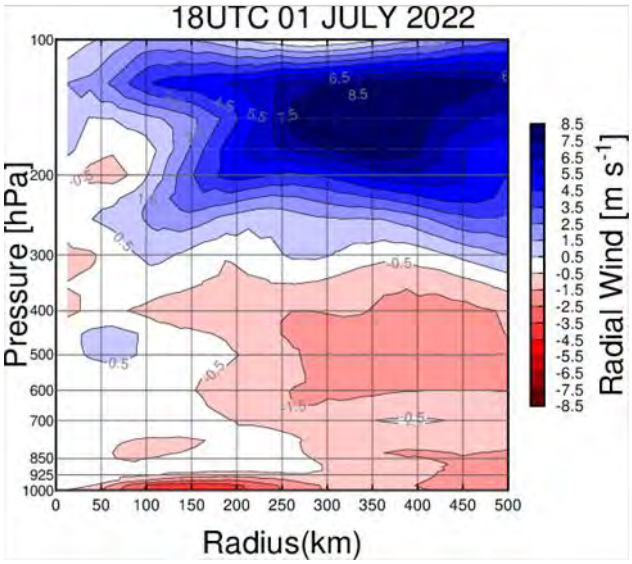

Fig.2 Radial-vertical distribution of the radial wind speed at 1800 UTC 1 July.

Comparisons of Wind Field derived from Radar observation and Numerical Model with Northward Track Typhoon in South Korea.

Jisun Lee[1], Dong-In Lee[1] and Cheol-Hwan You[1]

[1] *Atmospheric Environmental Research Institute, Pukyong National University, Busan, Korea*

Corresponding author: Jisun Lee, jisun_lee@pukyong.ac.kr

ABSTRACT

Typhoon damage has been rising annually, depending on the path, size, and intensity of the storms. In order to improve predictions based on observational data, numerous numerical modeling studies are being conducted. By examining the wind profiler data, Jeong et al. (2019) discovered that, depending on the train, the U-V distribution took one of three different forms: arc, round, or linear. Additionally, there was a significant correlation between the trajectories during landfall and the wind direction at 2 km and 4 km altitude. Then Lee et al. (2021) discussed the potential for predicting typhoon tracks by examining the wind field's characteristics with radar and a wind profiler, and calculating by using wind retrieval WISSDOM (WInd Synthesis System using Doppler Measurements), which was developed by Liou and Chang (2009) and Liou et al. (2012).

The goal of this study was to identify the characteristic of typhoon wind fields using radar data based on their paths and compare with the wind field derived from different numerical models (such as UM, KIM, GFS and ECMWF). The four typhoons in 2020 (Jangmi,Maysak, Bavi, Haishen) followed a path that was directly northward. The Korea Meteorological Administration (KMA) operated radars on Jeju Island (Gosan, Seongsan), Jindo, and Busan were collected, and the wind field retrieval WISSDOM was applied to calculate the wind fields of U, V, and W on each altitude from 1 km to 10 km. Also, three-hour intervals are chosen before, during, and after each typhoon's landfall.

First of all, as a result, the characteristics of the wind component U-V and W distribution were discovered that they are varied with height depending on the typhoon tracks moving northward on the east side and the west side of the Korean Peninsula.

Secondly, it was difficult to compare all three time steps of before/during/after the landfall as radar wind field since the time resolution of the models were much larger. Also, it was discovered that ECMWF was almost impossible to compare since the model only provide a limited amount of time steps and the altitude of wind component. Other numerical models have shown the limitation of deriving the SW wind with the typhoons in the west side of Korean peninsula. Detailed results will be discussed on the presentation during the conference.

A Preliminary Overview of Hurricane Fiona's Heavy Precipitation Aspects as it Approached Puerto Rico

Angelie Nieves Jiménez [a], Michael M. Bell [a], Ghassan Alaka[b], and Robert Rogers[b]

[a] *Colorado State University, Fort Collins, Colorado, USA*

[b] *NOAA/OAR/AOML Hurricane Research Division, Miami, Florida, USA*

Corresponding author: Angelie Nieves Jiménez, angelie.nieves-jimenez@colostate.edu

According to the records of Hurricane Fiona, this storm has been one of the strongest to make landfall in the Caribbean. Fiona rapidly intensified to a Category 1 storm before reaching Puerto Rico and after leaving the island kept intensifying until reaching Category 4. For Puerto Rico, the most concerning factor as the storm approached was the amount of precipitation the island was going to experience in 24 hours, which was recorded to be more than 20 inches. This work will analyze the environment of the storm prior to landfall and will study the dynamics the storm underwent as it approached the island. We hypothesize that there is a strong source of potential vorticity with associated moisture on the outer bands of the storm causing intense rainfall. This study will encompass an overview of the mechanisms affecting Hurricane Fiona's intensification and associated precipitation.

LROSE Tools to Estimate Surface Rain Rate

Ian Cornejo [a], Brenda Javornik [c], Angela Rowe [a], Jennifer DeHart [b], and Mike Dixon[c]

[a] *University of Wisconsin, Madison, WI, USA*

[b] *Colorado State University, Fort Collins, CO, USA*

[c] *National Center for Atmospheric Research, Boulder, CO, USA*

Corresponding author: Brenda Javornik, brenda@ucar.edu

The Lidar Radar Open Software Environment (LROSE) provides high-quality software tools that read and convert most binary radar and lidar data formats. The LROSE tools interactively display, quality control, and grid radar and lidar data. LROSE also provides tools for echo and wind analysis. The LROSE tools can be assemble into trusted, reproducible workflows that accomplish complex scientific tasks such as estimating surface rain rate. A common workflow to estimate surface rain rate helps to highlight some of the most popular tools: RadxConvert, RadxBeamblock, RadxRate, RadxQpe, and HawkEdit. At each step of the workflow, multiple parameters add flexibility and the opportunity to customize each of the tools. Once a workflow is tuned, shell scripts and files store all the steps and parameters for reproducibility.

Quality assessment of wind retrievals from SFMR of KMA/NIMS atmospheric research aircraft

Deok-Du Kang [a], Min-Seong KIM [a], Seung-Beom HAN [a], Kwang-Jae LEE [a],

Myoung-Hun Kang [a], Jong-Hoon Shin [a], Sueng-Pil JUNG [a], Tae-Young GOO [a]

[a] *National Institute of Atmospheric Sciences, KMA, Republic of KOREA*

Corresponding author: Deok-Du Kang, ddkang@korea.kr

The National Institute of Atmospheric Sciences (NIMS) atmospheric research aircraft (KingAir 350H) has been continuously operated to fulfill various mission objectives. The Severe Weather (SW) mission, in particular, aims to advance our understanding of severe weather phenomena such as heavy rainfall, snowfall and typhoons through advanced observation and improve the accuracy of numerical models. Also, accurately determining sea surface winds is crucial for maritime safety and weather forecasting. The Stepped Frequency Microwave Radiometer (SFMR), a C-band radiometer mounted on the underside of an atmospheric research aircraft, observes brightness temperature over the ocean to calculate sea surface wind speed and rain rate.

In this study, we compared sea surface winds derived from the SFMR, a high-resolution wind speed detection device, with those obtained from a maritime buoy located along the path of the aircraft. Also, we have demonstrated the effects of the calibration coefficients extracted from the calibration flight. Since June 2022, there had been 21 times flights for SW-mission and SFMR had recorded that the average wind speed was 8.7 m/s and maximum was 22.1 m/s. All cases were for the preceding observation of heavy rain on the Yellow sea. Sea surface wind speed were reproduced by applying the calibration coefficients produced from the calibration flight conducted on October 26, 2022, and were compared with those before the application and obtained from the maritime buoy. As a result, the correlation coefficient was improved by approximately 0.2, and the correlation was particularly improved in areas close to the coastline.

The Chalmers Cloud Ice Climatology: A spatially and temporally continuous record of ice hydrometeor concentrations

Simon Pfreundschuh[a,b], Aridrià Amell[b], and Patrick Eriksson[b]

[a] Colorado State University, *Fort Collins, Colorado, USA*

[b] Chalmers University of Technology, *Gothenburg, Sweden*

Corresponding author: Simon Pfreundschuh, s.pfreundschuh@gmail.com

Due to their continuous spatial and temporal coverage, infrared observations from geostationary satellites are a fundamental tool for studying convective systems. However, the raw brightness temperatures are only indirectly related to the properties of the observed clouds. Furthermore, while it is possible to estimate brightness temperatures from model simulations, it is not straightforward to relate potential deviations from observed brightness temperatures back to model deficiencies.

To overcome these limitations, we have developed a novel dataset of ice water content (IWC) and ice water path (IWP) that leverages deep neural networks to estimate these cloud properties from quasi-global (60° S - 60° N), gridded infrared observations. The machine-learning-based retrieval is trained using several years of collocations with the CloudSat 2C-ICE product. The underlying convolutional neural network learns to leverage spatial patterns in the input data, which allows it to produce skillful estimates of IWP and even IWC despite the limited spectral coverage of the input observations.

This presentation introduces the novel retrieval method and presents currently ongoing validation efforts. The retrieval is validated using independent CloudSat retrievals, ground-based cloud radar, and in-situ and remote-sensing measurements from two flight campaigns. The retrieval agrees well with independent measurements of IWP and IWC on both instantaneous and climatological time scales.

This novel ice-hydrometeor retrieval is used to create the Chalmers Cloud Ice Climatology (CCIC). CCIC provides quasi-global (-180 W - 180 E, 60 S - 60 N) coverage at three-hourly temporal resolution from 1981 and half-hourly from 2002 to the present. These unique properties make CCIC ideally suited for evaluating high-resolution climate models and studying cloud processes at regional scales. Moreover, since CCIC directly estimates ice hydrometeor concentrations, it is a natural choice for tracking convective systems and provides a more robust signal than raw brightness temperatures. The processing of the dataset is currently in progress, and the dataset will be made publicly available during the coming months.

A Magic Layer around -15°C:
Dynamical and Microphysical Processes

Gyuwon LEE [a], and Bo-Young Ye[b]

[a] *Department of Atmospheric Sciences, Center for Atmospheric REmote sensing (CARE), Kyungpook National University*

[b] *Weather Radar Center, Korean Meteorological Administration*

Corresponding author: Gyuwon Lee, gyuwon@knu.ac.kr

Microphysical and dynamical processes are intertwined, in particular, in diabatic feedback into atmospheric stability and supersaturation by upward motion. The intensive field experiment (ICE-POP 2028) is performed to reveal the dynamical and microphysical processes around -15°C layer.

The layer around -15°C to -17°C has a maximum excess vapor density over ice in the atmosphere saturated with respect to plane water. Thus, a lateral growth such as dendritic growth is dominant. In the literature, this layer showed distinctive signature of Z_{DR} maximum and K_{DP} maximum below. Many researchers explained this signature as dendritic growth but rapid growth of smaller pristine or planar crystal was need to explain rapid increase of K_{DP} maximum below. The existence of smaller ice particle was proved by bi-modal Doppler power spectra from vertical pointing cloud radar measurement. This research shows similar bi-modal spectra, and Z_{DR} and K_{DP} feature around this layer. In addition, we found mesoscale ascent below the layer from vertical pointing radar data in climatological sense. Thus, we speculate that new ice nucleation in increased supersaturation condition is most feasible explanation. This supersaturation can be explained by the combined effect of mesoscale ascent below and diabatic heating due to excess vaper density.

Extreme Rain Event and Related Microphysics in North Taiwan

Chi-June Jung [a], and Ben Jong-Dao Jou [a,b]

[a] *Department of Atmospheric Sciences, National Taiwan University, Taipei, Taiwan*

[b] *Center for Weather Climate and Disaster Research, National Taiwan University, Taipei, Taiwan*

Corresponding author: Dr. Ben Jong-Dao Jou, jouben@ntu.edu.tw

For this study, heavy rain was defined as gauge-measured hourly accumulated rainfall exceeding 40 mm. Compared to other non-typhoon events in north Taiwan, weak synoptic-forced heavy rain events have shorter duration and smaller spatial coverage but a slightly higher medium value of rain intensity. Notably, on 14 June 2015, the rain rate was one of the most extreme (at least 99th percentile of hourly rainfall) between 2014 to 2018.

On 14 June 2015, ground measurements suggested that the sea breeze efficiently transported moisture, leading to a higher amount of precipitable water. Analysis of radar-based hydrometeor identification and measured raindrop size distribution indicated that both ice-based and warm-rain processes contributed to the extreme precipitation. Graupel was abundant above the 0°C level, and the melted graupel increased raindrop concentration, resulting in a more intense rain rate. During the extreme rainfall stage (131.5 mm h^{-1}), the dominant process was considered to be breakup, which depended on local enhanced vertical wind shear caused by the cold pool. After the large breakup signature, higher concentrations of small raindrops may have further enhanced evaporative cooling.

More studies using TAHOPE/PRECIP field experiment database should be conducted to provide general conclusions.

Reference:

Jung, C.-J. and B. J.-D. Jou, 2023: Bulk microphysical characteristics of a heavy-rain complex thunderstorm system in the Taipei Basin. *Mon. Wea. Rev.*, 151, 877–896. DOI: 10.1175/MWR-D-22-0078.1

Microphysics of Heavy Rainfall Observed during the Prediction of Rainfall Extremes Campaign In the Pacific (PRECIP) 2022

Michael M. Bell [a], Jennifer DeHart [a], Chelsea Nam [a],

Ting-Yu Cha [b], Ming-Jen Yang [c], and Kazuhisa Tsuboki [d]

[a] *Colorado State University, Fort Collins, Colorado, USA*

[b] *National Center for Atmospheric Research, Boulder, Colorado, USA*

[c] *National Taiwan University, Taipei, Taiwan*

[d] *Institute for Space-Earth Environmental Research, Nagoya University, Nagoya, Japan*

Corresponding author: Michael M. Bell, mmbell@colostate.edu

The Prediction of Rainfall Extremes Campaign In the Pacific (PRECIP) collected novel observations in East Asia during the 2022 spring and summer to improve our understanding of the multi-scale dynamic, thermodynamic, and microphysical processes that produce extreme precipitation. The campaign was designed to maximize the chances of observing a variety of heavy rainfall events in the moisture-rich natural laboratory of the western North Pacific in order to find the commonalities across different weather phenomena. The U.S. instrumentation included the Colorado State University SEA-POL radar, radiosondes, disdrometers, and the National Center for Atmospheric Research S-Pol radar and three MicroPulse Differential Absorption LIDARs (DIALs). PRECIP was conducted in from May to August 2022 in partnership with the Taiwan TAHOPE and Japan T-PARCII experiments, which included research X-band radars and the operational Central Weather Bureau and Japan Meteorological Agency radar networks. An overview of the project and analysis of the new radar observations will be presented. Composites of microphysical characteristics retrieved from range-height vertical scans across a wide spectrum of precipitation events are combined with thermodynamic measurements from the radiosonde and DIALs over the 3-month project. The presentation will highlight the new field observations obtained from the field campaign radar network and the implications for improving our understanding of heavy rainfall.

Mammatus-Like Echo Structure along the Base of the Typhoon Outflow-Layer Clouds Observed by Ka-Band Radar

Tadayasu Ohigashi [a], Kazuhisa Tsuboki [b], Taro Shinoda [b], Haruya Minda [b], Moeto Kyushima [b], Hiroyuki Yamada [c], and Hironori Iwai [d]

[a] *National Research Institute for Earth Science and Disaster Resilience, Tsukuba, Japan*

[b] *Institute for Space-Earth Environmental Research, Nagoya University, Nagoya, Japan*

[c] *Department of Physics and Earth Sciences, Faculty of Science, University of the Ryukyus, Nishihara, Japan*

[d] *National Institute of Information and Communications Technology, Koganei, Japan*

Corresponding author: Tadayasu Ohigashi, ohigashi@bosai.go.jp

Upper-tropospheric clouds in the outflow layer of typhoons can significantly affect the track of typhoons (tropical cyclones) through radiation effects. In this study, the microstructure of the outflow-layer clouds of several typhoons was examined. Ka-band cloud radar observations of three typhoons for Chaba (2016), Cimaron (2018), and Neoguri (2019) around Japan revealed numerous protuberances in echoes along the base of the upper-level clouds, which are referred to as mammatus-like echoes. The outflow-layer clouds were present above 0°C levels and consisted of ice particles. The horizontal scale was 0.5-3 km, and the vertical scale was 0.3-1.5 km. The surface of the mammatus-like echo showed from smooth to irregular. The mammatus-like structure did not always appear when the typhoon outflow-layer clouds were formed. For Typhoon Chaba (2016), five radiosonde observations were conducted in the radar observation range. In all vertical profiles, neutral stratification with a nearly constant potential temperature layer was formed near the cloud base. Below that, there was a significantly dry layer with a relative humidity with respect to ice of <20%. For Typhoon Cimaron (2018), a 2-minute vertical observation was conducted within a 5-minute observation cycle. This vertical observation showed downward Doppler velocities in hanging echo regions, and upward Doppler velocities in between the hanging echoes. Considering the difference between positive and negative peaks of the Doppler velocities, upward and downward air motions of approximately 3 m s^{-1} were present around the mammatus-like echo layer. This vertical air motion was significantly larger than that in the upper part of the outflow-layer clouds. This study showed that the mammatus-like echo structure frequently occurred at the boundary between the outflow-layer clouds and the significantly dry layer below, with upward and downward air motions of several meters per second. This vertical motion is inferred to be caused by sublimation of ice particles from the outflow-layer clouds. These mammatus-like structures may contribute to mixing along the cloud base and promote dissipation of the outflow-layer clouds.

The Airborne Phased Array Radar (APAR) Observing Simulator (AOS): Part I - Implementation of the AOS Prototype

Wen-Chau Lee[1], Bradley W. Klotz[1], Jothiram Vivekanandan[1], Kevin Manning[2], George Bryan[2], Michael Bell [3], and Pavlos Kollias[4]

[1] NCAR/EOL, [2] NCAR/MMM, [3] Colorado State University, [4] Stony Brook University

Corresponding author: Wen-Chau Lee, wenchau@ucar.edu

Abstract:

Development of new observing systems is critical for the advancement of scientific understanding of weather phenomena. These instruments establish a proving ground for future operational transition while also providing tools for the research community. One of the issues with developing new instrumentation is the unknown performance characteristics of the instrument and the subsequent unknowns in uncertainty in measurements. Given the technological advancements that have occurred recently, the creation of end-to-end observing system simulators provides an opportunity to investigate the observing capabilities and limitations of instruments and reduce some of the risks associated with the performance of instrument development. This work aims to describe such a scenario for the Airborne Phased Array Radar (APAR). The APAR Observing Simulator (AOS) was developed to understand APAR's measurement capabilities for high-impact weather events. Using Cloud Model 1 (CM1) and Weather Research and Forecasting (WRF) model output to provide various storms of interest and their surrounding environments, simulated NCAR C-130 flights are operated within the model space. Radar moments are determined using the Cloud Resolving Model Radar Simulator (CR-SIM). The output can be examined directly or passed through additional tools to analyze various aspects of the data collected during each flight. This current work is the first of a two-part paper, where the first part describes the prototype version of AOS, including its design and functionality along with some initial APAR performance metrics related to a 3-D wind analysis. The second paper will focus on a more detailed analysis of the 3-D winds and dual-polarization products to showcase the usefulness of the AOS for generating reliable scientific products. The contents herein are presented in such a way as to provide insight into simulating APAR and to present a methodology for future simulation of radar observations.

Evaluating Microphysics and Precipitation Characteristics of Severe Weather Events with the Airborne Phased Array Radar (APAR) Observing Simulator

Bradley Klotz [a], Wen-Chau Lee [a], and Jothiranm Vivekanandan[a]

[a] *National Center for Atmospheric Research, Boulder, CO, USA*

Corresponding author: Bradley Klotz, bradklotz@ucar.edu

The current landscape of airborne weather radars in the United States consists of the operational Tail Doppler Radars (TDRs) on the NOAA WP-3D hurricane hunter aircraft and various cloud radars within the university community. With the retirement of the NSF ELectra DOppler RAdar (ELDORA) over ten years ago, there has been a gap in our ability to perform innovative research related to high-impact weather events, especially in remote locations. Therefore, NSF and the National Center for Atmospheric Research (NCAR) are in the process of developing a new and transformational airborne radar: the Airborne Phased Array Radar (APAR). This new radar is designed to fly on the NSF/NCAR C-130 aircraft and to provide both dual-Doppler and dual-polarization capabilities using agile scanning methods associated with PAR technology. While APAR is still in development, a tool was created at NCAR that allows scientists to test various uses of APAR in a controlled setting. The APAR Observing Simulator (AOS) uses model output and user-defined radar scan and flight parameters to provide realistic radar output that would be expected with APAR's given technical specifications.

Airborne radars provide a unique opportunity to understand high-impact weather events, such as hurricanes and mesoscale convective systems, due to their ability to sample large areas of a storm and to follow a storm as it propagates. Previous experiments with the AOS output investigated some of the radar's technical limitations related to flight and scan strategies, expected beam broadening away from the radar boresight, and attenuation comparisons with X-band radars (currently in use on the NOAA WP-3D aircraft). Evaluation of the Doppler winds and their comparison with known storm characteristics confirmed that APAR could provide this information with a high level of accuracy. These experiments show that at a minimum, APAR can support objectives that were designed for mechanically scanning tail Doppler radars. APAR is also equipped with dual-polarimetric capabilities, providing a new opportunity to study the microphysical and precipitation characteristics of these severe storms in new ways.

This presented work discusses the results of several experiments investigating topics related to determining particle identification (PID) distributions and Quantitative

Precipitation Estimates (QPE). The initial PID determination and analysis results suggest that the hydrometeor classifications match fairly well between the simulated cases and known distributions. For instance, the rain and snow distributions are well-represented, but there is a noticeable difference in the amount of ice crystals depicted in the simulated storms compared to observations. The information obtained from the PID classifications is used to help determine ice water content (IWC) and ice water path (IWP) in a hurricane case. The results from the QPE analysis indicate that specific methods are preferable for APAR, where "hybrid" rain rate determination schemes tend to provide more accurate results. These "hybrid" schemes use the hydrometeor classifications and dual-polarization parameters. New results associated with the hydrometeor classification scheme are discussed for application to APAR and how they can be utilized to provide more accurate estimates of particle fall speeds and vertical velocity.

Microphysical observation by newly-developed particle imaging radiosonde “Rainscope”

Kenji Suzuki [a], Yurika Hara [a], Rimpei Kamamoto [b], and Tetsuya Kawano [c]

[a] *Yamaguchi University, Yamaguchi, Japan*

[b] *Railway Technical Research Institute, Tokyo, Japan*

[c] *Kyushu University, Fukuoka, Japan*

Corresponding author: Kenji Suzuki, kenjis@yamaguchi-u.ac.jp

A new balloon-borne precipitation particle imaging radiosonde “Rainscope” have been developed. It captures a still image of falling particles by means of an electronic shutter when a precipitation particle crosses the built-in infrared sensor. The digitalization of the image enables clear particle images to be received even at a distance of several tens of kilometers from the receiving antenna. The development of the Rainscope has made it possible to acquire images that clearly recognize the outlines and irregularities of ice particles, as well as their state of aggregation and melting (Fig.1).

The Rainscope is also equipped with another infrared sensor, which records the time when a particle passes through the upper and lower sensors, enabling measurement of the velocity of falling precipitation particles. Vertical profile measurements of the fall velocity of precipitation particles can contribute to understanding microphysical processes within clouds and provide validation data for cloud resolution models. For the ground test, measurements of rain and snow by a ground-based Rainscope showed a raindrop size-fall velocity distribution similar to that of Altas et al. (1977). They were also in good agreement with the distributions obtained by Parsivel placed next to the Rainscope. In the test flight of the Rainscope into a stratiform cloud, raindrops were observed in the lower layers, and mostly melted particles, snowflakes in the process of melting, graupel, and snowflakes were observed above the freezing level. When multiple particles pass through the infrared sensor in succession, it is not possible to measure the fall velocity of each particle. However, even with a small number of samples, it was observed that the fall velocity varied depending on the type of precipitation particles (Fig.1).

The Rainscope was first deployed in the intensive observation campaign, which was conducted in Kyushu region during the Baiu rainy season in 2022. It was launched into convective clouds with active lightning and gust on 25 June 2022. It transmitted images of ice particle in the process of melting just below 0ºC, and frozen particles with semi-transparent and smooth outlines around 0ºC. And white and irregularly shaped graupel were observed across all layers up to -30ºC level. The clear particle images captured by the Rainscope enable us to get more detailed information of particle shapes, surface

conditions, and contours, making it easier to evaluate their shapes quantitatively. The circularity of graupel was smaller in upper layer. It has a longer circumference and more irregular shapes, suggesting an active riming process originated from ice crystals. On the other hand, graupel in lower layer with larger circularity was suggested to be originated from a frozen particle. The different graupel formation processes was considered to exist in convective clouds.

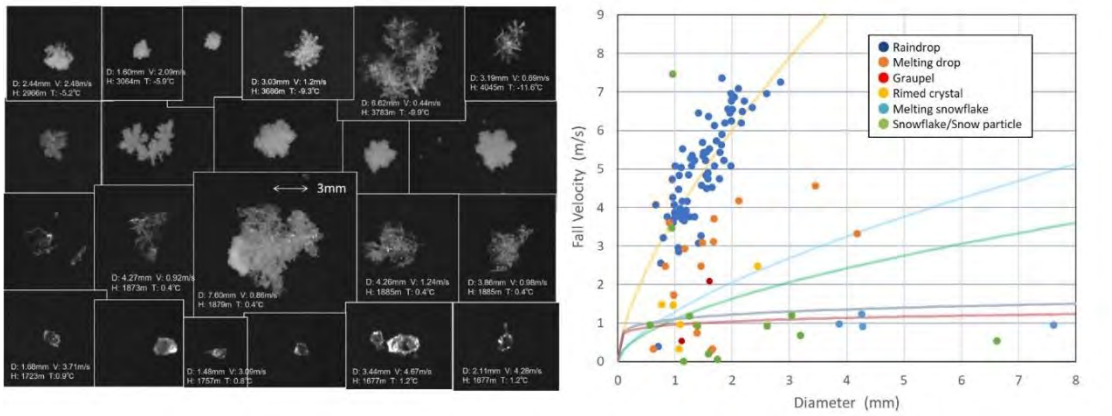

Fig. 1: Precipitation particle images (left) and particle size-fall velocity distributions (right) obtained from the Rainscope test flight into a stratiform cloud on 20 Feb. 2021.

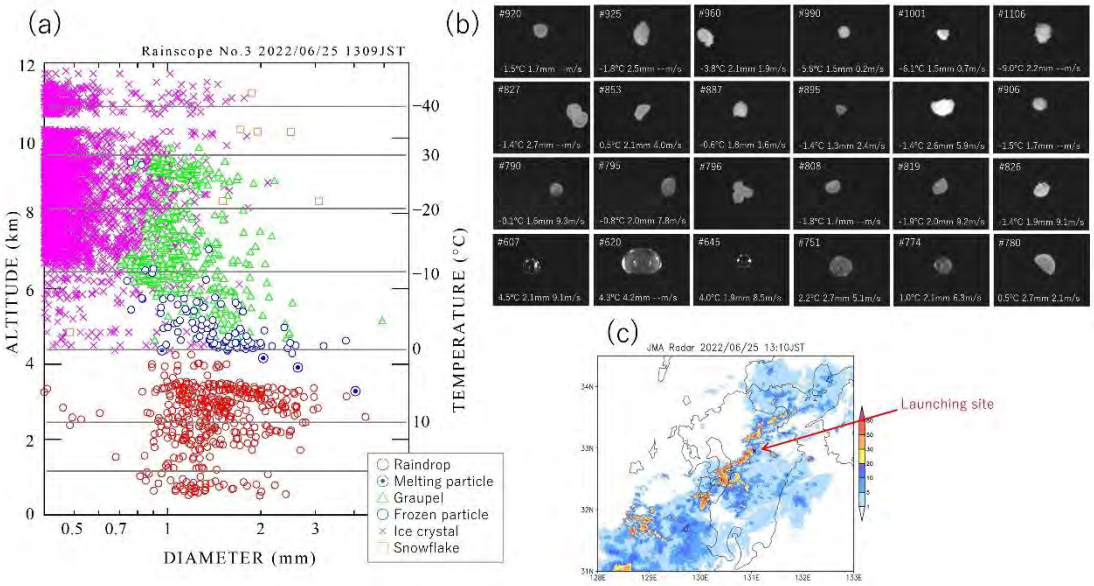

Fig. 2: (a) Particle size-altitude distribution obtained from Rainscope launching. Red circle: raindrop, medium-black circle: particles in the process of melting, blue circle: frozen particle, green triangle: graupel, pink x: ice crystal, orange square: snowflake. (b) Particle images, (c) JMA radar at 13:10 JST on 25 June 2022. The color bar indicates precipitation intensity, and the X in the figure indicates the Rainscope launching site.

Relationship Between the Warm Core and Typhoon Intensity Based on in Situ Measurements

Hiroyuki Yamada [a,c], Kosuke Ito [a,c], Soichiro Hirano [a], and Kazuhisa Tsuboki [b,c]

[a] *Faculty of Science, University of the Ryukyus, Nishihara, Okinawa, Japan*

[b] *ISEE, Nagoya University, Nagoya, Japan*

[c] *TRC, Yokohama National University, Yokohama, Kanagawa, Japan*

Corresponding author: Hiroyuki Yamada, yamada@sci.u-ryukyu.ac.jp

It is widely believed that the stronger a tropical cyclone, the larger the positive perturbation temperature (i.e., warm core) at the storm center, and that its maximum appears in the upper troposphere. A recent numerical study, on the other hand, argued that this maximum appears in the middle troposphere and pointed out that satellite-borne microwave sounders have insufficient resolution to measure temperature in the middle troposphere. The lack of in situ observations near the storm center in the middle to upper troposphere undoubtedly hinders our understanding of the relationship between the warm core and storm intensity. In the western North Pacific, we perform aircraft reconnaissance of intense typhoons since 2017, and have so far observed nine warm-core cases by dropsondes released from the upper troposphere (~14 km MSL). In addition, we have observed two other cases using radiosondes launched from the Okinawa Island. Furthermore, three more cases have been observed by operational upper-air soundings of the Japan Meteorological Agency in the Ryukyu Islands. In this study, we examine the relationship between perturbation temperature profiles and typhoon intensity based on these 14 cases of in situ measurements. The perturbation temperature is defined as a difference in temperature measured in the eye of a typhoon from that obtained in the environment (between 550 and 600 km from the center) at a constant pressure level. The perturbation temperature is averaged vertically in specific layers (900-250, 500-250, and 900-500 hPa). The minimum sea-level pressure (MSLP) observed in the eye is used as a proxy of storm intensity. First, we compare the MSLP and the mean perturbation temperature in 900-250 hPa (Fig. 1) and obtain a negative relationship with high coefficient of determination (R^2 of 0.94). This relationship enables us to estimate the MSLP from temperature with an error of about 10 hPa. We confirm that the correlation remains high (R^2 of 0.95) even if the mean perturbation temperature in the upper troposphere (500-250 hPa) is used. This result confirms that the upper tropospheric temperature measured by satellite-borne sounders can be employed as a proxy for typhoon intensity. Next, we examine the weighted height of perturbation temperature (Fig. 2), showing that the weight height is around 8 km regardless of the MSLP. In individual cases of intense typhoon, the maximum of perturbation temperature is embedded within a deep layer of nearly constant value. This is in contrast to many previous studies arguing that the height of maximum perturbation

temperature depends on typhoon intensity. The influence of the choice of a reference profile on the warm-core height will be discussed.

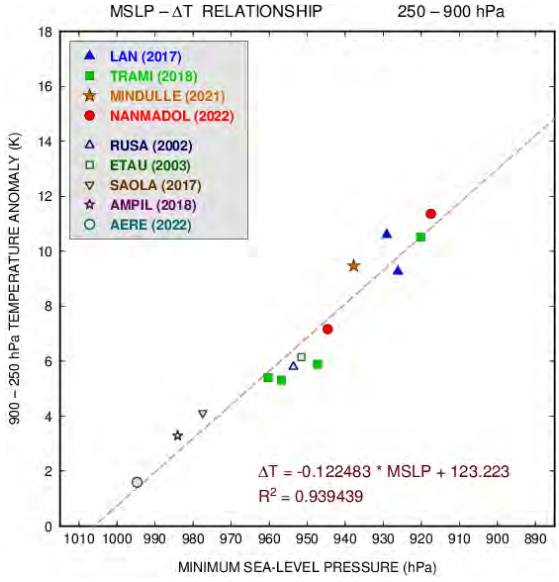

Fig. 1 Scatter plot and a regression line of the MSLP and perturbation temperature averaged between 900 and 250 hPa. Filled (outlined) symbols indicate aircraft (ground-based) typhoon eye soundings.

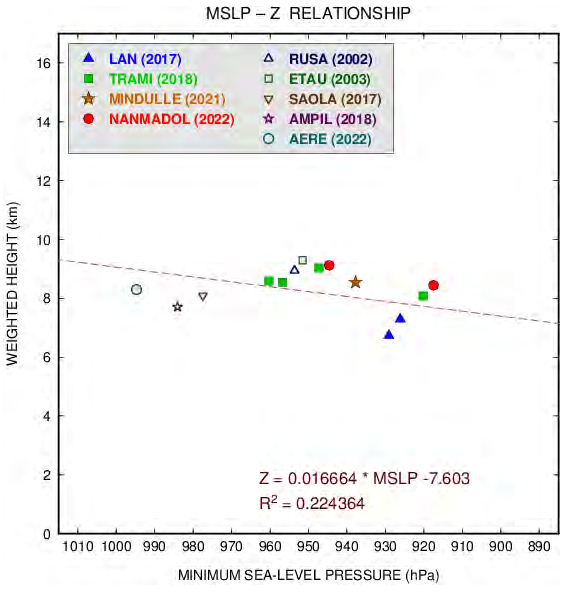

Fig. 2 Scatter plot and a regression line of the MSLP and the weighted height of perturbation temperature.

Dynamical and Microphysical Characteristics of Asymmetric Convection in the Outer Eyewall of Super Typhoon Lekima (2019)

Kun Zhao[a,b], Hao Huang [a,b], Qingqing Li[c,d], Huaning Dai[a,b]

[a] *Key Laboratory of Mesoscale Severe Weather/MOE and School of Atmospheric Science, Nanjing University, Nanjing, China*

[b] *Key Laboratory of Radar Meteorology, China Meteorology Administration, Nanjing, China*

[c] *Key Laboratory of Meteorological Disaster of the Ministry of Education, Nanjing University of Information Science and Technology, Nanjing, China*

[d] *State Key Laboratory of Severe Weather, Chinese Academy of Meteorological Sciences, Beijing, China*

Corresponding author: Kun Zhao, zhaokun@nju.edu.cn

Typhoon Lekima (2019) possessed a double-eyewall structure before making landfall in eastern China, with its outer eyewall showing quasi-periodic convective intensification. The microphysical signatures relevant to the asymmetric convection in the outer eyewall and the associated physical mechanisms were analyzed based on ground-based radar observations. The results indicate that the microphysical characteristics varied in quadrants. The phase locking that occurred between the vortex Rossby waves (VRWs) associated with the double eyewalls served as a plausible mechanism for the presence of repeated strong precipitation in the upshear regions of the outer eyewall, according to the radar reflectivity analysis. In the upshear-left outer eyewall, the convection was deepened on the inner edge due to the phase locking between the wavenumber-1 VRWs and the outward-moving wavenumber-2 VRWs sparked from the inner eyewall. With the updraft depressed by the filamentation effect and moat, warm rain was the predominant process contributing to the enhancement of rainfall. In contrast, the strongest precipitation occurred on the outer edge of the upshear-right outer eyewall, due to the phase locking between the strengthened wavenumber-1 VRWs and the wavenumber-2 VRWs. In this region, exuberant riming processes and graupel formation prevailed above the melting layer due to the strongest and more outward-tilted updrafts induced by the phase locking between the VRWs. A good deal of graupel melted into raindrops, along with significant accretion processes, produced intense rainfall with larger drop sizes.

A New Method to Estimate Circulations in Tropical Cyclones from Single-Doppler Radar Observations

Satoki Tsujino [a], Takeshi Horinouchi [b], and Udai Shimada [a]

[a] *Meteorological Research Institute, Tsukuba, Ibaraki, Japan*

[b] *Faculty of Environmental Earth Science, Hokkaido University, Sapporo, Hokkaido, Japan*

Corresponding author: Satoki Tsujino, satoki@mri-jma.go.jp

Doppler weather radars are a powerful tool for investigating the inner-core structure of tropical cyclones (TCs). The Doppler velocity from a single radar has no information on the wind component normal to the radar beam. Therefore, closure assumptions are needed to estimate the circulations of the TCs from single-Doppler radar observations. The Generalized Velocity Track Display (GVTD, Jou et al. 2008) technique used to estimate the TC circulations adopts the closure assumption of no asymmetric radial winds in the TC vortex.

The present study proposes a new closure assumption introducing asymmetric radial winds to improve the axisymmetric-circulations estimation, based on the geometry of the GVTD technique. Our new method can consider the asymmetric radial winds by using streamfunction based on the Helmholtz decomposition theorem of horizontal winds. As with GVTD, the new method retrieves TC circulations based on the Fourier decomposition of winds in the azimuthal direction and the least-square fit of the Doppler velocity from the single radar observation.

The new method and GVTD are applied to analytical vortices and a real typhoon (Haishen in 2020). For the analytical vortices with asymmetric winds in wavenumber-2 vortex Rossby waves, the axisymmetric tangential wind of V_{T0} retrieved by the new method (GVTD) has a relative error of less than 2% (10%) near the radius of maximum wind speed. For Typhoon Haishen, the GVTD-estimated V_{T0} has periodical fluctuations with an amplitude of about 5 m s^{-1} near the elliptical eyewall (Fig. 1a). The period of the fluctuations is approximately synchronized with the counterclockwise rotating period of the elliptical shape of the eyewall, suggesting pseudo-signals due to the closure assumption in GVTD. The periodical fluctuations are largely reduced in the estimated V_{T0} from the new method (Fig. 1b). We find that the new method can reduce the pseudo-signals of the GVTD-retrieved axisymmetric circulation in cases of asymmetric vortices. Furthermore, we clarify that a pattern of the estimated wavenumber-2 flows in Haishen is consistent with the flow pattern of an elliptical eyewall in a previous modeling study (Fig. 2).

Reference:

Jou et al. (2008): https://doi.org/10.1175/2007MWR2116.1

Tsujino et al. (2023): https://doi.org/10.51094/jxiv.299 (preprint)

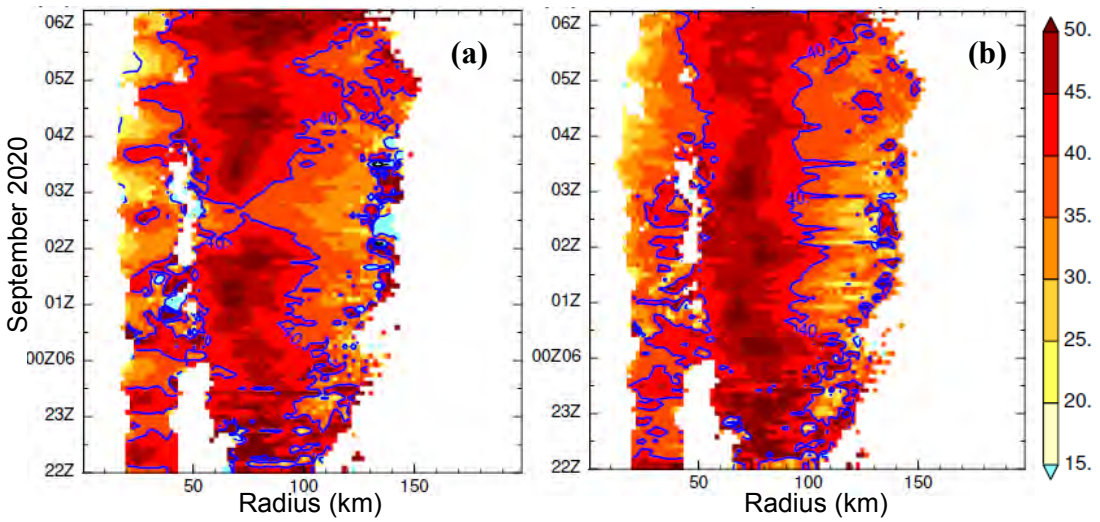

Fig. 1: Radius-time cross-sections of retrieved axisymmetric tangential winds (color; m s^{-1}) at the 2-km height in Haishen based on (a) GVTD and (b) our new method. The blue contours denote the axisymmetric tangential wind of 40 m s^{-1}.

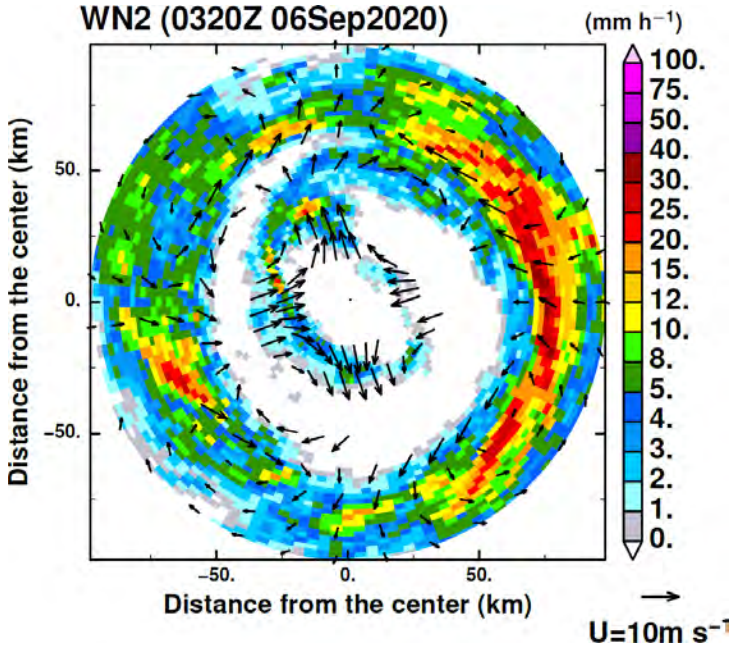

Fig. 2: Elliptical eyewalls in Typhoon Haishen (2020) captured by the JMA C-band operational Doppler radar at Naze. The color indicates the precipitation intensity (mm h^{-1}) converted from the radar reflectivity. The black arrows indicate the wavenumber-2 components of the rotating winds retrieved by the new method at 0320 UTC on 06 September 2020.

High-resolution 3D wind fields in Seoul City: Discrepancy with observations and potentially scientific applications

Chia-Lun Tsai[a,c], Kwonil Kim[c], Yu-Chieng Liou[b], and GyuWon Lee[c]

[a]*Department of Atmospheric Sciences, Chinese Culture University, Taipei, Taiwan*

[b]*Country Department of Atmospheric Sciences, National Central University, Jhongli, Taiwan*

[c]*Department of Astronomy and Atmospheric Sciences, Center for Atmospheric REmote sensing (CARE), Kyungpook National University, Daegu, South Korea*

Corresponding author: Chia-Lun Tsai, E-mail: CJL10@ulive.pccu.edu.tw

Very high-resolution 3-dimensional (3D) wind fields can be retrieved well over complex terrain via WISSDOM (Wind Synthesis System using Doppler Measurements) synthesis. This scheme was performed to derive reasonable 3D winds using lidar observations in Seoul city under clear-air conditions. A case was selected to evaluate the performance of retrieved winds due to colocated observations, including three towers and automatic weather stations (AWSs). The size of the test domain is 15 × 15 km^2 extended up to 2 km height mean sea level (MSL) with a remarkably high horizontal and vertical resolution of 50 m. The results indicate that the derived winds reveal good patterns with the observations. After a series of sensitivity tests with different weighting coefficients, the optimal setting was found. Compared to the original setting of WISSDOM, the average bias (root mean square deviation, RMSD) of wind speed between retrieved winds and tower observations was improved from 5.4 to 3.1 m s^{-1} (12.5 to 4 m s^{-1}). The average bias (RMSD) of wind speed between derived winds and the AWS was improved from 4.1 to 3.1 m s^{-1} (4.6 to 3.5 m s^{-1}). Although the performance of wind speed was improved, the bias and RMSD of wind speed did not change significantly in this case.

Predicting Rainfall Forecast Quality of Westbound Typhoons in Taiwan through Machine Learning

Chung-Chieh Wang [a], and Shin-Hau Chen [a]

[a] *Department of Earth Sciences, National Taiwan Normal University, Taipei, Taiwan*

Corresponding author: Chung-Chieh Wang, cwang@ntnu.edu.tw

Typhoon rainfall is both an important water resource and potential disaster in Taiwan, so its forecast quality and improvement are important. In this study, we have developed and tested a model through machine learning that provides objective guidance to indicate the credibility of each quantitative precipitation forecasts (QPFs) for typhoons soon after it is made. Specifically, time-lagged forecasts (out to 8 days) every 6 h by the 2.5-km Cloud-Resolving Storm Simulator (CReSS) for 10 westbound typhoons affecting Taiwan are used. A total of 105 parameters are selected from each run and those from nine typhoons are fed into the learning model to, after training, predict the similarity skill score (SSS) of total rainfall distributions when the storm is within 300 km from Taiwan's coast for the tenth storm. As a measure to the overall quality of the QPFs, the projected SSS thus serves as guidance for forecast confidence.

Results indicate that the model can capture the tendency of the actual SSS computed using observed rainfall for most cases, thereby informing the forecasters which QPFs are more trustworthy and which ones less so before the event. Such guidance is especially valuable at longer lead time, when the forecast uncertainty is relatively high, and thus our results are highly encouraging. Nevertheless, as machine learning can be viewed as a complicated statistical technique, when certain typhoon behaves differently from those used for training, the outcome would be an outlier and less useful. Some possible directions for further improvement are also discussed.

Can radar-based QPE reproduce the 201.9 mm hourly rainfall accumulation recorded at Zhengzhou, China?

Haoran Li[a,b], Dmitri Moisseev[b], Yali Luo[a,c], Liping Liu[a], Zheng Ruan[a], Liman Cui[d], and Xinghua Bao[a]

[a] *State Key Laboratory of Severe Weather, Chinese Academy of Meteorological Sciences, Beijing, China*

b Institute for Atmospheric and Earth System Research / Physics, Faculty of Science, University of Helsinki, Finland

c Collaborative Innovation Center on Forecast and Evaluation of Meteorological Disasters, Nanjing University of Information Science and Technology, Nanjing, China

d Henan Meteorological Observatory, Zhengzhou, China

Corresponding author: Haoran Li, lihr@cma.gov.com

Although radar-based quantitative precipitation estimation (QPE) has been widely investigated from various perspectives, very few studies have been devoted into extreme rainfall QPE. In this study, the performance of KDP-based QPE during the record-breaking Zhengzhou rainfall event occurred on 20 July 2021 was assessed. Firstly, OTT disdrometer observations were used as input to T-matrix simulation and different assumptions were made to construct R(KDP) estimators. Then, KDP estimates from three algorithms were compared for obtaining best KDP estimates, and gauge observations were used to evaluate R(KDP) estimates. Our results in general agree with previous known-truth tests, and provide more practical insights from the perspective of QPE applications. For rainfall rates below 100 mm h-1, R(KDP) agrees rather well with gauge observations, and the selection of KDP estimation method or controlling factor has minimal impact on QPE performance provided that the used controlling factor is not too extreme. For higher rain rates, significant underestimation was found for R(KDP), and a smaller window length results in higher KDP thus less underestimation of rain rates. We show that the "best KDP estimate"-based QPE cannot reproduce the gauge measurement of 201.9 mm h^{-1} with commonly used assumptions for R(KDP), and potential responsible factors were discussed. We further show that the gauge with the 201.9 mm h-1 report was located at the vicinity of local rainfall hot spots during 16:00 ~ 17:00 LST, while the 3-h rainfall accumulation center was located at the southwest of Zhengzhou city.

Applying the multi-scale radar ensemble data assimilation system to investigate the heavy precipitation episode during TAHOPE/PRECIP-IOP3

Shu-Chih Yang [a], Jing-Yueh Liu [a], Hao-Lun Yeh [a], Shu-Hua Chen [b], Wei-Yu Chang [a], Kao-Sheng Chung [a] and Pao-Liang Chang[c]

[a] *Dept. of Atmospheric Sciences, National Central University, Taoyuan, Taiwan*

[b] *University of California at Davis, USA*

[c] *Central Weather Burau, Taipei, Taiwan*

Corresponding author: Shu-Chih Yang, shuchih.yang@gmail.com

A multi-scale radar data assimilation (RDA) system has been established by applying the successive covariance localization to the WRF-Radar LETKF system. This study uses this multi-scale RDA system to investigate the convection development during the TAHOPE/PRECIP IOP3 event (from 6 to 8 June 2022) with the radial velocity and reflectivity of Wufenshan and SPol radar. The radar data are first QCed with the new version of RAKIT to remove the abnormal signals with concentric circles and along the beams. We conduct experiments using the convective-scale and multi-scale RDA systems with rapid cycles from 00 UTC 6 June to 00 UTC 7 June. Our goal is to understand the predictability of the convections initialized and intensified at the western coast of northern and middle Taiwan, as the mei-yu front approaching the northern Taiwan.

Compared to the convective-scale RDA experiment (RDA), the multi-scale RDA (MRDA) experiment exhibits broader wind correction, which enhances the wind speed over the Taiwan Strait and the near-surface offshore flow over the western coast of Taiwan. At 21 UTC on 6 June, a stronger convergence off western Taiwan is established and lasts several hours. Furthermore, the precipitable water is much higher off the coast in MRDA than RDA. As a result, MRDA generates much stronger convections along the shoreline of western Taiwan. Preliminary results show that the front location is one of the critical factors in sustaining the convergence and the long-hour convection development over the coast of western Taiwan. Although the precipitation prediction is generally improved in MRDA, the rainfall intensity is less optimal due to the deficit in representing the deep moisture layer offshore western Taiwan. During our presentation, we will provide more information about how we can further improve the representation of convection and precipitation by assimilation other types of observations under the multi-scale RDA system.

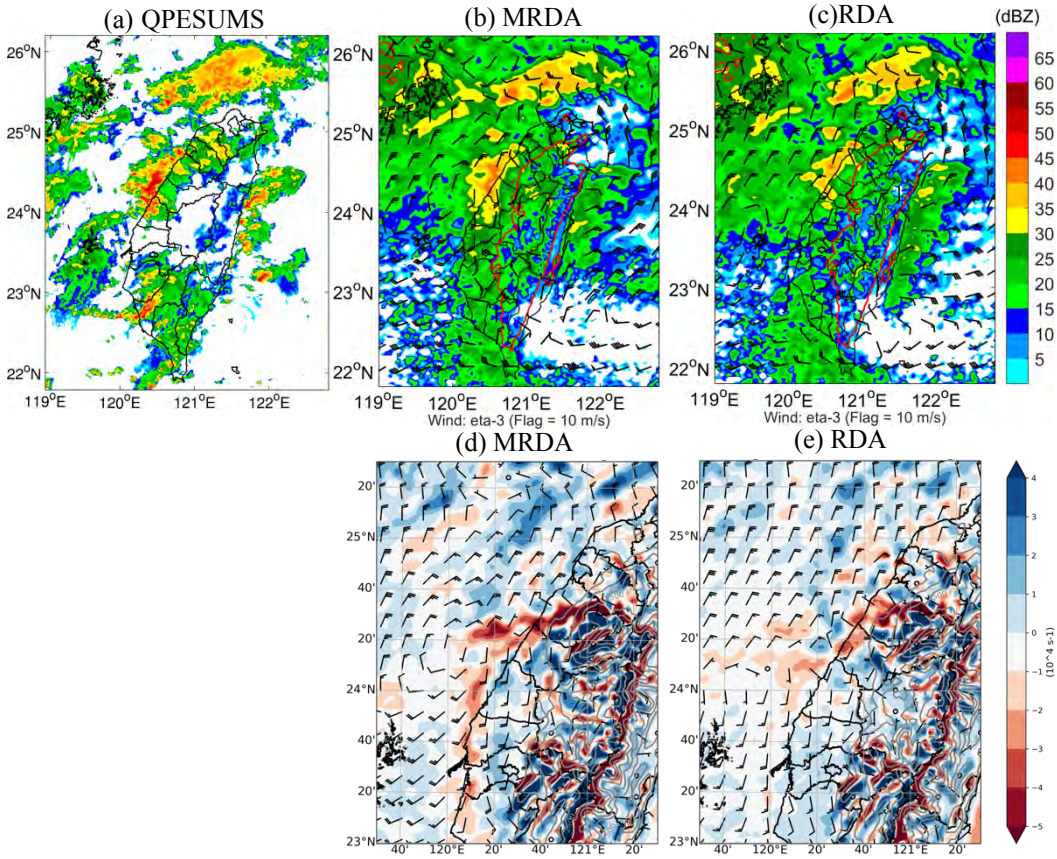

Figure 1. (a) Maximum composite reflectivity from CWB QPESUMS gridded radar data, and maximum reflectivity and horizontal wind at the 3rd model level from the (b) MRDA and (c) RDA analysis at 2300 UTC on 6 June, 2023. The convergence and horizontal wind at the 3rd model level from the (d) MRDA and (e) RDA analysis.

What controlled the low-level moisture transport during the extreme precipitation in Henan Province of China in July 2021?

Hao-Yan Liu [a,b], **Jian-Feng Gu** [c], Yuqing Wang[d], and Jing Xu[e]

[a] *Key Laboratory of Marine Hazards Forecasting, Ministry of Natural Resources, Hohai University, Nanjing, China*

[b] *College of Oceanography, Hohai University, Nanjing, China*

[c] *Key Laboratory of Mesoscale Severe Weather/Ministry of Education, School of Atmospheric Sciences, Nanjing University, Nanjing, Jiangsu Province, China*

[d] *International Pacific Research Center and Department of Atmospheric Sciences, School of Ocean and Earth Science and Technology, University of Hawaii at Manoa, Honolulu, Hawaii*

[e] *State Key Laboratory of Severe Weather, Chinese Academy of Meteorological Sciences, China Meteorological Administration, Beijing, China*

Corresponding author: Jian-Feng Gu, jfgu@nju.edu.cn

Abstract: A record-breaking precipitation event occurred in Henan province of China in July 2021 (217HP). To identify the moisture source of the event, ensemble experiments with 120 members were conducted in this study. Results show that the precipitable water during this extreme event was primarily contributed by the low-level southeasterly (LLSE) water vapor transport. The LLSE was largely enhanced by the pressure gradient force maintained by the western Pacific subtropical high and further amplified by the latent heat release in the rainfall system over Henan. The positive moisture advection by the LLSE and evaporative water occurred below 950 hPa and was redistributed into higher levels by the LLSE jet-enhanced sub-grid vertical turbulent transport. As a result, the combination of enhanced LLSE centered around 950 hPa and the increase of moisture below 850 hPa were the main drivers for the continuous strengthening of LLSE moisture transport, with the former playing the dominant role. It is also found that not only the presence but also the intensity of LLSE jet were important for reproducing the extreme rainfall. The impact of binary tropical cyclones In-Fa and Cempaka on the low-level moisture transport was also examined. We found that In-Fa (2021) presented uncertain impact on 217HP, while Cempaka (2021) was found to be unfavorable for 217HP. Different from the LLSE water vapor transport, Cempaka mainly acted to weaken the southwesterly to the southwest of Henan by reducing the pressure gradient, and impeded the water vapor transport towards Henan.

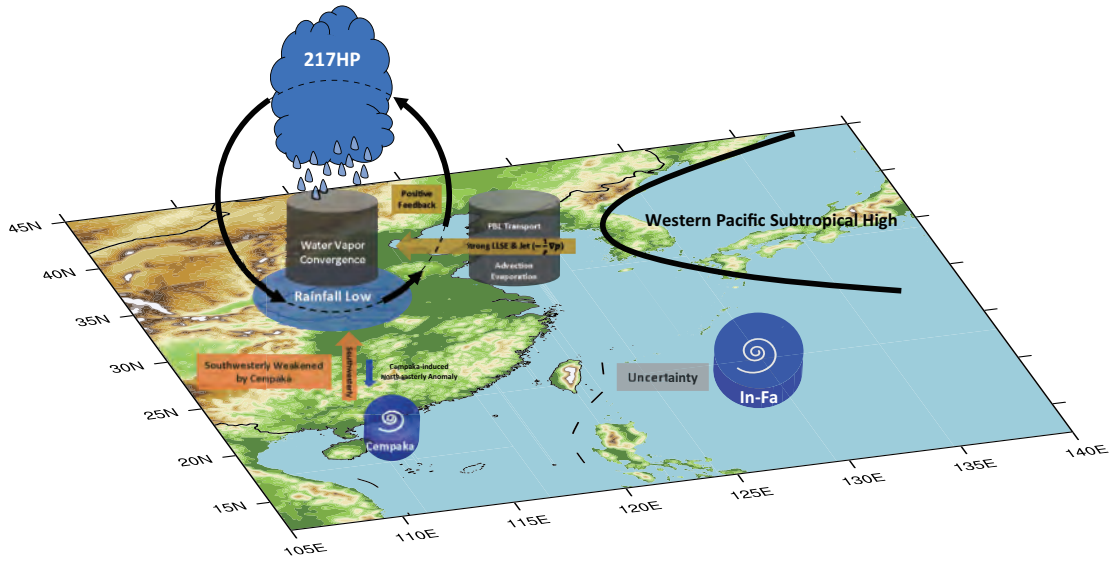

Figure 1. Schematic diagram of processes affecting moisture transport during 217HP. The source of precipitable water over Henan was mainly from the advection and evaporation below 950 hPa and PBL process above 950 hPa to the southeast of Henan, which were primarily driven by the strong LLSE (brown arrow). The LLSE was triggered and maintained by the WPSH to Henan's east and accelerated by the local rainfall system over Henan. Driven by the LLSE moisture transport, the local rainfall system over Henan lowered the local pressure and enhanced the LLSE moisture transport, further strengthening the heavy rainfall through positive feedback. Typhoon In-Fa showed large uncertainty on the heavy rainfall during 0000 UTC 18 July to 0000 UTC 21 July, while Cempaka impeded the heavy rainfall through weakening the southwesterly (orange arrow) moisture transport into Henan. The colored shadings represent the terrain height.

Impacts of Coastal Terrain on Warm-Sector Heavy-Rain-Producing MCSs in Southern China

Murong Zhang[a,d], Kristen L. Rasmussen[b], Zhiyong Meng[a], and Yipeng Huang[c]

[a] *Department of Atmospheric and Oceanic Sciences, Peking University, Beijing, China*

[b] *Department of Atmospheric Sciences, Colorado State University, Fort Collins, Colorado*

[c] *Xiamen Key Laboratory of Straits Meteorology, Xiamen Meteorological Bureau, Xiamen, China*

[d] *College of Ocean and Earth Sciences, Xiamen University, Xiamen, China*

Corresponding author: Zhiyong Meng, zymeng@pku.edu.cn

Warm-sector heavy rainfall in southern China refers to the heavy rainfall that occurs within a weakly-forced synoptic environment under the influence of monsoonal airflows. It is usually located near the southern coast, and is characterized by poor predictability and a close relationship with coastal terrain. This study investigates the impacts of coastal terrain on the initiation, organization and heavy-rainfall potential of MCSs in warm-sector heavy rainfall over southern China using quasi-idealized WRF simulations and terrain-modification experiments.

Typical warm-sector heavy rainfall events were selected to produce composite environments that forced the simulations. MCSs in these events all initiated in the early morning and developed into quasi-linear convective systems along the coast with a prominent backbuilding process. When the small coastal terrain is removed, the maximum 12-h rainfall accumulation decreases by ~46%. The convection initiation is advanced ~2 h with the help of orographic lifting associated with flow interaction with the coastal hills in the control experiment. Moreover, the coastal terrain weakens near-surface winds and thus decreases the deep-layer vertical wind shear component perpendicular to the coast and increases the component parallel to the coast; the coastal terrain also concentrates the moisture and instability over the coastal region by weakening the boundary layer jet. These modifications lead to faster upscale growth of convection and eventually a well-organized MCS. The coastal terrain is beneficial for backbuilding convection and thus persistent rainfall by providing orographic lifting for new cells on the western end of the MCS, and by facilitating a stronger and more stagnant cold pool, which stimulates new cells near its rear edge. The role of coastal terrain in the development of warm-sector heavy-rain-producing MCS is schematically demonstrated in Fig.1.

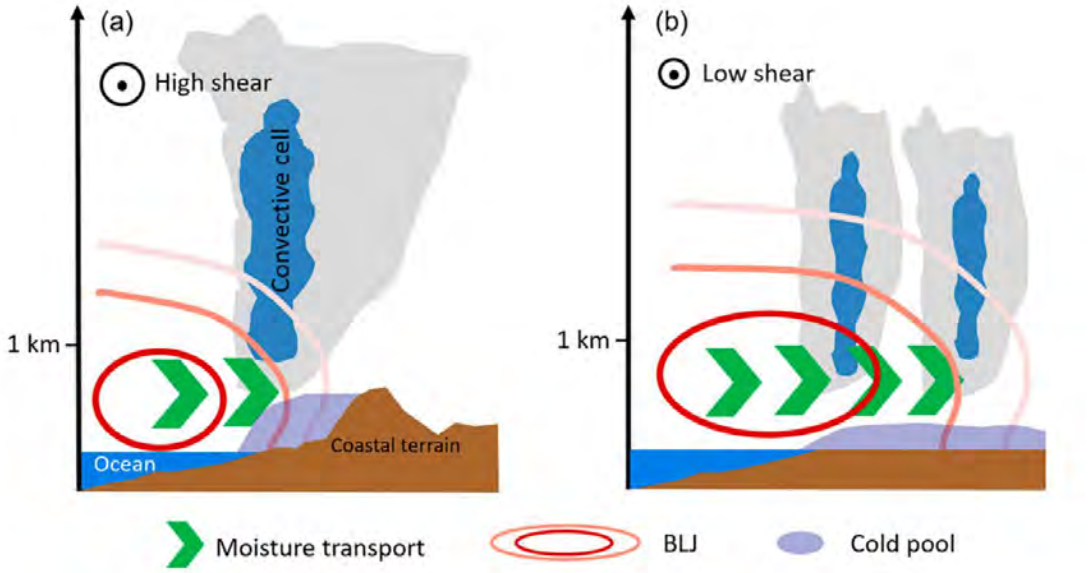

Fig. 1. Schematic diagram of the impacts of coastal terrain on warm-sector heavy-rain-producing MCSs. BLJ (red contour), moisture transport (green arrow), cold pool (light purple blob), environmental vertical wind shear (denoted on the top left) conditions, and convective cells (shading clusters) in (a) control run and (b) no-coastal-terrain run.

Current and Future Convective Storm Modes over CONUS from GPM Observations and Convection-permitting Regional Climate Model Simulations

Hungjui Yu [a], Kristen L. Rasmussen [a], Steven A. Rutledge, and Brenda Dolan[b]

[a] *Department of Atmospheric Science, Colorado State University, Fort Colloins, CO, USA*

Corresponding author: Hungjui Yu, hungjui@rams.colostate.edu

High-resolution convection-permitting regional climate model simulations employing the pseudo- global warming (PGW) approach are used to examine climatological changes in reflectivity and convective storm modes over the contiguous United States (CONUS). Two continuous 13-year convection-permitting regional climate simulations were conducted using (1) ERA-Interim reanalysis (CTRL simulation) and (2) ERA-Interim reanalysis plus a climate perturbation for the RCP8.5 scenario (PGW simulation). Four different storm modes, including deep convective cores, wide convective cores, deep and wide convective cores, and broad stratiform regions (DCC, WCC, DWCC, and BSR), are classified and analyzed in both the CTRL and PGW simulations using an objective algorithm that has been previously applied to space-borne precipitation radar observations. The 13-year CTRL simulation has a similar storm mode climatology, including spatial patterns of storm modes, compared to 9 years of Global Precipitation Measurement (GPM) Ku-band radar observations. The CTRL simulation shows prominent convective mode (DCC, WCC, and DWCC) occurrences over the southern Rocky Mountains, Great Plains, and from the Gulf of Mexico to the western Atlantic. Stratiform precipitation (BSRs) is concentrated over the northwestern coast and eastern part of the CONUS. In the PGW scenario, the simulations show an expansion and increase in the area and frequency for each convective mode throughout all seasons, with DCCs and DWCCs increasing the most (~180% and ~250%), indicating a more favorable environment for the development of intense convection in a future climate. The model performs well in representing the climatological patterns of storm mode occurrences and spatial distributions compared to GPM, despite some differences. Detailed comparisons of horizontal and vertical structures within the storm modes in the current and future climate will be presented. In summary, the objective method used for storm mode classification in satellite observations is for the first time deployed in a high-resolution convection-permitting model simulation, and it serves as a good approach to investigate changes in three-dimensional storm structures under different climate scenarios.

Multifractal Properties of Water Vapor Flux, Turbulence, and Precipitation Particles Distribution in Organizing Process of Mesoscale Convective Systems

Akiyuki ONO[a], Kosei YAMAGUCHI[b], Eiichi NAKAKITA[b]

[a] *Graduate School of Engineering, Kyoto University, Kyoto City, Kyoto, Japan*

[b] *Disaster Prevention Research Institute, Kyoto University, Uji City, Kyoto, Japan*

Corresponding author: Akiyuki ONO, ono.akiyuki.76n@st.kyoto-u.ac.jp

Mesoscale convective systems (MCSs) are high-risk phenomena that can cause serious disasters in the watersheds and rivers of Japan. Few studies have characterized the temporal and spatial patterns of the atmospheric fields in which MCSs are organized in a multifractal manner. Multifractal analysis quantitatively evaluates the shading of the physical quantity of interest to determine whether the field is monofractal, expressed as a uniform scaling index, or multifractal, consisting of a variety of indices. The objective of this study is to analyze the multifractal nature of the solid-phase precipitation particle distribution estimated from the water vapor flux, turbulent kinetic energy (TKE), and radar three-dimensional observations in a reproduced experiment, focusing on linear convection systems.

Multifractal analysis was performed using the method of Ono et al. (2022) for a line-shaped rainband that occurred on July 15, 2012. The horizontal/vertical grid resolution was set to 500 m/(average) 250 m and the computational domain was set to 600x600x61 layers centered in the Kinki region (Fig.1). The data were obtained from four X-band polarimetric radars in the Kinki region under the jurisdiction of the Ministry of Land, Infrastructure, Transport and Tourism, which made three-dimensional observations every five minutes. The mixing ratio of hail was estimated and analyzed using the polarization parameters above the melting layer.

Figures 2(a), 2(b) show the results of the multifractal analysis of the water vapor flux and TKE in the simulations. The generalized dimension D_7, which represents the multifractality of the water vapor flux, decreased about 30 min before rainfall intensity above 50 mm h^{-1} was observed at the surface. The result shows that the water vapor flux field with a moist lower layer before the onset of convection was close to a monofractal. On the other hand, the multifractality is strengthened when convection was generated and the extreme values of the water vapor flux associated with the updraft are expanded in the vertical direction. Before the onset of heavy rainfall the spectra are almost constant, indicating that the distribution is close to a monofractal, while TKE exhibits strong multifractal behavior at the onset of convective system (indicated by the warm

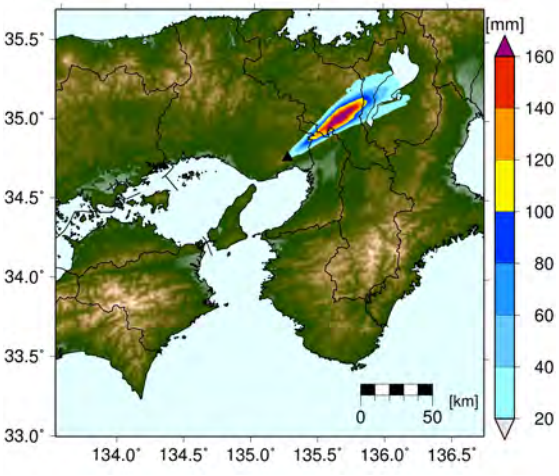

Figure 1: Computation region and 6hr accumulated rainfall obtained by X-band radars.

color), D_q increases slightly and the spectrum maintains a constant shape. This behavior of TKE was observed about 20 min before the formation of the zonal precipitation area, suggesting that it is one of the signals seen when the convective system is organized as a convective system.

The graupel area reached its first peak before and after the date, and reached its second peak when a zonal precipitation area was formed and expanded in Fig.2(c). Multifractal analysis of the estimated graupel mixing ratio showed that the multifractal state changed from strong to near monofractal after 0130 JST. Since there is a certain upper limit to the mass of precipitation particles, it is suggested that the distribution of ice-phase precipitation particles after the development of the convection system remained close to a monofractal state with little difference in scaling properties by maintaining a generally constant particle size distribution.

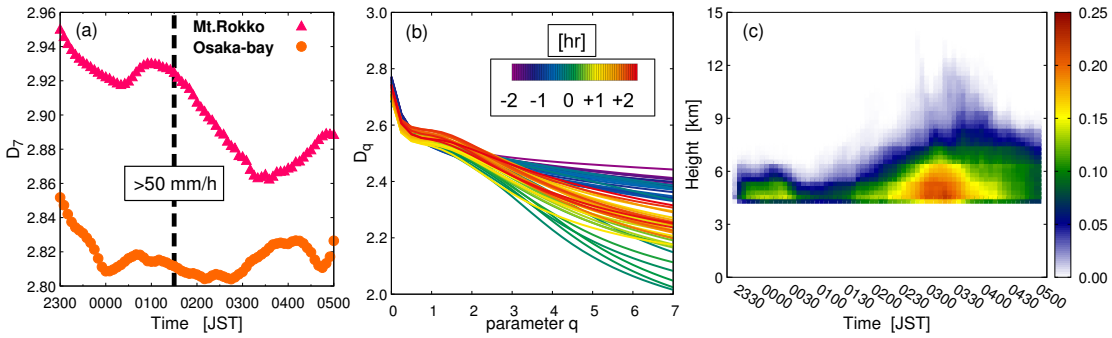

Figure 2: Multifractal spectrum of (a) water vapor flux and (b) TKE.

Acknowledgment: This research was supported by JSPS Grant-in-Aid for JSPS Fellows Grant Number JP22J13778, JST SPRING Grant Number JPMJSP2110, and JSPS KAKENHI JP15H05765, JP20H02258. The MSM and SST dataset was provided by Japan Meteorological Agency, Japan. The XRAIN observation data was provided by Ministry of Land, Infrastructure, and Tourism, Japan.

References

[1] Ono. A., Yamaguchi. K., and Nakakita. E., 2022. Multifractal Properties of Water Vapor Flux and Precipitation Particles in Line-shaped rain band. Journal of Japan Society of Civil Engineers, Ser. B1 (Hydraulic Engineering), 78, 2, 319-324.

Moisture Transport and Buoyancy in the Front and Wake of Tropical Convective Systems: HAMSR Sounding Observations in NASA CPEX Campaigns

Sun Wong [a], Mathias Schreier [a,], and Bjorn Lambrigtsen[a]

[a] JPL, California Institute of Technology, *Pasadena, CA, USA*

Corresponding author: Sun.Wong@jpl.nasa.gov

Moisture supply is an essential factor in modulating development of convection in the tropical atmosphere and, hence, modulating the movement of tropical convective systems. HAMSR, a microwave sounder, was mounted on the NASA DC-8 aircraft during NASA CPEX-AW (2021 August-September) and CPEX-CV (2022 September) campaigns and measured the temperature and specific humidity profiles in both clear and cloudy conditions when the aircraft flied through convective systems in the tropical Atlantic. The HAMSR measurements are also collocated with IMERG precipitation rate estimates and MERRA-2 moisture transport parameters to provide a thorough picture of how atmospheric thermodynamic conditions and moisture budgets in and around convective systems influence the systems' development and propagation. We use the HAMSR temperature and moisture profiles to calculate buoyancy profiles at the front and wake of tropical convective systems, including convection associated with a tropical storm and African Easterly Waves, and establish how buoyancy profiles are related to synoptic scale moisture transport and column moisture content. We found that a well-organized convective system is associated with a clear dipole pattern of moist and dry advection, with the moist (dry) advection located at the front (wake) of the dynamical convergence associated with the systems. Couplets of dry/moist anomalies with nearby cold anomalies (see Fig. 1) are stronger in the front of convective systems than the wake, reducing negative buoyancy in the PBL and weakening the convective inhibition. Such mechanism favors a thermodynamic condition of convective initiation in the front of the systems. Consequently, the systems and the associated precipitation propagate into the front direction where the moist advection is located by generating new convection in that direction. The aircraft also encountered cases of Saharan Air Layer, over which HAMSR can detect a strong temperature inversion associated with a large dry anomaly, providing a thermodynamic condition that hinders the growth of convection.

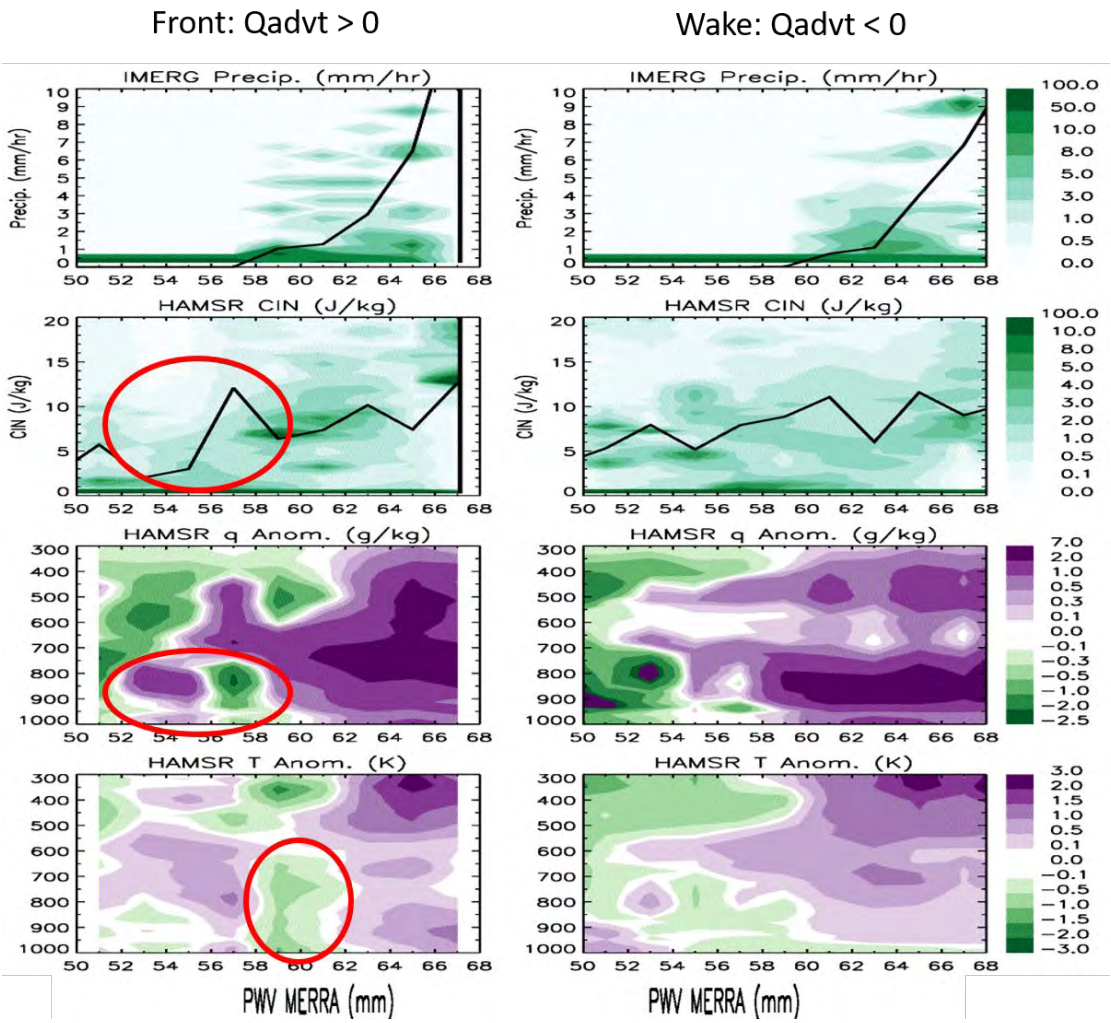

Figure 1 Composites of (top) IMERG rain rates (mm/hr), (2nd row) convection inhibition (CIN, J/kg) derived from HAMSR soundings, (3rd row) specific humidity anomalies (q Anom., g/kg), and (bottom) temperature anomalies (T Anom., K) as function of MERRA-2 precipitable water vapor (mm) for the front (left column) and wake (right colum) of convective systems encountered during 3 days of the NASA CPEX-AW campaign in late August to early September of 2021.

Initial Insights into Tropical Oceanic Mesoscale Convective Systems from the NASA Convective Processes Experiment – Cabo Verde (CPEX-CV)

Angela Rowe[a], Benjamin Rodenkirch[a], Giselle Martine[a], Ed Zipser [b], Mani Rajagopal[b], Sun Wong[c], John Cooney[d], Svetla Hristova-Veleva[c], Naoko Sakaeda[e], Kris Bedka[d], E. P. Nowottnick[f], A. R. Amin[d], J. Zawislak[f]

[a] *University of Wisconsin-Madison, Madison, WI, U.S.A.*

[b] *University of Utah, Salt Lake City, UT, U.S.A.*

[c] *Jet Propulsion Laboratory, Pasadena, CA, U.S.A.*

[d] *NASA Langley Research Center, Hampton, VA, U.S.A.*

[e] *University of Oklahoma, Norman, OK, U.S.A.*

[f] *NASA Goddard Space Flight Center, Greenbelt, MD, U.S.A.*

[g] *NOAA Aircraft Operations Center, Lakeland, FL, U.S.A.*

Corresponding author: Angela Rowe, akrowe@wisc.edu

Previous studies using airborne field measurements, reanalysis datasets, spaceborne instrumentation, and model output have long inferred relationships between the intensity, lifecycle, and impacts of mesoscale convective systems (MCS) with their environment across tropical oceanic basins. However, these relationships have varied depending on the datasets used, methods to calculate these metrics, and which oceanic basin being studied. In an effort to better understand these relationships, and with future spaceborne missions aiming to improve these global measurements including winds and moisture in the near-storm environment, the NASA Convective Processes Experiment (CPEX) field campaign series have approached these goals through a unique airborne payload. With 2017's CPEX and 2021's CPEX-Aerosols Wind (CPEX-AW), measurements were collected over the Gulf of Mexico, Caribbean, and Western Atlantic, while the recent 2022 CPEX-Cabo Verde (CPEX-CV) campaign focused on the eastern Atlantic off the west African Coast. Equipped with a multi-frequency radar, lidars, radiometer, dropsondes, and in situ measurements, the DC-8 sampled a range of convective systems and environments during these campaigns.

This presentation will introduce the mission objectives, flight strategies, and unique airborne payload of CPEX-CV, describe initial results linking MCSs with their environment in the context of CPEX and CPEX-AW and of satellite-based precipitation estimates, and highlight collaborative research opportunities from these unique datasets. Particular attention will be given to a CPEX-CV flight in which convective lifecycle

was sampled within a weak African Easterly Wave that eventually was linked to Hurricane Ian in the west Atlantic.

A review of research on the record-breaking precipitation event in Henan Province of China, July 2021

Qinghong Zhang [a,b], Rumeng Li [a], and Juanzhen Sun[c] Feng Lu[d], Jun Xu[e] , Fan Zhang[b]

[a] *Department of Atmospheric & Oceanic sciences, School of Physics, Beijing 100871, China*

[b] *HIWeather International Coordination Office, Chinese Academy of Meteorological Sciences, Beijing 100081, China*

[c] *National Center for Atmospheric Science, Boulder, Colorado*

[d] *Innovation Center for Feng Yun Meteorological Satellite, National Satellite Meteorological Center (National Center for Space Weather), China Meteorological Administrations, Beijing 100049, China*

[e] *National Meteorological Center of China, Beijing 100081, China*

Corresponding author: Qinghong Zhang, qzhang@pku.edu.cn

A record-breaking precipitation event caused 398 deaths and 20.06 billion RMB economic losses in Henan Province of China in July 2021. A maximum 24-h (1-h) precipitation of 624 mm (201.9mm) was observed at the Zhengzhou weather station. However, all global operational forecast models failed to predict the intensity and location of maximum precipitation for the event. This high social impact event has drawn much attention from the research community. This presentation provides a high-level review of the event and its research from the perspectives of observations, analysis, dynamics, predictability, and the connection with climate warming and urbanization.

Global reanalysis revealed obvious abnormality in large-scale circulation patterns that resulted in abundant moisture supplies in the region of interest (Figure 1). The circulation pattern in July 19−21, 2021 were previously observed in only 1.6% of all summer days in the past 42 years. However, the extreme large-scale circulation pattern could not completely explain the record-breaking event; other dynamic processes related to mesoscale convective storms may have been contributing factors. Based on high-resolution model simulation and data assimilation, the rainstorm was found to formed via the sequential merging of three convective cells, which were initiated along the convergence bands in a meso-beta-scale low-pressure system (mesolow). Three mesoscale systems (a mesoscale low pressure system, a barrier jet and downslope gravity current) contributed to the local intensification of the rainstorm (Figure 2). Further, observational analysis suggested that an abrupt increase of graupel through microphysical processes contributed to the record-breaking precipitation.

Although these findings aided in our understanding of the extreme rainfall event, preliminary analysis indicated that the practical predictability of the extreme rainfall for this event was rather low. The contrary influences of climate warming and urbanization on precipitation extremes as revealed by two studies could add further challenges to the predictability. We concluded by emphasizing that data sharing and

collaboration between meteorological and hydrological researchers would be crucial in the future research on high-impact weather events.

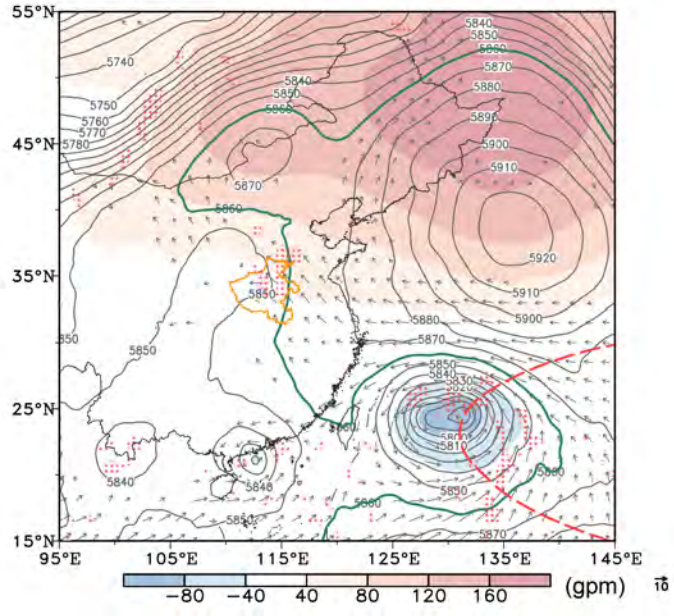

Figure 1 Geopotential height (contour) and its anomalies (shaded, unit: gpm) at 500 hPa from July 19 to 21, 2021. The green solid line and red dashed line denote the 5,860 gpm contour in the three-day period and associated climatology in the period 1980−2021, respectively. The vectors correspond to 925 hPa wind with a velocity > 4 m/s. Red dots represent 200 hPa divergence > 10^{-5} s^{-1}. The orange line is the boundary of Henan Province.

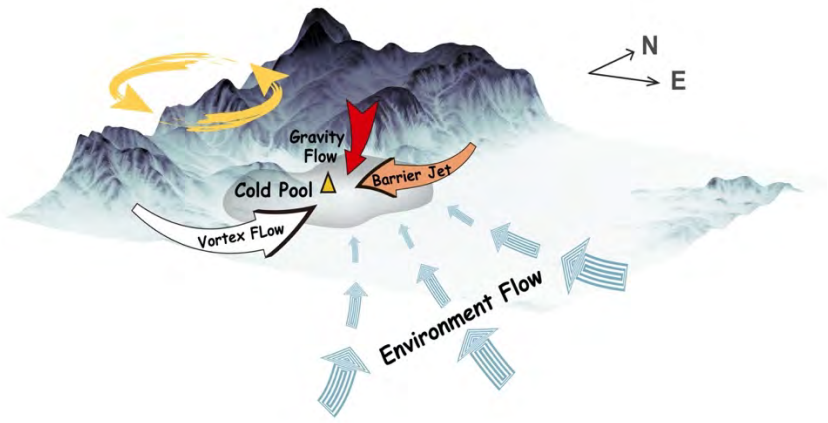

Figure 2 Schematic diagram of the multiscale dynamical processes responsible for the extreme hourly rainfall in Zhengzhou on July 21, 2021. Golden triangle is the location of Zhengzhou city. The turquoise, white, red, and brown arrows represent the environmental flow, the southwesterly flow from the mesolow, the gravity flow original from the top of Taihang Mountains, and the barrier jet, respectively. The light yellow circular arrows indicate the mid-level circulation of the mesolow.

Assessing the Predictability of Derecho-Producing Mesoscale Convective Systems Using a Convection-Allowing Ensemble

Bruno Ribeiro [a], Lance Bosart [a], and Steven Weiss[b]

[a] Department of Atmospheric and Environmental Sciences, University at Albany, Albany, NY

[b] *Storm Prediction Center, Norman, OK (retired)*

Corresponding author: Bruno Ribeiro, bribeiro@albany.edu

Derechos produced by progressive mesoscale convective systems (MCSs) during the warm season are often associated with low predictability. The convective initiation and upscale growth into a MCS and subsequent propagation as a bow echo system depend upon mesoscale and storm-scale processes that are often not well handled by convection-allowing models. In this study, a 10-member convection-allowing ensemble using the Model for Prediction Across Scales (MPAS) is run for twenty warm-season progressive derechos that occurred in the United States. The main goal is to explore differences in members that produced a progressive MCS and members that did not. The MPAS mesh is global and has 60 km spacing over most of the globe decreasing to 3 km over the area where the derecho occurred. The ensemble is initialized using Global Ensemble Forecasting System (GEFS) analyses from five days before the event to the day of the event, thus fifty forecasts of the same derecho are run with five different lead times. The hourly maximum wind speed at the lowest model level is used as a severe wind gust surrogate. The members are then classified based on four aspects: convective mode, severe wind initiation timing, displacement of the severe wind axis and severe wind areal coverage. Composites of more successful members (i.e., members that produced a progressive MCS similar to observations) with less successful members were created to explore the main physical processes leading to different forecasts in the ensemble. There is higher CAPE, weaker convective inhibition and stronger warm advection in the more successful members compared to less successful members that produced storms at the right time and location but with the wrong convective mode or members that did not produce storms. More successful members were also capable of producing greater precipitation in the 3 h before derecho initiation (defined as the time of the first observed wind report), leading to a larger 2-m temperature decrease due to faster intensification of the cold pool. Therefore, stronger forcing for ascent, higher instability and lower convective inhibition, which favor stronger convection and faster cold-pool intensification in the early stages of the derecho, appear to be related to upscale growth into a progressive MCS.

Sources of Forecast Errors for Extreme-Rain-Producing Mesoscale Convective Systems

Russ S. Schumacher [a], and Aaron J. Hill [a]

[a] *Department of Atmospheric Science, Colorado State University, Fort Collins, Colorado, USA*

Corresponding author: Russ Schumacher, russ.schumacher@colostate.edu

Mesoscale convective systems (MCSs) produce a large proportion of the extreme rainfall events in the United States and around the world. Considerable progress has been made in the understanding and prediction of these MCSs, but their details remain very challenging to forecast. This presentation will investigate the reasons for errors in the timing, location, and rainfall production in model forecasts of heavily raining MCSs. In particular, the MCSs of 26-28 July 2022, which led to devastating flooding in eastern Kentucky, will be examined. As is often the case for extreme-rain-producing MCSs, numerical weather prediction models correctly indicated that heavy rain would occur somewhere in the general region where it was observed, but with large differences in the location and precipitation amounts. These differences were largely connected to uncertainties in the water vapor in the inflow to the MCS: model forecasts with ample low-level moisture correctly predicted extreme precipitation, but those with relatively dry inflow produced only modest rainfall accumulations. These findings are consistent with other past studies of MCS forecast errors, and underscore the importance of accurately observing boundary-layer moisture in predicting warm-season heavy rainfall.

Shrinking Circulation of Tropical Cyclones in the Warming Climate?

Buo-Fu Chen[a], Boyo Chen[a], and Chun-Min Hsiao[b]

[a]*Center for Weather Climate and Disaster Research, National Taiwan University, Taipei, Taiwan*

[b]*Weather Forecast Center, Central Weather Bureau, Taipei, Taiwan*

Corresponding author: Buo-Fu Chen, bfchen@ntu.edu.tw

Understanding trends and variability of tropical cyclone (TC) activity, intensity, and size in the past provides a critical basis for researching future TC projections in the changing climate. From the perspective of type-II error avoidance, the anthropogenic influences are linked to TC poleward migration, TC-associated extreme precipitation, and an increased proportion of major hurricanes or typhoons. However, uncertainty in the subjective-analyzed historical datasets leads to relatively low confidence in the assessed and projected responses of TC to climate change. Also, little literature can discuss the TC size and structure in the changing climate due to insufficient data.

Here, we construct a new dataset of accurate structural reanalysis for global TCs since the 1980s with a deep learning approach. Our deep learning model is trained on a uniquely-labeled dataset integrating TC best-track data and numerical model reanalysis of TCs during 2004−2016, enabling the model to convert multi-channel satellite imagery to a 0−750-km wind profile of the axisymmetric TC surface winds. The model performance is verified based on independent satellite ASCAT and SAR datasets of accurate and direct wind observation for 2017−19 TCs.

As this novel dataset is suitable for calculating the overall TC energy/circulation, we examined the climatological trends of intensity (V_{max}) and 50~600-km averaged relative angular momentum (AM) for historical TCs from 1981 to 2020. Based on the homogenized V_{max} data, we find an increased probability that the storm would reach V_{max} over 100 kt once it becomes a typhoon/hurricane. However, no significant V_{max} trends are found for the major typhoon/hurricane proportion to all samples. Furthermore, a decreasing trend of annual-mean TC AM is found for global TCs, as well as a ~20% decrease in large-AM (75^{th} percentile) TC proportion. However, a ~10% increase in extremely-large-AM (95^{th} percentile) TC proportion is found. It is hypothesized that the overall shrinking circulation may be related to the poleward migration of TC tracks to lower SST and higher VWS regions. However, for some still developing TCs, the high-latitude Coriolis torque may contribute to additional growth of TC outer circulation. We anticipate this deep learning approach can provide better data for further investigating physical mechanisms that explain the climate TC trends, accessing the influences from intertwined natural variabilities to those trends, and verifying the simulation of TC structure in the numerical climate model.

Ingredients-based approach to understanding mesoscale processes in numerous heavy rainfall events in Taiwan

Extreme rainfall is a high impact weather phenomenon that profoundly affects people around the world, but our fundamental understanding and quantitative forecast skill for these events remains limited. To address these important scientific and forecast challenges, the Prediction of Rainfall Extremes Campaign In the Pacific (PRECIP) field experiment in summer 2022 aimed to improve our understanding of the multi-scale dynamic and thermodynamic processes that produce extreme precipitation in the moisture-rich regions of Taiwan and Yonaguni Island, Japan. In this presentation, three topics will be covered: (1) Climatological perspectives on the frequency and occurrence of mesoscale storm modes and their associated ingredients from the TRMM satellite and ERA5 reanalysis, (2) Analysis of the impact of terrain modification on mesoscale storm modes associated with a record-breaking Meiyu front event over Taiwan, and (3) Analysis of several PRECIP 2022 case studies and their associated mesoscale storm modes, comparisons with satellite observations, and the atmospheric ingredients supporting such events. When combined, these three topics will provide a broad picture of ingredients supporting mesoscale storm modes associated with heavy rainfall in Taiwan, with an aim of generalizing our understanding of heavy rainfall processes on a global scale.

Sensitivity of Tropical Oceanic Convection to Horizontal Model Resolution in Idealized Simulations Forced with PRECIP Observations

Rosimar Rios-Berrios[a] *and George H. Bryan*[a]

[a] *National Center for Atmospheric Research, Boulder, CO, USA*

Corresponding author: Rosimar Rios-Berrios, rberrios@ucaar.edu

Recent studies have shown that tropical oceanic phenomena, including equatorial waves and organized rainfall systems, are better represented by models with explicitly resolved convection than with a convective parameterization. However, other studies suggest that typical convection-permitting resolution (i.e., 1-5 km grid spacing) is insufficient to resolve the narrow nature of tropical convective updrafts. Those same studies suggest that a convective parameterization is needed, even at sub-10-km grid spacing, to accurately represent tropical convection including extreme rainfall. To address these issues, this study seeks to investigate the sensitivity of tropical oceanic convection to horizontal model resolution using a hierarchy of model simulations—using grid spacings all the way from 15 km to 50 m. The simulations are initialized with an observed sounding from the 29 July 2022 extreme rainfall event that was sampled in detail during the Prediction of Rainfall Extremes Campaign in the Pacific. Distributions of rainfall rate and simulated reflectivity are compared to understand the similarities and differences amongst different resolutions. A comparison against statistics from radar and disdrometer observations further helps establish the advantages and deficiencies of each model resolution.

Intense Surface Winds from Gravity Wave Breaking in Simulations of a Destructive Macroburst

Russ S. Schumacher [a], Samuel J. Childs[a], and Rebecca D. Adams-Selin [b]

[a] *Department of Atmospheric Science, Colorado State University, Fort Collins, Colorado, USA*

[b] *Verisk Atmospheric and Environmental Research, Bellevue, Nebraska*

Corresponding author: Russ Schumacher, russ.schumacher@colostate.edu

Shortly after 0600 UTC (midnight local time) 9 June 2020, a convective line produced severe winds across parts of northeast Colorado that caused extensive damage, especially in the town of Akron. High-resolution observations showed gusts exceeding 50 m s^{-1}, accompanied by extremely large pressure fluctuations, including a 5-hPa pressure surge in 19 s immediately following the strongest winds and a 15-hPa pressure drop in the following 3 min. Numerical simulations of this event (using the WRF Model) and with horizontally homogeneous initial conditions (using Cloud Model 1) reveal that the severe winds in this event were associated with gravity wave dynamics. In a very stable postfrontal environment, elevated convection initiated and led to a long-lived gravity wave. Strong low-level vertical wind shear supported the amplification and eventual breaking of this wave, resulting in at least two sequential strong downbursts. This wave-breaking mechanism is different from the usual downburst mechanism associated with negative buoyancy resulting from latent cooling. The model output reproduces key features of the high-resolution observations, including similar convective structures, large temperature and pressure fluctuations, and intense near-surface wind speeds. The findings of this study reveal a series of previously unexplored mesoscale and storm-scale processes that can result in destructive winds.

Effects of Initial and Boundary Conditions on Heavy Rainfall Prediction over the Yellow Sea: Validation with Dropsonde Measurements

Jiwon Hwang[a] and Dong-Hyun Cha[a]

[a] *Department of Urban & Environmental Engineering, Ulsan National Institute of Science and Technology, 50 UNIST-gil, Ulju-gun, Ulsan 689-798, South Korea*

Corresponding author: Dong-Hyun Cha, dhcha@unist.ac.kr

The objective of this study was to examine the effect of initial and boundary conditions on the forecast of heavy rainfall over the Yellow Sea and Korean Peninsula using the Weather Research and Forecasting (WRF) model initialized by two operational global model analyses from NCEP and ECWMF. Before applying the two analysis fields to the WRF model, it was found that the temperature and relative humidity difference of the ECMWF analysis against the dropsonde data were overall less than those of the NCEP analysis. In general, the ECMWF analysis depicted atmospheric conditions that were warmer and wetter than the NCEP analysis. This difference was most pronounced below 850 hPa in the lower atmosphere. The WRF model with the initial and lateral boundary conditions from the ECMWF analysis had a better performance of the heavy rainfall forecast over the Yellow Sea compared to that from the NCEP analysis. Based on these findings, it is suggested that the use of ECMWF analysis data will attribute to a more precise simulation of unstable and fast-growing convection systems. These findings indicate that the quality of the initial field has a significant impact on the effectiveness of numerical weather forecasting models.

Linking Microphysical Processes to Rainfall Intensity and Duration in Complex Terrain

Angela Rowe[a], Ian Cornejo[a], Kristen Rasmussen[b], Alison Nugent[c]

[a] *University of Wisconsin-Madison, Madison, WI, U.S.A.*

[b] *Colorado State University, Fort Collins, CO, U.S.A.*

[c] *University of Hawai'i at Mānoa, Honolulu, HI, U.S.A.*

Corresponding author: Angela Rowe, akrowe@wisc.edu

Extreme rainfall remains a forecasting challenge, with events spanning a spectrum of high intensities and short durations to weaker precipitation intensity over longer durations. In a moisture-rich environment, ingredients and processes leading to extreme rainfall are likely to vary across this spectrum, with varying roles of strong vertical velocity with high precipitation efficiencies and horizontal forcing replenishing the moisture. Steep topography modifies these ingredients and processes, with impacts on precipitation location, intensity, and duration that complicates our understanding and prediction capabilities. The 2022 Prediction of Rainfall Extremes Campaign in the Pacific (PRECIP) in Taiwan and Japan aimed to address these unknowns and challenges through observing rainfall events across the intensity/duration spectrum, including those occurring during the Mei-Yu/Baiu season, diurnally driven afternoon convection, and tropical cyclone influences. Measurements from the dual-polarization research radar (S-Pol), deployed throughout the nearly 3-month campaign in northwest Taiwan, provide high-resolution, continuous observations of both heavy and non-heavy rainfall over both the steep terrain and nearby water to investigate common and unique microphysical processes leading to heavy rainfall in Taiwan and the role the topography plays in modifying those processes. This presentation will describe the hypotheses driving these microphysical measurements in the context of previous campaigns and a look into the range of rainfall events captured during PRECIP 2022 including S-Pol observations. Additionally, pathways forward using this exciting dataset will be presented to address this microphysical aspect of our overarching goal to improve understanding and prediction of heavy rainfall.

Integrated Physical Analysis of Past Line-shaped Convective Systems for Mechanisms Investigation

Kana Fukuda[a], Yukari Naka[b], and Eiichi Nakakita[b]

[a] *Graduate School of Engineering, Kyoto University, Osaka, Japan*

[b] *DPRI, Kyoto University, Kyoto, Japan*

Corresponding author: Yukari Naka, naka@hmd.dpri.kyoto-u.ac.jp

In Japan, line-shaped convective systems with Baiu front have caused many heavy rainfall events triggered disasters recently. It is important for disaster prevention to investigate mechanisms of line-shaped convective systems. In addition, the consideration of spatial and temporal characteristics of rainfall is necessary because the difference of spatial and temporal scale makes a difference of characteristics of disasters. Then, the purpose of this research is to analyze past events of line-shaped convective systems considering spatial and temporal characteristics.

At first, we detected line-shaped convective system events from the spatial distribution of 3-hour rainfall of Rader-AMeDAS (Automated Meteorological Data Acquisition System) from 2006 to 2020 by ellipse approximation, and classified them into two types, type-A and type-B. As shown on the Figure1, type-A is large scale and occurs near convergence of Baiu front, while type-B is small scale and occurs more than 100km away from Baiu front. Figure 2 represents the occurrence location of each type detected by ellipse approximation, and shows that events of type-A (red) occur all over Japan, while that of type-B (blue) mainly occur Pacific Ocean side.

After the classification, we analyzed environment conditions when line-shaped convective systems occur. Firstly, we checked vertical profiles of water vapor mixing ratio and EPT (Equivalent Potential Temperature). According to the profile of water vapor mixing ratio, the atmospheric condition when type-A occur is humid from bottom to middle layer, while that of type-B occurrence has much humid air at bottom layer. In addition, the profile of EPT shows type-B is more convective instable than type-A. Secondly, we focused on spatial distribution of environmental parameters of CAPE (Convective Available Potential Energy) and BRN (Bulk Richardson Number). CAPE means atmospheric instability represented by the vertical integration of buoyancy, and BRN is the ratio of buoyancy to turbulence and is said to be about 32 when line-shaped convective systems occur by previous research (Nakakita et al., 2000). As a result, we found type-B has large CAPE and BRN of type-B tend to be almost equal to 32 locally at occurrence area. Lastly, we made hodograph of each type, and it showed type-B has vertically change in direction of wind.

Therefore, we found differences of occurrence location and environment between types. Moreover, this research shows type-B occurs at more limited and idealized environment than type-A. Considering below results, we suppose that the large convergence of Baiu front significantly influences on occurrence of type-A and the

environmental condition when type-A occur is not necessarily idealized. On the other hand, without external force of large convergence, environmental condition of type-B is supposed to be limited and idealized. In the future, using more numerous past events, we will quantitively analyze environment of line-shaped convective systems occurring and developing.

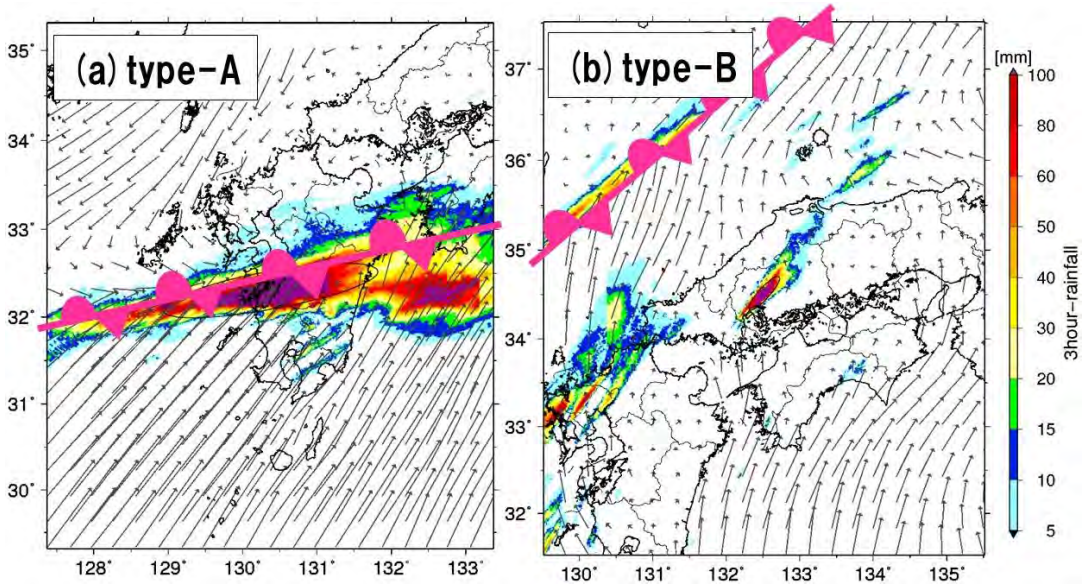

Figure 1. Spatial distribution of 3-hour rainfall obtained from Rader-AMeDAS: (a) example of type-A at Kumamoto, Japan (2020/7/4 20:00(UTC)), (b) example of type-B at Hiroshima, Japan (2014/8/19 19:00(UTC)). Pink line shows Baiu front, and black solid arrows show water vapor flux based on MSM (Meso Scale Model).

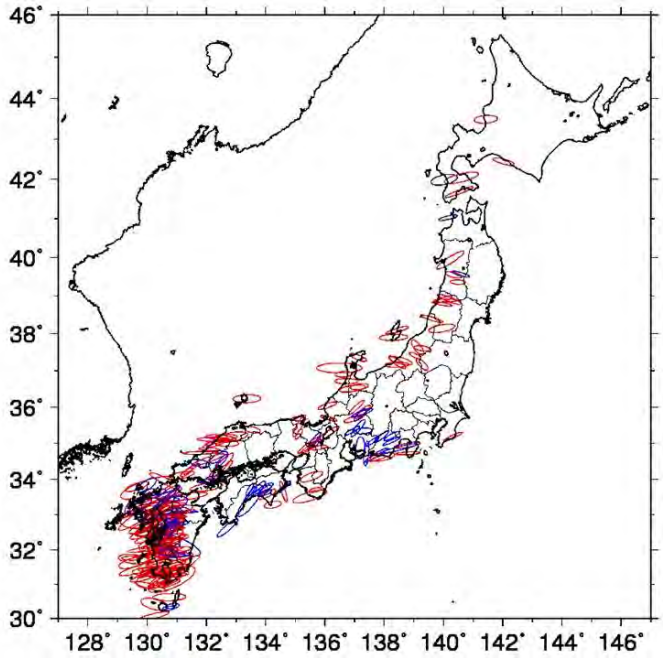

Figure 2. Map of Japan plotted occurrence location detected by ellipse approximation. Red line represents type-A and blue line represents type-B, respectively.

References

Nakakita, E., Yagami, T. and Ikebuchi, S.: Characteristics of Generation and Propagation of Localized Heavy Rainfall over Nasu Region in 1998, Annual Journal of Hydraulic Engineering, Vol 44, pp.109-114, 2000, February.

Case study of cold-air damming induce intensive winter precipitation in northeast Taiwan

Yung-Chuan Yang[a], and Wei-Yu Chang [a]

[a] *National Central University, Taoyuan, Taiwan*

Corresponding author: Wei-Yu. Chang, wychang@g.ncu.edu.tw

The field campaign YESR (Yilan Experiment of Severe Rainfall) with high spatiotemporal resolution observations aims to examine the thermal structure and dynamics processes of winter precipitation in the Lanyang plain of northeast Taiwan. The physical processes of a intensive precipitation event with about 70 mm daily accumulated rainfall was investigated. Based on the thermal analysis from ST (Storm Tracker mini-radiosonde) data, a pronounced cold advection flow is found in the interior of Lanyang plain. The colder air was advected by the inland southward flow downstream of the synoptic cold-high in the north. The prevailing northeasterly wind collided the interior north-northeasterly and facilitated the developments of convections. This feature is revealed by 3-D kinematic fields from the Multiple–Doppler Radar Three-Dimensional Wind Synthesis Method (WISSDOM). The precipitation further intensified as the development of the cold-air damming due to the terrain blocking. These results indicate the importance of sub-scale flow of precipitation system induced by the complex terrain of Yilan.

Investigating the Relationships Between Rotation and Heavy Rainfall Along the Mei-yu Front During PRECIP 2022

Jennifer C. DeHart [a], Michael M. Bell [a], and Tyler Barbero[a]

[a] *Colorado State University, Fort Collins, CO, USA*

Corresponding author: Jennifer DeHart, jcdehart@colostate.edu

Extreme rainfall is an important weather phenomenon due to the high potential for loss of life and property; however, our forecast skill remains limited, especially on smaller spatial scales. Recent research has shown a positive relationship between the strength of low-level mesoscale rotation and rainfall rates through nonlinear dynamic accelerations driven by negative pressure perturbations. This relationship has been explored in continental convective storms and a landfalling tropical storm, but has not yet been explored in the context of mei-yu frontal precipitation. Recent results from a numerical simulation show a positive relationship between potential vorticity and rainfall rates in association with meridional moisture flux and isentropic ascent along the mei-yu front. Other nonlinear interactions between vorticity and the boundary layer can also produce localized ascent. The relationships between rotation and rainfall, and which of these mechanisms plays a role in the context of mei-yu frontal precipitation, remain to be explored.

This study analyzes Doppler radar data from operational and research radars collected during the NSF-funded Prediction of Rainfall Extremes Campaign in the Pacific (PRECIP) experiment held in Taiwan and southern Japan in 2022. Multi-Doppler analyses generated by the Spline Analysis at Mesoscale Utilizing Radar and Aircraft Instrumentation (SAMURAI) application are used to compare the kinematic and precipitation structures during the 2022 mei-yu period. The three-dimensional analyses provide best estimates of vertical motion, vorticity, and precipitation characteristics to evaluate the relationship between rotation, ascent, and rainfall intensity. This study examines convection over two intensive operating periods during the 2022 mei-yu season to examine the statistical relationships between these quantities on different spatial scales.

Synoptic Pattern Classification of Heavy Rainfall Systems in Monsoon Season over the Korean Peninsula

Seungyeon Lee [a,b,c] and Seon Ki Park[a,b,c]

[a] *Department of Climate and Energy Systems Engineering, Ewha Womans University, Seoul, Republic of Korea*

[b] *Center for Climate/Environment Change Prediction Research, Ewha Womans University, Seoul, Republic of Korea*

[c] *Severe Storm Research Center, Ewha Womans University, Seoul, Republic of Korea*

Corresponding author: Seon Ki Park, spark@ewha.ac.kr

The monsoon season in the Korean Peninsula (KP) usually brings about concentrated heavy rainfall events, leading to significant human and property losses. In August 2022, the monsoon front stalled in the central region of the KP; the maximum hourly rainfall exceeded the capacity of Seoul's drainage system. The 24-hour maximum rainfall recorded was 435mm, resulting in severe flooding. To enhance early prediction of future monsoon occurrences, particularly in discerning differences among cases that occur in various regions, this study aims to classify the synoptic weather patterns of monsoons in the KP. Principal components analysis (PCA) and K-means clustering were utilized to classify the synoptic weather patterns of monsoons that took place from 2000 to 2022. The fifth generation of the European Centre for Medium-Range Weather Forecasts (ECMWF) reanalysis data (ERA5) was used to determine the most significant variables in distinguishing between different types of heavy rainfall cases in the monsoon season over the KP. We investigate whether this method can effectively classify the differences in heavy rainfall regions — the central, southern and northern regions in the KP. This study also identifies the most influential variables that differentiate between different types of heavy rainfall events, including atmospheric pressure, temperature, humidity, and wind. The synoptic pattern classification of heavy rainfall systems in the monsoon season over the Korean Peninsula is crucial in predicting future weather events, particularly in discerning differences among cases that occur in various regions. This study can provide a basis for predicting future heavy rainfall in monsoon season over the characteristic regions in the KP.

Development of the Rapid Refresh Forecast System Data Assimilation System (RDAS) for an Expected Operational Implementation in 2024

For: 15th International Conference on Mesoscale Convective Systems (ICMCS-XV)
https://icmcs15.colostate.edu/

Terra Ladwig, NOAA/OAR/GSL Boulder, CO, USA;
David Dowell, NOAA GSL
Chunhua Zhou, CU/CIRES@ NOAA GSL
Ming Hu, NOAA GSL
Ruifang Li, NOAA GSL
Amanda Back, CSU/CIRA@ NOAA GSL
Stephen Weygandt, NOAA GSL
Curtis Alexander, NOAA GSL
Donald Lippi, Lynker@ NOAA NWS NCEP EMC
Shun Liu, NOAA NWS NCEP EMC
Ting Lei, Lynker@ NOAA NWS NCEP EMC
Sho Yokota, JMA and UCAR Visiting Scientist @ NOAA NWS NCEP EMC
Jili Dong, SAIC@ NOAA NWS NCEP EMC
Matthew Pyle, NOAA NWS NCEP EMC
Jacob R. Carley, NOAA NWS NCEP EMC

Successful data assimilation is of paramount importance for initializing numerical models. The Rapid Refresh Forecast System (RRFS) is NOAA's next generation regional convection-allowing ensemble forecast system within the wider Unified Forecast System (UFS) community. NOAA's Global Systems Laboratory (GSL) and NOAA's Environmental Modeling Center (EMC) are developing the hourly Data Assimilation System to initialize RRFS version 1, known as RDAS, which is expected to be implemented in 2024.

The RDAS includes two components. (1) A 30 member ensemble with hourly EnKF assimilation of conventional and radar observations. RDAS-EnKF provides initial conditions for ensemble forecasts. RDAS-EnKF also provides storm-scale ensemble covariance information for (2) hourly 3DEnVar assimilation of conventional and radar observations to initialize deterministic control forecasts. The control is used periodically to recenter the ensemble members.

This presentation will introduce the details of RDAS as well as share results from warm season convective events. Key areas of development for RDAS are the initialization of the convective scale ensemble and the maintenance ensemble spread during the data assimilation cycling. Both of these data assimilation system aspects are important for improving severe thunderstorm forecasts. During development we have investigated sensitivity to localization lengths, inflation to prior spread parameters, recentering frequency, and ensemble initialization frequency. Results from Spring 2022 and Summer 2022 retrospective testing have narrowed the RDAS parameter choices. Real-time results from Spring 2023 severe convective cases will also be presented. Lastly progress towards operational implementation and remaining science questions will be discussed.

Gravity Waves Associated with Frontal Rainfall as a Preconditioning Mechanism for Warm-Sector Heavy Rainfall in South China

Hongpei Yang [a], Yu Du [a], and Zijian Chen[a]

[a] *School of Atmospheric Sciences, Sun Yat-sen University, and Southern Marine Science and Engineering Guangdong Laboratory (Zhuhai), Zhuhai, China*

Corresponding author: Du Yu, duyu7@mail.sysu.edu.cn

This study investigates the convective preconditioning mechanisms for nocturnal coastal heavy rainfall in the warm-sector of a quasi-stationary front in South China on 10–11 May 2014. We conducted cloud-permitting numerical simulations and found that, in addition to mesoscale lifting provided by double low-level jets, convective preconditioning played a vital role in this event. The preconditioning was characterized by mid-level moistening and destabilization with wave-like variation over the region, which was induced by gravity waves associated with low-level ascent and high-level descent (n=2 wave). These hydrostatic waves propagated southeastward at a speed of ~27 m s^{-1}. The low-level upward motions of the waves were strongest at approximately 3 km AGL, and greatly enhanced relative humidity through adiabatic cooling and vertical transport of water vapor. These gravity waves are mainly generated during the evolution of northern frontal rainfall forced by synoptic forcings. As frontal rainfall strengthened, low-level diabatic cooling from rainwater evaporation triggered n=2 waves, further enhancing relative humidity along wave path. This process is confirmed through vertical Flourier decomposition of the vertical temperature profile over the frontal region. A sensitivity experiment with an earlier initial condition failed to reproduce the preconditioning process by gravity waves and the occurrence of warm-sector heavy rainfall at the coast. The western part of frontal rainfall stimulated in the sensitivity experiment developed earlier and more stably, resulting in weaker wave amplitudes and a mismatch between the region of mid-level moistening and the strong lifting area associated with double low-level jets. Overall, this study sheds light on the key relationship between frontal and warm-sector heavy rainfall, bridged by gravity waves.

Numerical Study of Near-Cloud Aviation Turbulence Encounters over East Asia

Soo-Hyun Kim [a] and Jung-Hoon [a]

[a] *School of Earth and Environmental Sciences, Seoul National University, Seoul, Korea*

Corresponding author: Prof. Jung-Hoon Kim, jhkim99@snu.ac.kr

Turbulence associated with convective clouds is referred to as convectively induced turbulence (CIT). The CIT occurs within the cloud as well as in cloud-free air above or near convective clouds (near-cloud aviation turbulence, NCT). Because in-cloud CIT can be detected by monitoring in-flight radar echoes and satellite images, predicting NCT in advance is more significant for a safe air travel. Although there have been investigated generation mechanisms of NCT using numerical simulations and observations in the world, further studies on NCT frequently occurred over East Asia have been required. In this regard, current study examines the generation mechanisms of moderate-or-greater (MOG)-intensity turbulence cases occurred over East Asia using convection-permitting scale simulation. On 2 December 2019, a commercial aircraft traveling across the northern Pacific Ocean encountered MOG-level turbulence near convective clouds developed along well-organized surface front. The numerical simulation is conducted using the Advanced Research Weather Research and Forecasting model v4.3.3 with five domains with horizontal grid spacings from 9 to 0.111 km. It is found that there are convectively induced modifications in large-scale flow near turbulence incident regions: 1) strong bulk vertical wind shear is evident near downstream regions of deep convection and 2) areas of moist static instability. In the vertical cross sections, it is found that strong vertical wind shear and flow deformation below and above enhanced jet due to deep convection exist. The current simulated results indicate that a combination of vertical wind shear, flow deformation, and convective gravity waves and their breaking can be related to the southern cluster of current NCT cases. On the other hand, shear instability due to strong vertical wind shear mainly induced by enhanced upper-level jet may be associated with the northern cluster of the NCT cases. The detailed analysis of the finest domain (domain 5) will be presented in the conference.

Acknowledgement: This work is funded by the Korean Meteorological Administration Research and Development Program under Grant KMI2022-00310 and also supported by the Basic Science Research Program through the National Research Foundation (NRF) funded by the Ministry of Education (grant no. 2022R1I1A1A01071708).

Numerical experiments on quasi-stationary band-shaped convective systems formed by self-organization processes under horizontally homogeneous virtual environments

Miteki Satoh and Yasutaka Wakazuki

Graduate School of Science and Engineering, Ibaraki University, Mito, Japan

Corresponding author: Miteki Satoh, zubizudar@gmail.com

Abstract

In recent years, disasters caused by torrential rain have become more frequent in Japan. Many of these disasters are caused by quasi-stationary band-shaped convective systems that cause locally heavy rainfall for several hours. However, the primary formation causes of the quasi-stationary band-shaped convective system are considered to be complicated and case-by-case. This study investigated processes of generating quasi-stationary band-shaped convective systems by self-organization processes under horizontally homogeneous environments without topography. In particular, we focused on cases where a pre-existing convective system modifies the surrounding atmospheric circulation. The modified circulation adjusts the convective system into a quasi-stationary band-shaped convective system.

We conducted numerical experiments with the JMA non-hydrostatic model. An environmental atmospheric vertical profile was extracted from objective analysis data for the torrential rainfall event in Hiroshima, Japan, on August 20, 2014. The Air Lifting Blending (ALB) method, developed by Wakazuki and Satoh (2021), was used as the bogus to initiate cumulonimbus clouds. Two types of ALB bogus were applied: wide-range circulation and locally closed circulation versions.

Comparison between experiments with two different types of ALB bogus showed that a band-shaped convective system was formed only with the wide-range circulation ALB. This result suggests that a meso-β-scale low-level convergence maintained by the advection effect is essential for successive generations of convections.

Next, we focus on generating a band-shaped convective system formed in the affection of the preceding deep meso-β-scale convective system with a locally closed ALB bogus. Here, we used a locally closed ALB bogus because it seems to be reasonable as naturally generated boundary layer turbulence. The system's formation was triggered by the widespread low-level convergence formed by the prior convective system. Here, sensitivity experiments were conducted with different vertical profiles of temperature, relative humidity, and horizontal wind velocities. The experiment results showed that a distinct quasi-stationary band-shaped convective system was formed under the low LFC environment (Fig.1). A cold pool was not

enormously intensified in the low LFC experiment. However, the widespread low-level convergence formed by the prior convective system had been modified into a band-shaped convergence zone on the upwind side of the cold pool (Fig.2). Finally, a distinct quasi-stationary band-shaped convective system was generated along the convergence zone. In case the environmental low-level wind speed was slow, the generated convective system showed stationarity due to the slow-moving features of the convergence zone.

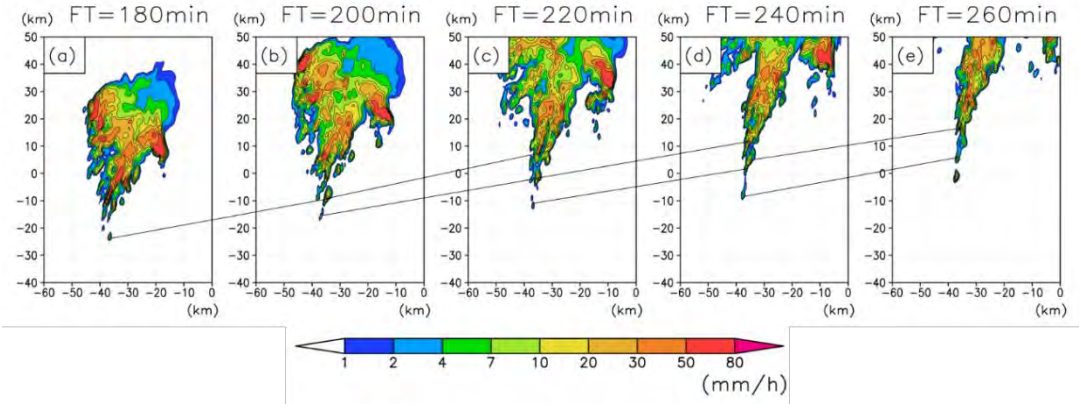

Fig.1 Temporal variation of precipitation (mm hr^{-1}) for a case in which the LFC is low. The solid black lines indicate the tracks of convective cells on the upstream side of the convective system.

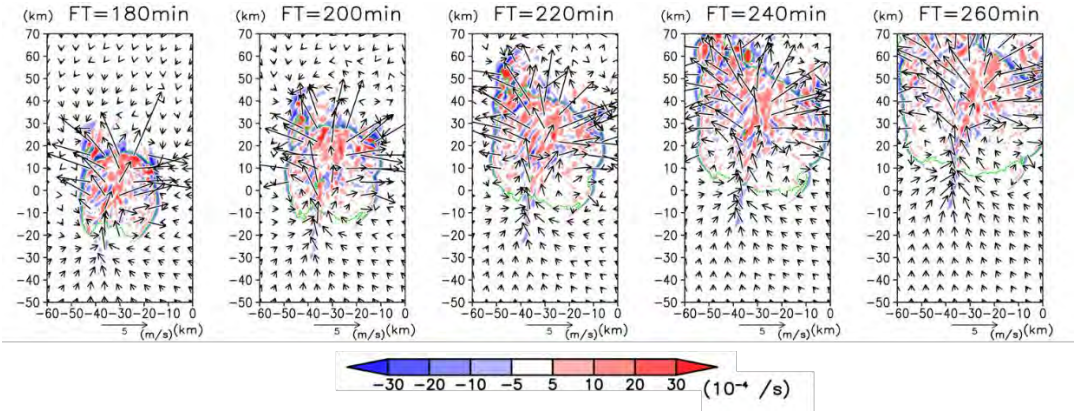

Fig.2 Temporal variation of divergence at the height of 200 m. The shaded represents divergence (10^{-4} s^{-1}), and the solid green line represents the edge of the cold pool.

The Impact of Coastal Marine Boundary Layer Jet on Rainfall in South China

Yu Du[a], Yian Shen[a], Xiaoqing Li[a], and Guixing Chen[a]

[a] *Sun Yat-sen University, Zhuhai, Guangdong, China*

Corresponding author: Yu Du, duyu7@mail.sysu.edu.cn

The characteristics of coastal marine boundary layer jets (BLJs) over South China Sea (SCS) and their impacts on rainfall are examined using scientific-research-ship observations, satellite data, and reanalysis data. Typically, the BLJs exhibit a maximum intensity at night and reach their peak at 950 hPa. They are formed by the large-scale diurnal land-sea thermal contrasts under the background of the monsoon flow. Two main BLJs are found, one on each side of Hainan Island (named BLJ-WEST and BLJ-EAST), which are always strengthened jointly. The emergence of the BLJs leads to increased rainfall in South China, particularly in areas downstream of each BLJ. The response of rainfall to the BLJs is mainly attributed to convergence at the terminus of each BLJ, terrain-induced lifting, and relevant atmospheric stratification. Coastal rainfall downstream of the BLJ-WEST is much weaker than that downstream of the BLJ-EAST because of higher CIN over the Beibu Gulf, which is caused by lower temperature lapse rates and adiabatic heating in the lee of the Annamite Range. The inland rainfall increases along with BLJ intensity, whereas coastal rainfall reaches a maximum in the presence of moderate BLJs rather than stronger BLJs. Stronger BLJs induce stronger dynamic lifting but higher CIN near the coastal area. Therefore, anomalous dynamic lifting, moisture flux convergence, and CAPE/CIN associated with BLJ intensity jointly result in anomalous rainfall.

The sensitivity of the simulated BLJ and associated precipitation in South China to different planetary boundary layer parameterization schemes is further investigated. Results show that both too strong or too weak BLJs in the model are unfavorable for extreme rainfall in South China. The differences in BLJs' strength among PBL schemes are attributed to varying simulated low-level vortex on the northern side of the BLJ through veering ageostrophic winds. The intensity of the simulated low-level vortex is affected by variations in boundary layer mixing over land and associated vertical temperature stratification under different PBL schemes.

References:

Du, Y.[#] Y. Shen, and G. Chen, 2022: Influence of Coastal Marine Boundary Layer Jets on Rainfall in South China. Adv. Amos. Sci., 39, 782-801.

Shen Y. and **Y. Du**[#]**,** 2023: Sensitivity of boundary layer parameterization schemes in a marine boundary layer jet and associated precipitation during a coastal warm-sector heavy rainfall event. *Front. Earth Sci.* 10:1085136.

Li, X., and **Y. Du**[#], 2021: Statistical Relationships Between Two Types of Heavy Rainfall and Low-Level Jets in South China. J. Climate, 34, 8549-8566

The Isotopic Composition of Rainfall on a Subtropical Mountainous Island

Giuseppe Torri[a], Alison D. Nugent[a], and Brian N. Popp[b]

[a] *Department of Atmospheric Sciences, University of Hawai'i at Mānoa, Honolulu, HI, USA*

[b] *Department of Earth Sciences, University of Hawai'i at Mānoa, Honolulu, HI, USA*

Corresponding author: Giuseppe Torri, gtorri@hawaii.edu

Tropical islands are some of the most biodiverse and vulnerable places on Earth. Water resources help maintain the delicate balance on which tropical island ecosystems and populations depend. Hydrogen and oxygen isotope analysis is a powerful tool for studying the water cycle on tropical islands, although the scarcity of long-term and high-frequency data makes interpretation challenging. A new dataset is presented based on a weekly collection of the H and O isotopic composition of rainfall on the island of O'ahu, Hawai'i, beginning in July 2019 and still ongoing. During this time, different weather conditions have affected the island, each producing precipitation with different isotopic ratios: precipitation from upper-level lows was found to have the lowest isotopic ratios, while trade wind showers had the highest. These data also show some differences between the windward and leeward sides of the island, the latter being associated with higher rainfall isotope ratios due to increased rain evaporation. As an example of such differences, the amount effect is not observed at all sites. The measured deuterium excess shows a pronounced seasonal cycle, which is attributed to different origins of the air masses responsible for rainfall in the winter and summer months. The local meteoric water line is then determined and compared with similar lines for O'ahu and other Hawaiian islands. Finally, a comparison is made with data collected on Hawai'i Island over a longer period of time, and it is shown that the isotopic composition of precipitation exhibits significant interannual variability.

Topographic Influence on the Spectrum of Storm Modes Associated with Heavy Rainfall during the 2021 "PRE"-CIP Field Campaign in Northern Colorado

Zoe A. Douglas [a] and Kristen L. Rasmussen [a]

[a] *Colorado State University, Fort Collins, Colorado, United States*

Corresponding author: Zoe A. Douglas, zoedoug@colostate.edu

Extreme rainfall is a high-impact weather phenomenon that profoundly affects people around the world, but our fundamental understanding and quantitative forecast skill for these events remains limited. To better understand and improve forecast skill for extreme rainfall events, the Prediction of Rainfall Extremes Campaign in the Pacific (PRECIP) planned to observe the spectrum of heavy rainfall events of various intensities and durations in the moisture-rich environment of Taiwan during the summer of 2020, but was delayed until 2022 due to the global pandemic. As a result of this unanticipated delay, the PRECIP science team conducted the Preparatory Rockies Experiment for the Campaign in the Pacific ("PRE"-CIP), which observed rainfall over northern Colorado during the summer of 2021 using Colorado State University's CHIVO and CHILL ground-based research radars and radiosondes. Extreme precipitation features are identified in these radar datasets between May and August 2021 and organized into storm modes based on prior research on the Tropical Rainfall Measuring Mission (TRMM) satellite's Precipitation Radar. An "ingredients-based" approach provides a theoretical framework to separate the storm modes into a spectrum of storm intensity and duration during the entire "PRE"-CIP field project, allowing us to connect storm modes to the topography, diurnal cycle, and overall rainfall characteristics in northern Colorado. Using these rainfall characteristics and storm durations identified through storm tracking algorithms, we populate the intensity-duration phase space with storm mode observations from "PRE"-CIP for comparison with the theoretical intensity-duration framework that drives the science behind the field campaign. Ultimately, this analysis is important for the eventual comparison of extreme precipitation in a semi-arid midlatitude region ("PRE"-CIP) and a moisture-rich tropical environment (PRECIP), thus providing a more complete picture of extreme rainfall and contributing to an enhanced global understanding of the commonalities of heavy rainfall processes.

Synoptic Control on the Initiation and Rainfall Characteristics of Warm-season MCSs over the South China Coast

Chenli Wang [a,b], Xingchao Chen [b], Kun Zhao [a], and Chin-Hsuan Peng [b]

[a] *Key Laboratory of Mesoscale Severe Weather/MOE and School of Atmospheric Science, Nanjing University, Nanjing, and State Key Laboratory of Severe Weather and Joint Center for Atmospheric Radar Research of CMA/NJU, Beijing, China*

[b] *Department of Meteorology and Atmospheric Science, and Center for Advanced Data Assimilation and Predictability Techniques, The Pennsylvania State University, University Park, Pennsylvania, USA*

Corresponding author: Chenli Wang, chenliwang@smail.nju.edu.cn

The South China coast (SCC) experiences frequent heavy rainfall every warm season (May-September). Objective classification analysis shows that the majority of warm season precipitation (>80%) occurs under three typical synoptic patterns: the southerly monsoon pattern (P1), the southwesterly monsoon pattern (P2), and the low-level vortex pattern (P3). Using 20 years of satellite observations and cloud tracking, we found that mesoscale convective systems (MCSs) play a pivotal role in generating precipitation under all three synoptic patterns, accounting for 60-80% of the total rainfall. In contrast, non-deep convection contributes 10-20%, while non-MCS deep convection makes up less than 20% of the total precipitation. Our analysis also shows that the majority of the MCSs contributing to the precipitation over the SCC were initiated locally under all three synoptic patterns. This underscores the crucial role of locally initiated MCSs in driving warm-season precipitation over the SCC, as opposed to propagating MCSs. MCS precipitation under synoptic patterns P1 and P2 tends to originate along the coastline in the early morning (early afternoon) and then propagates offshore (onshore), likely influenced by the diurnal land (sea) breeze circulation. Conversely, under synoptic pattern P3, nocturnal MCS precipitation initiates near the coastline at midnight and then propagates offshore, merging with the widespread offshore precipitation. Compared to the other two synoptic patterns, the onshore precipitation during the afternoon under P3 is significantly weaker and its onshore propagation distance is shorter. Statistical correlation analysis further shows that the pre-MCS deep-layer wind shear (from surface to 500 hPa) over the SCC, the upstream convective available potential energy, and the lower-tropospheric moisture transport from open ocean play important roles in modulating the maximum precipitation area, maximum precipitation intensity, and maximum hourly precipitation of MCSs under the three synoptic patterns. The potential physical mechanisms will also be discussed in the talk.

Effects of the land–sea contrast and topography on diurnal cycle of precipitation over the Bay of Bengal

ZiJian Chen[a] and Yu Du[a]

[a] *School of Atmospheric Sciences, Sun Yat-sen University, ZhuHai, GuangDong Province, China*

Corresponding author: Yu Du, duyu7@mail.sysu.edu.cn

Over the Bay of Bengal, a pronounced diurnal offshore propagating signal of rainfall is observed from the high-resolution precipitation products. Series of numerical model experiments reveal that this phenomenon is closely related to the land-sea breeze excited by diurnal heating over the west coast of the Bay of Bengal. These experiments imply that the inertia-gravity waves generated by land-sea breeze play an important role in the initiation and offshore propagation of mesoscale convective systems (MCSs) over the bay, and their phase speed are good match for the propagation speed of rainfall. From these experiments, we also find that offshore propagating signal still exists after removing orography or turning off latent heating from MCSs over land areas. These tests imply that terrain and diurnal MCSs over east coast of India have secondary but not critical effects on the offshore propagation of rainfall. Boundary layer heating depth relative to orography and latent heating from MCSs over land areas both affect the amplitude, phase and phase speed of the inertia-gravity waves triggered by land-sea breeze. For higher mountains or stronger convection over land, gravity waves with faster propagating speed and stronger amplitude are triggered by the deeper boundary layer, accompanying with faster propagation of rainfall.

Orographic controls on precipitation intensity and duration associated with a Mei-yu front

Ian Cornejo [a], Angela Rowe[a], and Kristen Rasmussen[b]

[a] *University of Wisconsin - Madison, Madison, Wisconsin, United States of America*

[b] *Colorado State University, Fort Collins, Colorado, United States of America*

Corresponding author: Ian Cornejo, icornejo@wisc.edu

Taiwan frequently receives extreme rainfall associated with seasonal Mei-yu fronts that encounter Taiwan's steep and complex topography. One such Mei-yu case occurred 1-3 June 2017 when severe flooding and landslides occurred as a result of over 600 mm of rainfall in 12 hours near Taipei basin and over 1500 mm of rainfall in 2 days near the Central Mountain Range (CMR). This Mei-yu front event is simulated using the Weather Research and Forecasting (WRF) model with halved terrain as a sensitivity test to better understand the orographic mechanisms that modify the intensity, duration, and location of extreme rainfall.

The reduction in terrain height in WRF produced a decrease in rainfall duration and accumulation in Northern Taiwan and a decrease in rainfall duration, intensity, and accumulation over the CMR. The reductions in Northern Taiwan are linked to a weaker orographic barrier jet resulting from a lowered terrain height. With a weaker barrier jet, the front propagates south faster, decreasing the time rainfall accrues in Northern Taiwan. The reductions in rainfall intensity and duration over the CMR are partially explained by a lack of orographic enhancements to Mei-yu frontogenesis near the terrain. A prominent feature missing with the reduced terrain is a redirection of postfrontal westerly winds attributed to orographic deformation. These orographically deforming winds converge with prefrontal flow to maintain the Mei-yu front. These orographic features will be further explored using observations of heavy rainfall Mei-yu events captured during the 2022 Prediction of Rainfall Extremes Campaign in the Pacific (PRECIP) field campaign.

Three-Dimensional Variational Multi-Doppler Wind Retrieval over complex terrain

Ting-Yu Cha [a], and Michael M. Bell[b]

[a] *National Center for Atmospheric Research, Boulder, Colorado, United States*

[b] *Department of Atmospheric Science, Colorado State University, Fort Collins, Colorado, United States*

Corresponding author: Ting-Yu Cha, tycha@ucar.edu

Airflow interactions with complex terrain can greatly enhance the potential for extreme precipitation events and alter the structure and intensity of the precipitating cloud systems, but these events are difficult to understand and forecast, partly due to limited direct in-situ measurements to sample wind and thermodynamic fields. Doppler radar can provide the capability to monitor extreme rainfall events over land, but our understanding of airflow modulated by orographic interactions remains limited. In this study, a new Doppler radar technique is developed to retrieve three-dimensional wind fields in precipitation over complex terrain. New boundary conditions are implemented in a variational multi-Doppler radar technique to represent the topographic forcing and surface impermeability.

A series of observing simulation sensitivity experiments using a full-physics model and radar emulator simulating rainfall from Typhoon Chanthu (2021) over Taiwan are conducted to evaluate the retrieval accuracy and parameter settings. Analysis from real radar observations from Chanthu demonstrates that the improved retrieval technique can advance scientific analyses for the underlying dynamics of orographic precipitation using radar observations.

Global Warming Intensifies Mesoscale Convective Systems During the Record-breaking Rainfall Event in July 2021 in Henan Province, China

Zhongxi Lin

Peking University, China

Mesoscale convective systems (MCS) merged and sustained in the record-breaking heavy rainfall event during 19-21 July 2021 in Henan Province, China. Whether warming climate enhances the intensity or area of MCS is crucial for understanding the changing risk of extreme rainfall events under global warming. Ensemble simulations based on the Weather Research and Forecasting (WRF) is adopted. The human-induced warming and moistening at approximately 0.8 degree Celsius, which is derived from the difference of Historical and ALL-Nat experiments in CMIP6, is added to the initial and boundary condition. With MCS-tracking algorithm, the results suggests that the total rainfall volume and maximum rainfall intensity in the MCS region both increases by ~10%. During developing phases, the spatial areas of MCSs are 10%~40% larger in a warmer condition, which is contributed by the more favorable unstable conditions. For extreme hourly precipitation, the probability distributions of extreme rainfall grids inside MCS (larger than 100 mm/h) increase up to 50% in warming climate, which greatly aggravate the threat of flood. In addition, during the two hourly rainfall peaks, the maximum precipitation is enhanced by 15%~23%. Furthermore, vertical velocity is enhanced by 10% and the cloud top is raised by 0.5 km, and moisture is more adequate in a warming scenario which is beneficial for consisting extreme rainfall. Thus, the flood risk managements should take the changes of MCSs characteristics due to warming climate into account, to encounter the future threat of extreme rainfall event.

Initiations of Mesoscale Convective Systems in the Middle Reaches of the Yangtze River Basin Based on FY-4A Satellite Data: Statistical Characteristics and Environmental Conditions

Ya-Nan Fu [a,b], Jian-Hua Sun [a,b,c], Shen-Ming Fu [d], Yuan-Chun Zhang [a], Zheng Ma [a]

[a] *Key Laboratory of Cloud-Precipitation Physics and Severe Storms, Institute of Atmospheric Physics, Chinese Academy of Sciences, Beijing, China*

[b] *University of Chinese Academy of Sciences, Beijing, China*

[c] *Collaborative Innovation Center on Forecast and Evaluation of Meteorological Disasters, Nanjing University of Information Science and Technology, Nanjing, Jiangsu Province, China*

[d] *International Center for Climate and Environment Sciences, Institute of Atmospheric Physics, Chinese Academy of Sciences, Beijing, China*

Corresponding author: Dr. Jian-Hua Sun sjh@mail.iap.ac.cn

Based on the brightness temperature observed by the Fengyun-4A satellite, eight hundred mesoscale convective systems (MCSs) are identified in the middle reaches of the Yangtze River Basin (YRB) during the warm seasons (April–September) of 2018–2021, which are categorized into the quasistationary (QS) type and the outward-moving (OM; i.e., vacating the source region) type. The daily circulations of June, July and August, during which MCSs occur most frequently, are objectively classified into three patterns using the k-means algorithm, and the environmental conditions of MCS initiation are further compared and analyzed. The main conclusions are described as follows:

(1) Among the four main moving paths (i.e., northeast path, southeast path, northwest path and southwest path) of QS MCSs, the occurrence frequency in the southeast path is the highest. The QS MCSs are mostly initiated over mountainous areas and then propagate to the plains. The moving trajectories of OM MCSs are classified into three paths, namely, northeast path, southeast path and southwest path, among which the southeast path has the largest amount of OM MCSs.

(2) The QS MCSs primarily occur in July and August and are mainly initiated in the afternoon. The OM MCSs mostly occur in June and July with two initiation peaks at noon and late night, respectively, corresponding to the afternoon peak and morning peak of the typical precipitation associated with Mei-yu fronts. QS MCSs are mainly initiated in mountainous areas and caused by local thermal effects, while OM MCSs are mostly triggered in plain areas, which is related to synoptic circulation forcings.

(3) The OM MCSs move faster than the QS MCSs and mostly propagate eastward. The durations and maximum extents of QS MCSs show no obvious differences among different months, while those of OM MCSs vary among different months. The lowest brightness temperatures of QS MCSs mostly appear in the afternoon, but those of the OM MCSs exhibit no obvious diurnal variation.

(4) Circulations of 285 MCS days, without direct influencings from tropical cyclones, are classified into 3 patterns using the k-means algorithm. The composite circulation of Pattern-I (P1) is consistent with the typical circulation of the Mei-yu front,

and those of Pattern-II (P2) and Pattern-III (P3) are dominated by the northwesterly and the weak southerly, respectively. The mean initiation frequencies of the QS MCSs in P1 and P3 are the same and that in P2 is the lowest. The OM MCSs are initiated the most in P1, followed by P2, and they are initiated the least in P3.

(5) Analysis of the environmental conditions suggests that a) the low-level wind speed in P1 is relatively high, and the MCS initiations in P1 may be accompanied by low-level jets, which is more favorable for OM MCS initiation and propagation; b) the circulation in P2 is dominated by northwesterlies with a relatively stable layer in the low-level troposphere; and c) the southerly in P3 accompanied by adiabatic warming establishes a dry-adiabatic or even a superadiabatic layer and further lowers the stability.

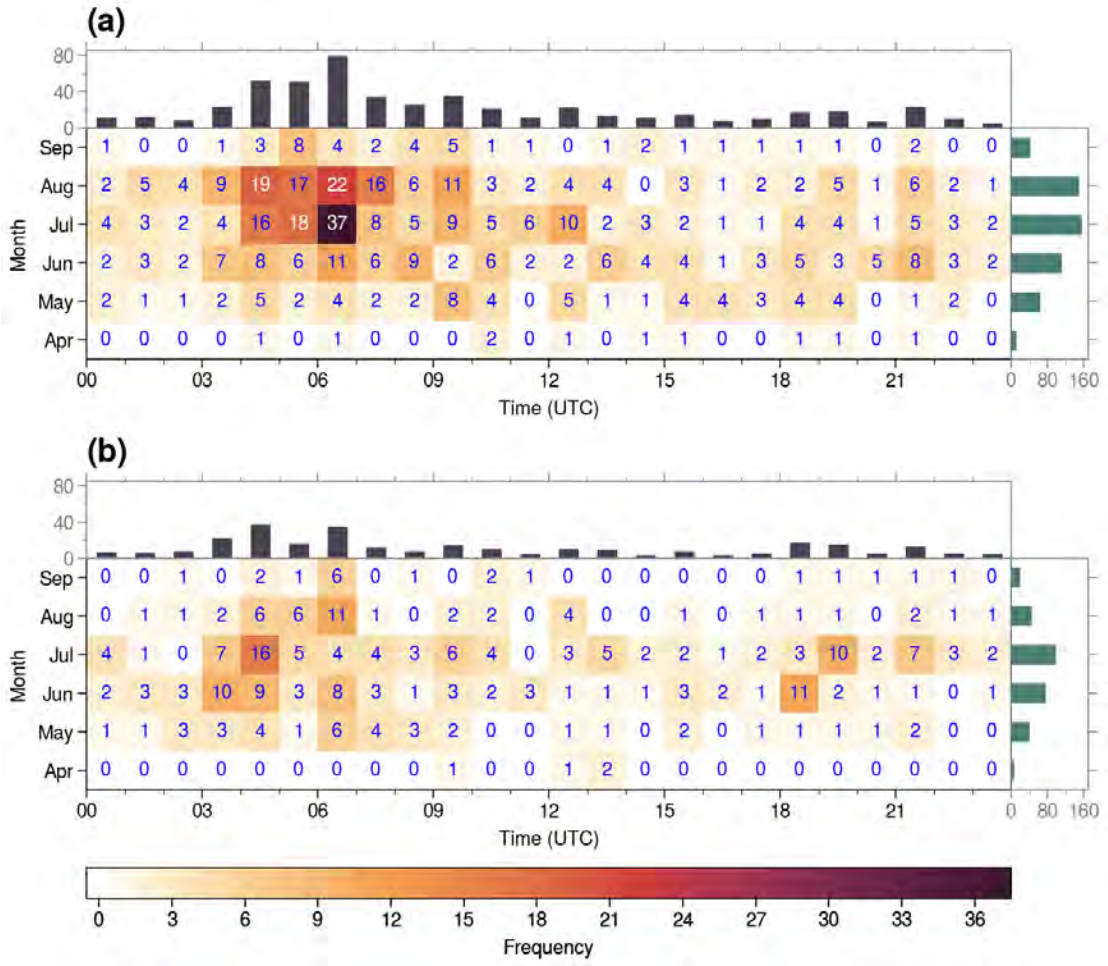

Figure 1. Monthly and diurnal distributions of the QS MCS frequency (a) and the OM MCS frequency (b) in the middle reaches of the YRB during the warm seasons (April–September) of 2018–2021. The horizontal axis represents the initiation time (UTC). The color shading symbolizes the occurrence frequency of MCSs.

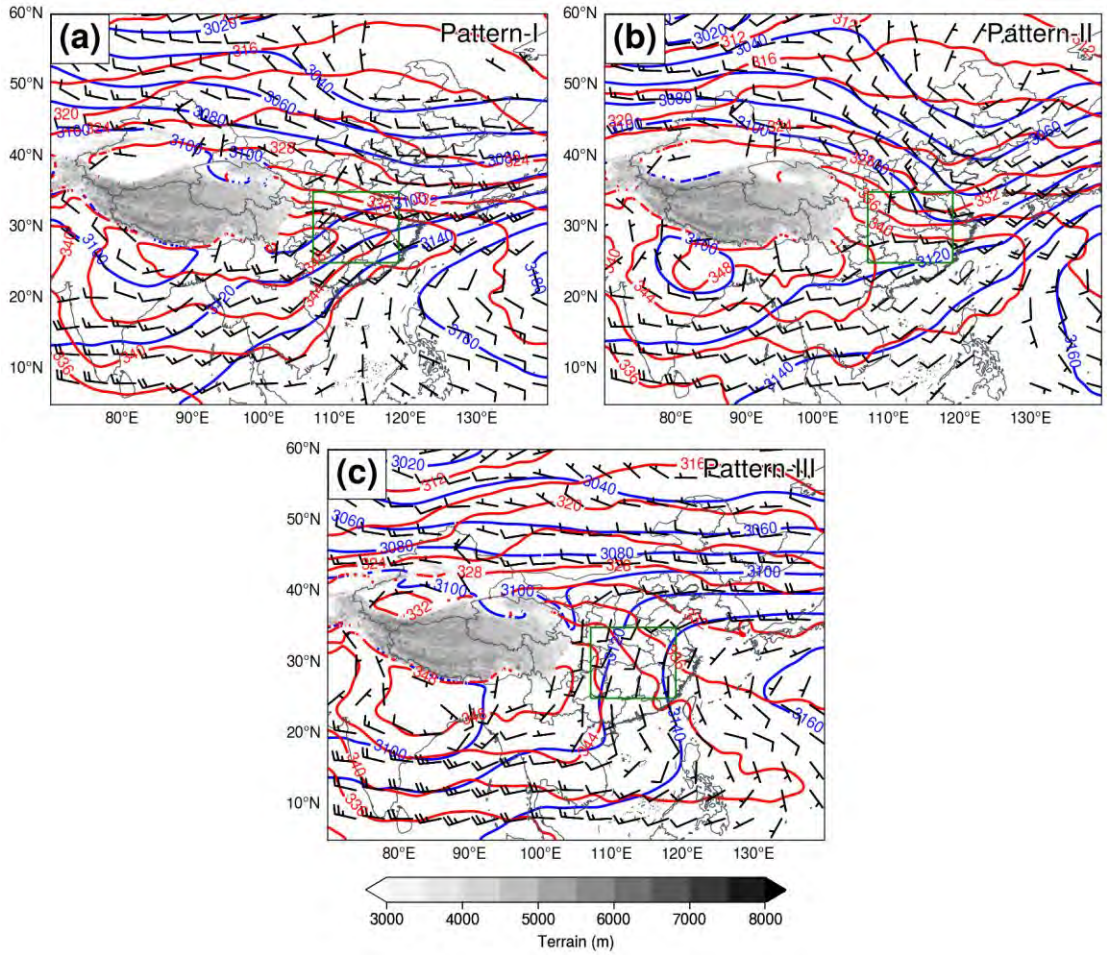

Figure 9. The composite geopotential fields (blue contours, gpm), equivalent potential temperature fields (red contours, K) and wind fields (wind barbs, m s−1) at 700 hPa of Pattern-I (a), Pattern-II (b) and Pattern-III (c), respectively. A half (full) barb represents 2 m s−1 (4 m s−1). The green rectangle marks the middle reaches of the YRB. The gray shading represents terrain heights (m).

Precipitation characteristics of mesoscale convective systems over East Asia: regional difference and seasonal variations, the added value of convection-permitting simulation, and the sensitivity of simulated MCS to the different treatment of deep convection

Puxi Li [a], Haoming Chen [a], Kalli Furtado [b], Mark Muetzelfeldt [c] and Reinhard Schiemann [c]

[a] *State Key Laboratory of Severe Weather, Chinese Academy of Meteorological Sciences, China Meteorological Administration, Beijing 100081, China*

[b] *Met Office, Exeter, UK*

[c] *National Centre for Atmospheric Science, Department of Meteorology, University of Reading, Reading, UK*

Corresponding author: Puxi Li, lipx@lasg.iap.ac.cn

In this talk, we will first introduce our study focusing on the regional differences and seasonal variations of MCS precipitation characteristics over East Asia, by using an iterative rain cell tracking method to identify and track MCS precipitation during 2008-2016. Our results show that the middle-to-lower reaches of the Yangtze River basin (YRB-ML) receives the largest amount and exhibits the most pronounced seasonal cycle of MCS precipitation in eastern China. MCS precipitation over YRB-ML can exceed 2.6 mm d^{-1} in June, contributing over 30.0% of April to July total rainfall. Particularly long-lived MCSs occur over the eastern periphery of the Tibetan Plateau (ETP), 25% of MCSs over the ETP persist for more than 18 hours in spring. In addition, spring MCSs feature larger rainfall areas, longer durations and faster propagation speeds. Summer MCSs have a higher precipitation intensity, and more pronounced diurnal cycle except for southeastern China, where MCSs have similar precipitation intensity in spring and summer. There is less MCS precipitation in autumn, but an MCS precipitation center over the ETP still persists. Then, by choosing a typical heavy rainfall event hit eastern China during Mei-yu season in 2016, featured by high precipitation intensity, long duration and huge rainfall accumulations, we conducted a series of numerical experiment (one global run ~20km, and two regional convection-permitting simulations: ~4km and ~2km) and investigated the added value of convection-permitting simulations in simulating the MCS precipitation characteristics. We found that convection-permitting models better simulate the rainfall pattern, the diurnal cycle of precipitation, the small disturbances with the rain-bands, and also reduce the spurious topographical rainfall simulated by the global model, although there is a tendency for heavy rainfall to be too intense in convection-permitting simulations. Finally in this talk, we will also briefly introduce the sensitivity of simulated MCSs over East Asia to the treatment of convection in a high-resolution GCM at O(10km).

Here the sensitivity of MCSs simulated by a global atmosphere-only climate model to different treatments of convection (with and without parametrized convection, and a hybrid representation of convection) have been investigated. In general, explicit convection better simulates the diurnal variability of MCSs over the eastern China, and is able to represent the distinctive diurnal variations of MCS precipitation over complex terrain particularly well, such as the eastern TP and the complex terrain of central-northern China. It is shown that explicit convection is better at simulating the timing of initiation and subsequent propagating features of the MCS, resulting in better diurnal variations and further a better spatial pattern of summer mean MCS precipitation. All three experiments simulate MCS rainfall areas which are notably smaller than those in observations, but with much stronger rainfall intensities, implying that these biases in simulated MCS morphological characteristics are not sensitive to the different treatment of convection.

Five-year climatology and composite study of precipitation bands associated with extratropical cyclones over the British Isles

Tianhang Zhang [a], and David M. Schultz [a,b]

[a] *Centre for Atmospheric Science, Department of Earth and Environmental Sciences, University of Manchester, Manchester, United Kingdom*

[b] *Centre for Crisis Studies and Mitigation, University of Manchester, Manchester, United Kingdom*

Corresponding author: Tianhang Zhang, tianhang.zhang@postgrad.manchester.ac.uk

ABSTRACT

A five-year climatology and composite study of precipitation bands associated with extratropical cyclones over the British Isles from April 2017 to March 2022 are constructed. A total of 249 single bands were manually identified from radar network mosaics in association with 167 cyclones identified from surface maps. More bands formed over water near the coast than over inland areas, and most had a meridional orientation. The average lengths of bands at the times of formation and maximum length were 290 and 460 km, respectively; only 20% of bands reached a maximum length exceeding 600 km. The number of bands decreased with increasing duration, with 31% of bands lasting for 2–3 h, with bands lasting more than 10 h uncommon. The bands were classified into six categories, with occluded-frontal bands, warm-frontal bands, and cold-frontal bands being the most frequent. Occluded-frontal and warm-frontal bands commonly occurred west of Scotland and in the east quadrant relative to their parent cyclones. In contrast, cold-frontal bands commonly occurred southwest of Great Britain and in the south quadrant relative to their parent cyclones. Composites for northwest–southeast occluded-frontal and warm-frontal bands west of Scotland, and southwest–northeast cold-frontal bands southwest of Great Britain, show the different synoptic environments that favor bands. The low-level jet transports moisture into the band and is similar to the location and scale of the composite bands, similar to that of an atmospheric river. These results are compared to previous studies on bands from the United States.

Tracking Mesoscale Convection Systems in the US in E3SMv1 with Multiscale Modeling Framework

Wei-Ching Hsu[a], Gabriel J. Kooperman[a], Walter M. Hannah[b], Kevin A. Reed[c], Akintomide A. Akinsanola[d,e], and Angeline G. Pendergrass[f,g]

[a]Department of Geography, University of Georgia, Athens, GA.

[b]Atmospheric, *Earth and Energy Division, Lawrence Livermore National Laboratory, Livermore, CA.*

[c]*School of Marine and Atmospheric Sciences, Stony Brook University, Stony Brook, NY.*

[d]*Department of Earth and Environmental Sciences, University of Illinois Chicago, Chicago, IL.*

[e]*Environmental Science Division, Argonne National Laboratory, Lemont, IL.*

[f]*Climate and Global Dynamics Laboratory, National Center for Atmospheric Research, Boulder, CO.*

[g]*Department of Earth and Atmospheric Sciences, Cornell University, Ithaca, NY.*

Corresponding author: Wei-Ching Hsu, weiching@uga.edu

Organized mesoscale convective systems (MCSs) over the continental US (CONUS) are often linked to significant amounts of precipitation, especially during the spring and summer. However, current global models with conventional configurations cannot reasonably capture MCSs, their characteristics, and the associated precipitation. In this study, we investigated the representation of the MCSs in three configurations of the Energy Exascale Earth System Model (E3SMv1) over the Central and Eastern CONUS. To identify MCSs, we developed a tracking algorithm solely based on the outgoing longwave radiation using the software TempestExtremems, in order to examine the biases in the representation of MCSs and precipitation separately. Our results suggest that the two conventionally parameterized simulations, with low (~150 km) and high (~25km) horizontal resolutions, respectively, underestimate the high-level cloud ice associated with deep convection and fail to capture MCSs. On the other hand, although with a low horizontal resolution (~150km), the multiscale modeling framework (MMF) configuration reasonably captures MCSs. Nonetheless, biases in MCS characteristics are still evident in the MMF simulation, including: the spatial distribution of MCSs and related precipitation shifted eastward and diurnal timing lagging observation, especially during the summer. These biases are linked to biases in the low-level humidity and the moisture transport associated with the low-level jet. Moreover, a comparison between the two conventionally parameterized simulations indicates that the high resolution used in this study does not reduce the biases in the low-level environment. In conclusion, explicit representation of kilometer-scale convective organization, as in the MMF configuration, is a useful approach to reasonably capture MCSs over CONUS.

Rainfall Nowcasting Performance of the Extrapolation Adjusted by Model Prediction (ExAMP) Blending Scheme

Chih-Chien Tsai [a], Chung-Yi Lin [a], Jia-Chyi Liou [a], Hsin-Hao Liao [a], Yu-Chun Chen [a], Kao-Shen Chung [b], Ben Jong-Dao Jou [c], and Yi-Chiang Yu [a]

[a] *National Science and Technology Center for Disaster Reduction, New Taipei City, Taiwan*

[b] *Department of Atmospheric Sciences, National Central University, Taoyuan City, Taiwan*

[c] *Department of Atmospheric Sciences, National Taiwan University, Taipei City, Taiwan*

Corresponding author: Chih-Chien Tsai, tsaicc@ncdr.nat.gov.tw

This study evaluates the extrapolation adjusted by model prediction (ExAMP) scheme for its skill and strategies in rainfall nowcasting. The scheme leverages the contrasting strengths of extrapolation and NWP model predictions and blends them to provide accurate rainfall estimates. The current study utilizes the MAPLE and WRF models for extrapolation and intensity adjustment, respectively, and implements seven different strategies for 150-min rainfall nowcasting across 37 sampled periods from seven heavy rainfall events. Results indicate that the superior strategy of MAPLE for rainfall nowcasting is achieved by extrapolating the current rainfall rate estimated from the lowest dual-polarimetric radar observations using hybrid QPE relationships. Furthermore, the ExAMP scheme that blends the MAPLE and WRF forecasts can surpass both components in 150-min rainfall nowcasting. However, the empirical innovation limitation, which is beneficial for blending composite reflectivities, can be too restrictive for blending rainfall rates with a much larger range of values. Spatial examination of two contrasting events reveals that the ExAMP scheme without the innovation limitation performs best in grasping rainfall strengthening and weakening in different areas. The scheme is effective in intensity correction instead of pattern correction, and skill statistics separately at rainfall strengthening and weakening gauges further prove its effectiveness despite extrapolation biases.

Sensitivity of Precipitation Diurnal Variation Forecast to the Cumulus Parameterization

Haixia Mei[a], Xin-Zhong Liang[b,c], and Mingjian Zeng[a]

[a] Key Laboratory of Transportation Meteorology of China Meteorological Administration, Nanjing Joint Institute for Atmospheric Sciences,Nanjing, Jiangsu, China

[b] Earth System Science Interdisciplinary Center, University of Maryland,College Park, Maryland, USA

[c] College of Atmospheric Science, Nanjing University of Information Science and Technology, Nanjing, Jiangsu, China

Corresponding author: Haixia Mei, meihaixiameihaixia@163.com

This study investigates the effects of call frequency for cumulus parameterization on forecasting diurnal precipitation variation through the double nesting approach. It is demonstrated by reinitized 36-hr forecasts during the plum rainy season June 19-July 20,2016 in Jiangsu Province in China. In the outer domain at 15km grid, the control run applying the KF cumulus scheme of 30 min the interval predicts two precipitation peaks in the early morning and early afternoon as observed, but siginificantly overesimates the precipitation intensity. The afternoon precipitation peak is twice higher, while the evening valley and the early morning peak are also significantly over-forecasted. At the coarse grid, cumulus parameterizations affects the consumption of instability energy, which govern the subgrid convective precipitation process. Increasing the KF call frequency facilitates the timely triggering and full development of convective activities during the daytime. This increases the subgrid precipitation and decrease the gridscale precipitation alleviating the delay of daytime precipitation, and thus reduce the over-forecast of the low valley and early-morning precipitation. In particular, the KF scheme at a high-frequency predicts the weakest CAPE and consequently the most realistic precipitation diurnal variation in the coarse grid. In the inner domain at 1 km grid, precipitation is explicitly resloved by the cloud microphysics processes which is driven by the water vapor and instability energy inflows from the coarse grid through the lateral boundary conditions. Increasing the KF frequency in the outer domain reduces the water vapor excess remaining in the low troposphere, and thus provides less water vapor supply across the bounaries to weaken the precipitation over-forecast in the early morning and daytime in the inner domain. Above all, KF scheme at high frequency most realistically predicts the daytime precipitation peak.

Precipitation Nowcasting Based on an Optimized Deep Learning Model Trained with Heterogeneous Weather Data

Dian-You Chen[a], Chia-Tung Chang[a], and Buo-Fu Chen[a]

[a] *Center for Weather and Climate Disaster Research, National Taiwan University, Taipei, Taiwan*

Corresponding author: Buo-Fu Chen, bfchen777@gmail.com

Due to the threat of extreme rainfall associated with mesoscale convective systems and summer afternoon thunderstorms, very short-term quantitative precipitation forecasting during 0−3 h is critical in Taiwan. In this study, deep learning models are developed for high-resolution quantitative precipitation nowcasting in Taiwan up to 3 h ahead. The baseline model based on the convolutional recurrent neural network is trained with a dataset containing radar reflectivity and rain rates at a granularity of 10 min. As previous works tend to produce overprediction in low-rainfall regions, the currently proposed model is improved and further driven by highly related heterogeneous weather data, including visible channel satellite observation, environmental winds, and environmental thermo-dynamical profiles. **Note that an innovative "PONI module" is added to the deep learning model to integrate a variety of heterogeneous data with various spatial and temporal characteristics.** Moreover, model performance is evaluated from statistical and spatial rescaling perspectives represented by $R = \bar{R} + R'$, where R denotes original rainfall, $\bar{R}$ and R' are spatial moving averages and the values deviated from $\bar{R}$, respectively. Statistical verification shows that the $\bar{R}$ of the new model outperforms the previous model, while the performance of R' is comparable. The new model integrated with heterogeneous data selected upon domain knowledge can restrain the nowcasts that overestimate in low-rainfall regions. Finally, quasi-operational verifications against other state-of-the-art techniques in Taiwan Central Weather Bureau are presented as follow: (1) the CSI of the first-hour prediction from deep learning model is comparable with QPESUMS-QPF and better than RWRF and iTeen. (2) 3h ahead prediction CSIs of RWRF and iTeen are inferior to the performance of deep learning model owing to the misprediction of rainfall regions.

Ensemble-based Adaptive Observation for Improving Sea Fog Prediction in Coastal Regions around the Bohai Sea: A Case Study based on Cold-front Synoptic Pattern

Huiqin Hu[a], Chengqing Ruan[b], and Xiaolin Yu[c]

[a] *Qingdao University of Science and Technology, Qingdao, Shandong Province, China*

[b] *North China Sea Marine Forecasting Center of State Oceanic Administration, Qingdao, Shandong Province, China*

[c] *Ocean University of China, Qingdao, Shandong Province, China*

Corresponding author: Huiqin Hu, serenahuhq@sina.com

Sea fog is a weather phenomenon that occurs at sea or in coastal regions, and reduces the atmospheric horizontal visibility to below 1 km due to an abundance of tiny water droplets or ice crystals suspended in the boundary layer. For regions with a high frequency of fog occurrence and heavy sea traffic, such as the Bohai Sea, sea fog has become a high-impact weather phenomenon. However, accurate numerical predictions of sea fog are still challenging. Providing more realistic ICs through assimilating supplemental observations is a potentially effective way to improve the numerical prediction of sea fog. Therefore, observation strategies are urgently needed to determine what types of observations and where should be deployed.

This study explored the observation strategy and effectiveness of synoptic-scale adaptive observation for improving sea fog prediction in the Bohai Sea based on a poorly-forecast fog event with cold-front synoptic pattern (CFSP). An ensemble Kalman filter data assimilation system for the Weather Research and Forecasting Model was adopted with ensemble sensitivity analysis (ESA). By comparing observation impacts (estimated from an ensemble) among different meteorological observation variables and pressure levels, temperature at both 850 hPa and surface (850-SFC temperature) was selected as the targeting observation type. Area with large observation impact for 850-SFC temperature was predicted to be located over the transition region of a low to the northwest and a high to the southeast. This area developed southward with the low and moved eastward with the low–high system (Fig. 1), which could be explained by main features of CFSP. Both experiments with assimilating simulated and real observations showed that assimilating 850-SFC temperature observation in areas with larger predicted observation impacts generally yield better fog coverage forecast than that with smaller impacts (Fig. 2). However, effectiveness of adaptive observation was reduced when real observations rather than

simulated observations were assimilated, which is possibly due to some actual factors such as observation and model errors.

Results of this study highlight importance of improved initial condition over the low-high-system transition region on improving fog prediction, and provide scientific guidance for implementing an observation network for fog forecasting over the Bohai Sea.

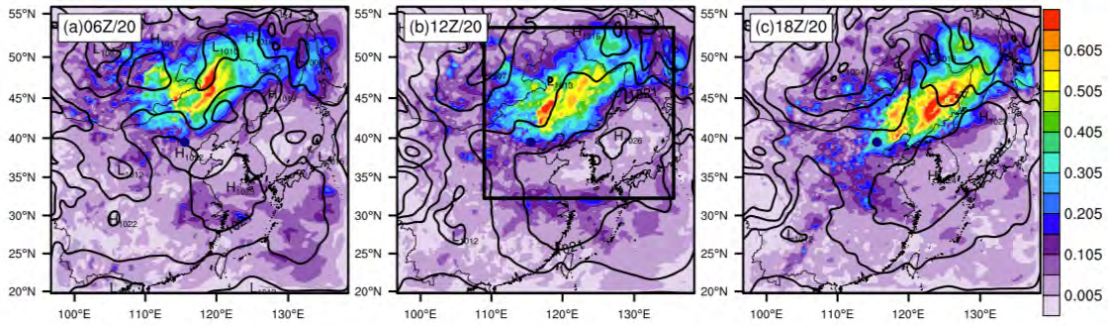

Fig.1 Sea level pressure (contour line) for TRUE run, and impact factor (shaded; units: e^{-2}) of FPR at the verification time in the verification region to 850-SFC temperature observations in D1 at 06:00 UTC (a), 12:00 UTC (b), and 18:00 UTC (c) on February 20, 2007, respectively. Large rectangular box in (b) denotes region used to locate different single synthetic/real observation for examining the effectiveness of adaptive observation. Navy dot in each subplot denotes location of Beijing.

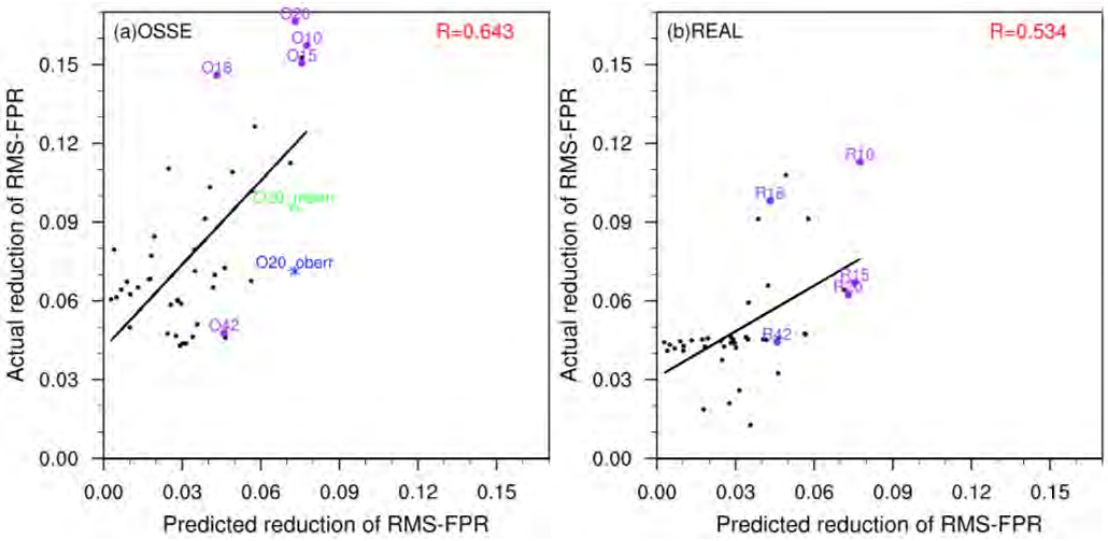

Fig.2 Scatterplot and linear regressions between predicted and actual reductions in root mean square error (RMSE) of FPR in verification region at verification time for experiments of assimilating simulated (OSSEs; a) and real observations (REAL; b), respectively.

The Roles of Low-level Jets in "21·7" Henan Extremely Persistent Heavy Rainfall Event

Yuhan Luo [a] and Yu Du [a]

[a] *SunYat-sen University, Zhuhai, Guangdong, China*

Corresponding author: Yu Du, duyu7@mail.sysu.edu.cn

An extremely heavy rainfall event lasting from 17 to 22 July 2021 occurred in Henan Province of China with accumulated precipitation of more than 1000 mm in the 6-day period that exceeded its mean annual precipitation. The present study examines the roles of the persistent low-level jets (LLJs) in maintaining the precipitation using surface station observations and reanalysis datasets.

The LLJs triggered strong ascent motions and carried moisture mainly from the outflow of typhoon "Infa". The varying directions of LLJs well corresponded to the south-north shifts of rainfall. The precipitation rate reached a maximum during 20-21 July as the LLJs strengthened and expanded vertically into double LLJs including synoptic-weather-system-related LLJs (SLLJs) at 850-700 hPa and boundary-layer jets (BLJs) at ~950 hPa. The coupling of the SLLJ and BLJ provided the mid- and low-level convergence on 20 July, whereas the SLLJ produced mid-level divergence at its entrance that coupled with low-level convergence at the terminus of the BLJ on 21 July.

The formation mechanisms of the two types of LLJs are further examined. The SLLJs and the low-pressure vortex (or inverse trough) varied synchronously as a whole, which were affected by the southwestward movement of the WPSH in the rainiest period. The lasting large total pressure gradient force at low levels also maintained the strength of low-level geostrophic winds and thus sustained the BLJs on synoptic scale. In addition to the synoptic scale, evident diurnal varying signals of the BLJ were found in its zonal and meridional wind components, Coriolis forces and fictional forces. The low-level perturbation winds rotated clockwise due to the inertial oscillation (Blackadar mechanism). The opposite geostrophic wind deviations parallel to the orography during the daytime and nighttime reflected the effect of Holton mechanism on the nocturnal BLJs. The Du-Rotunno 1D model further verified the combined effects of Holton and Blackadar mechanisms in diurnal variation of the BLJs in this event. The nocturnal intensification of the BLJs yielded the nocturnal rainfall peaks during the persistent heavy rainfall event via nocturnal strengthening dynamic and moisture convergence.

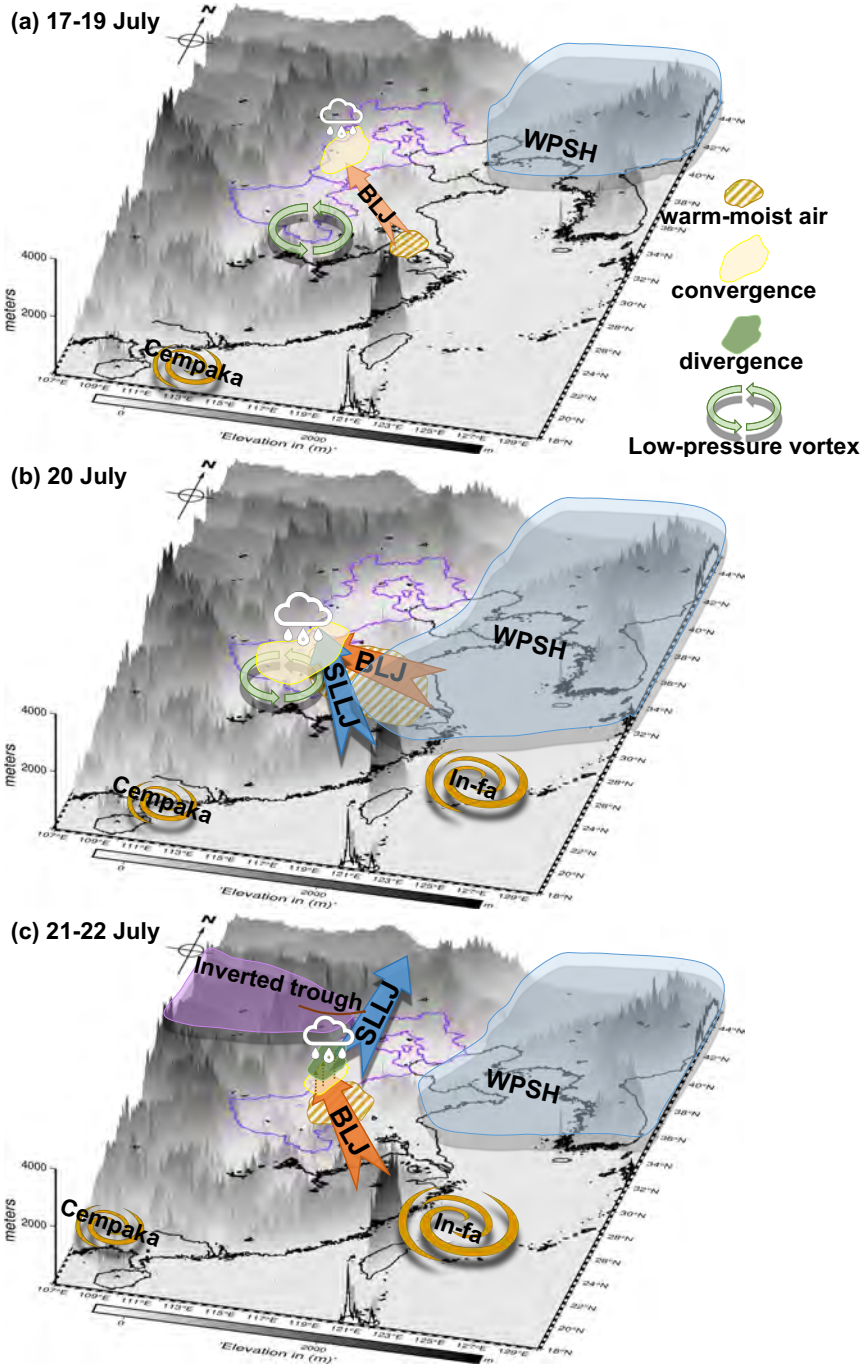

Fig. 1. Conceptual diagram of the persistent rainfall processes associated with BLJs and SLLJs in "21·7" rainfall event. (a) On 17-19 July, the southeasterly BLJ impinged the terrain and triggered convergence at the exit region of the BLJ to start the rainfall process. (b) On 20 July, the BLJ was intensified and turned to easterly, resulting in a southward movement of precipitation. The SLLJ was driven by the high pressure gradient between the WPSH and the low-pressure vortex. The low- and mid- level convergence occur at the exit region of the BLJ and the left region of the SLLJ. (c) On 21-22 July, the SLLJ moved northward with the inverted trough and produced divergence at the entrance region in the mid-level, which was coupled with the convergence at the exit region of the BLJ and thus maintained the northward shifting rainfall.

Analysis on Weather Situations of the Ultralight Aircraft Incident on 7 January 2021 over the Complex Terrain in Southern Taiwan Based on the Mesonet Array and Radar Measurements

Tai-Hwa Hor[a], Tian-Yow Shyu[a], Chiung-Kuang Chu[b]
[a] *Lunghwa University of Sci. and Tech., Taiwan, ROC*
[b] *Inspection Office, Air Force Combat Command, ROC*

Abstract

At 1635TST (UTC+8) on 7 January 2021, the Pingtung County Fire Bureau received a report about a burning plane identified as an ultralight CTLSi aircraft with the serial number AJ-2199. The aircraft departed from Runway 26 of Jiehao airfield in Gaoshu Township, Pingtung County at about 1420TST to perform orientation with a planned flight route. Before the release of the Occurrence Investigation Report by TTSB (Taiwan Transportation Safety Board), the study plans to organize a mesonet array of six weather stations in spacing of 6~18km on 07 January 2021, including hourly data collected by five CWB (Central Weather Bureau) weather stations plus the METAR data of Pingtung Air Force Base as well as the radar observations (Fig. 1a). The preliminary findings illustrated that the SW flow between 850hPa and 700hPa levels brought abundant moisture air inland over the complex topography and spectacular mountainous features in the south Taiwan area. The visibility reduced from 4000m to 3200m before the takeoff with light rain as well as scattered clouds in altitude of 600ft (~183m) and overcast in altitude of 1600ft (~488m) at 1400TST. During the possible flight period between 1420TST~1530TST, the radar map emphasized the scattered and weak echoes in 15-20 dBZ (Fig. 1b), and it kept in light rain and bad visibility due to the scattered low clouds. The preliminary findings were that the persistent light rain and scattered low clouds over the complex hillside area might reduce the visibility sharply.

After the release of the Occurrence Investigation Report by TTSB on 10 Dec 2021, it confirms that the estimated visibility at the plane takeoff was about 1000m, accompanying with persistent drizzle/light rain. Since the ultralight plane may only be operated under VMC (visual meteorological conditions) in cloud ceiling of 1500ft (~457m) and visibility of 5000m, the IFR (instrument flight rules) operation is permitted if the aircraft is equipped with the appropriate instrumentation. Therefore, the conclusions between the previous study and the TTSB report are quite consistent, implying that the real-time meteorological services are quite significant to popular light aviation activities for recreation and sports in Taiwan.

Keywords: ultralight aircraft incident, mesonet array.

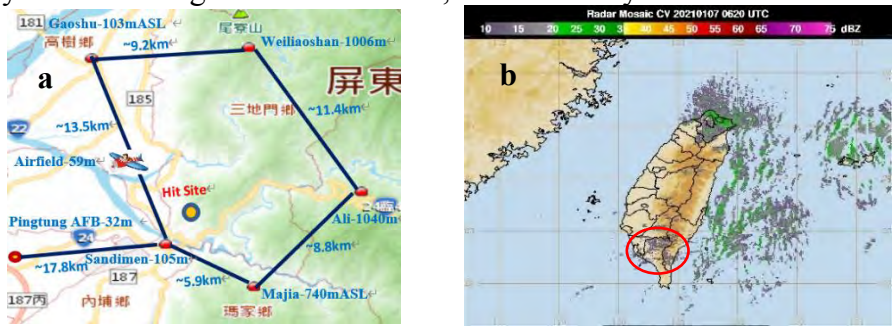

Fig. 1 (a) The mesonet array of six weather stations in spacing of 6~18km on 07 January 2021.The hit site of the ultralight AJ-2199 aircraft is located at 22.72959ºN and 120.642942ºE. (b) The radar mosaic CV map in Taiwan at 1420 TST(UTC+8) on 07 January 2021. The red circle covers the mesonet array.

Corresponding author: Tai-Hwa Hor, taihwahor@gmail.com

Ingredient-based analysis for extreme rainfall events in Taiwan

Tianqi Zuo[1], Alison D. Nugent[1], Kristen Rasmussen[2], Angela Rowe[3], Hungjui Yu[2]

[1] *University of Hawai'i at Manoa, Honolulu, HI*

[2] *Colorado State University, Fort Collins, CO*

[3] *University of Wisconsin-Madison, Madison, WI*

Corresponding author: Tianqi Zuo, tianqi@hawaii.edu

Extreme rainfall is a high impact weather phenomenon that affects people globally. Extreme rainfall events typically result from high intensity rain rates, long duration rainfall, or a combination of the two. Previous studies have found multiple synoptic and mesoscale environments or ingredients that are favorable for extreme rainfall to occur, such as conditionally or potentially unstable airflow accompanying a moist low-level jet, complex topography, and quasi-stationary synoptic-scale systems.

Taiwan is a global hotspot that frequently receives a variety of extreme rainfall events. With the goal of improving our understanding and predictability of extreme rainfall events, we are investigating how atmospheric ingredients combine together to produce a spectrum of extreme precipitation. Both historical rain gauge observations and the recently collected Prediction of Rainfall Extremes Campaign In the Pacific (PRECIP) field data from boreal summer 2022 are viewed with an Intensity-Duration framework. In addition, because the interaction between atmospheric ingredients and topography is often non-linear, we use the linear theory model for orographic precipitation (LTOP) to simplify the complex. It is find that duration matters more than intensity for extreme precipitation when combined with complex topography, and the LTOP model has the ability to captured the observed spatial distributions of rainfall.

Polarimetric Characteristics of a Stranded Meiyu Rainband in North Taiwan

Wu, Zong-Lin[1] and Ben Jong-Dao Jou[1, 2]

[1] Center for Weather and Climate Disaster Research, National Taiwan University, Taipei, Taiwan

[2]Department of Atmospheric Science, National Taiwan University, Taipei, Taiwan

Abstract

From the night of June 1 to the early morning of June 2, 2017, Taiwan experienced a heavy rainfall event caused by a stationary front. The front tangled in the northern Taiwan for nearly 10 hours, bringing in more than 600 mm of staggering rainfall. Based on the frontal movement characteristics, the study divides this heavy rainfall event into three periods: southward movement period (p1), quasi-stationary period (p2), and second southward movement period (p3), respectively.

During p1, the rainband landed at northern tip of Taiwan on 1800 UTC, June 1 and brought heavy rain to the area with 150 mm in few hours. Then the rainband moved southward to Taipei Basin, slowed down and weakened. In p2, the main rainband possessed a narrower area over NW coast. The prefrontal convection merged into the main rainband and intensified and brought heavy rainfall over the area. At the end of this period, the rainband retreated northward to stayed in the northern ocean. In p3, the rainband moved southward again and entered Taipei Basin (~ 0200 UTC, June 2). Large number of convective cells developed and merged with the rainband at the leading edge of the front, resulting in heaviest rainfall for the event.

Earlier researches have shown in this case, the front was stalled by the low-level jet caused by Taiwan terrain. In this study, we focus on discussing the possible role of this barrier jet on modulating the rainfall. The S-band polarimetric radar at Wu-Feng-Shan (RCWF) is used to document the rainfall characteristics of the stranded rainband in these three periods. The preliminary results show in p1, the maximum Zdr and Kdp in rainband is about 2.5 dB and 2 deg km^{-1} and in p2, Zdr and Kdp increased to 3.5 dB and 3 deg km^{-1} when prefrontal convections merged with the main rainband at the northwest coast of Taiwan. This is the time when Taipei basin experienced heavy rainfall. In p3, Zdr and Kdp decreased again. It is suggested the complete evolution was strongly modulated by the low-level jet over the NW coast of Taiwan.

Corresponding author: Dr. Ben Jong-Dao Jou, jouben43@gmail.com

Comparison of Two Post-Monsoon Heavy Rainfall Events in South Korea

Minseo Yu [a], Sujeong Lim[b,c], and Seungyeon Lee[a,b,c], Seon Ki Park[a,b,c]

[a] *Department of Climate and Energy Systems Engineering, Ewha Womans University, Seoul, Republic of Korea*

[b] *Center for Climate/Environment Change Prediction Research, Ewha Womans University, Seoul, Republic of Korea*

[c] *Severe Storm Research Center, Ewha Womans University, Seoul, Republic of Korea*

Corresponding author: Seon Ki Park, spark@ewha.ac.kr

In this study, we analyzed two heavy rainfall events occurred in July 2011 and August 2022, respectively, in South Korea, which were caused by atmospheric instability after the monsoon (Changma) period. Both occurred when a blocking high was located in the northeast of the Korean Peninsula (KP). Meanwhile, over the KP, warm humid air was supplied to the low-level atmosphere from the North Pacific High (NPH), whereas cold and dry air flew into the mid-level of the troposphere along the trough located in the north of KP — causing strong instability. The southwesterly low-level jet stream supplied heat and moisture to the KP, which was located under the divergence area of the upper-level jet stream, causing strong convection and low-level and forming deep convective clouds. Satellite images from the infrared channel show cloud cells growing and combining with themselves while passing the west coast of KP. The K-index and lifted index values also showed a high possibility of heavy rain due to static instability. Because the NPH expanded northward in 2011 and westward in 2022 than usual, the 2011 case showed a relatively scattered rainfall area under a stationary front while the 2022 case had a concentrated, definite horizontal rainband.

Observed Microphysical Characteristics of Orographic Precipitation Associated with Typhoon Chanthu (2021)

Tsubaki Hosokawa [a] and Cheng-Ku Yu [a]

[a] *Department of Atmospheric Sciences, National Taiwan University, Taipei, Taiwan*

Corresponding author: Tsubaki Hosokawa, d10229006@ntu.edu.tw

This study aims to document microphysical characteristics of precipitation enhancement over Da-Tun Mountain (DT) of northern Taiwan associated with Typhoon Chanthu (2021) using two Doppler radars, one of which is dual-polarized, a dense rain gauge network and disdrometers. Chanthu approached the DT area as it moved northward along the eastern coast of Taiwan and brought heavy precipitation over northern Taiwan. Rain gauge observations indicated a 48-h accumulated rainfall of 234 mm near the mountain ridge of DT. In this event, there were two distinct TC background precipitation types influenced the DT area; outer rainband (stage1, Fig. 1a) and weak stratiform (stage 2, Fig. 1b). There was a noticeable rainfall enhancement over the mountainous region compared to the surrounding coastal areas (Fig. 1c, d). The orographic enhancement of rainfall was the greatest during stage 1 and decreased during stage 2. Primary rainfall was brought by the mature outer rainband with vertically extending radar echoes accompanying midlevel updrafts (~2.0 m s^{-1}). After the rainband passage, weak stratiform precipitation characterized by distinct bright-band signatures with weak vertical air motions influenced the analysis domain. The Froude number was greater than unity, and dual-Doppler wind field captured intensifying upslope lifting over the northeast-southwest oriented barrier of DT, corresponding to the approach of Chanthu. Disdrometer observation at Anbu showed a higher number concentration of midsize drops during stage 1 and a lower number concentration of midsize drops for stage 2 (Fig. 2a-b). The maximum mass-weighted mean diameter (D_m) reached 2.5 mm at Anbu while 1.75 mm over the Taipei basin (not shown), demonstrating the significance of the size increase over the mountain. Polarimetric parameters showed an increase in radar reflectivity (Z_{HH}), differential reflectivity (Z_{DR}), and specific differential phase shift (K_{DP}) below the melting level (Fig. 2c-e). These polarimetric characteristics imply drop-size and liquid water content increase due to the warm-rain process, namely collision-coalescence. Interestingly, the K_{DP} increase was more prominent for stage 1, suggesting the higher concentration of raindrops was the primary contributor to the heavy precipitation during this stage, which was consistent with the disdrometer observation (Fig. 2b). On the other hand, stage 2 was characterized by lower number concentration with small K_{DP}. It was speculated that the increase in drop size supported the persistent rainfall enhancement during stage 2. These results clarified how the orographic effect and background precipitation types modulated microphysical processes, influenced particle size distributions, and eventually contributed to heavy precipitation over DT.

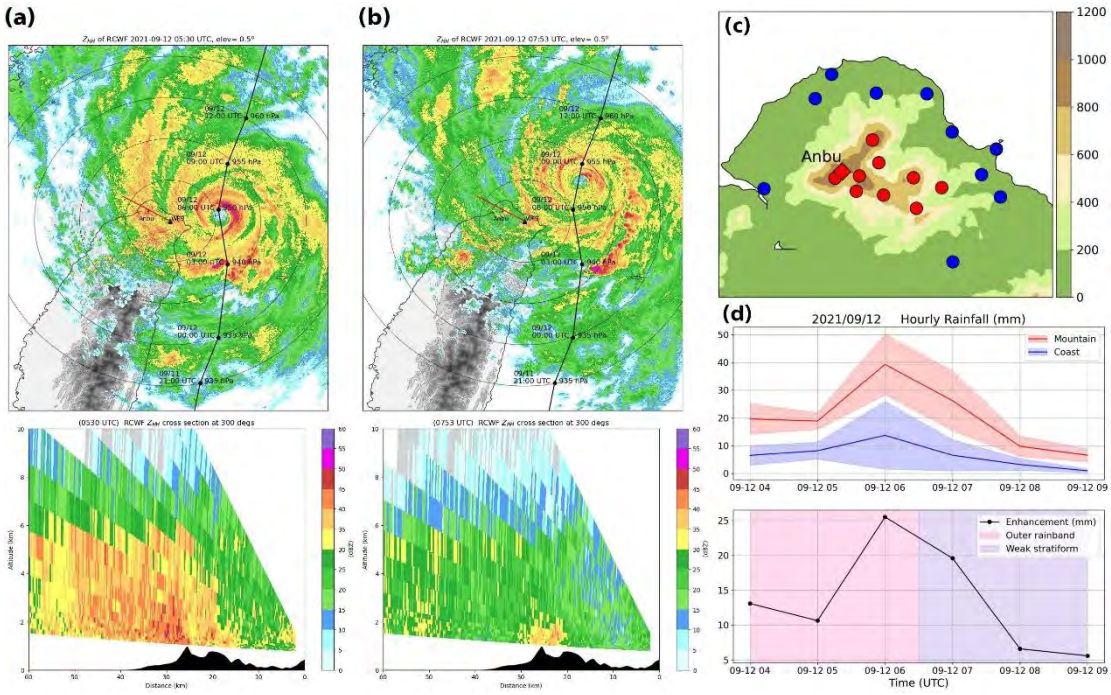

Fig. 1. (a)-(b) Radar reflectivity distributions by the lowest-available (0.5°) plan position indicator (PPI) from WFS radar with best track (black line with makers) from Japan Meteorological Agency (JMA) (top), and vertical cross-sections along red lines with topography cross-section (bottom). (c) Terrain height around DT and rain gauge locations of Mountain (red) and Coast (blue) groups. (d) Time series of hourly rainfall accumulation of each group mean (top) and the difference between Mountain and Coast groups (bottom).

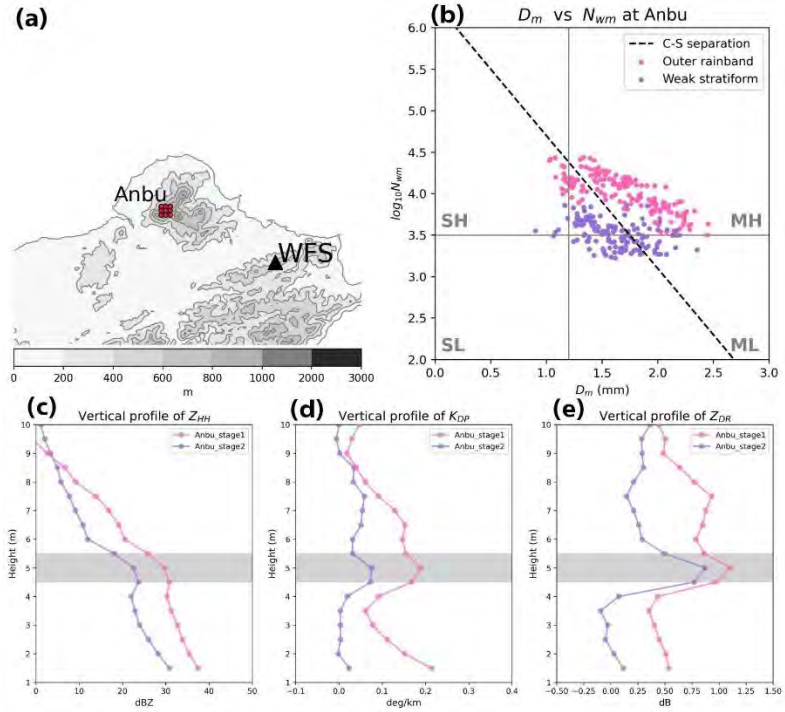

Fig. 2. (a) Sample grids for vertical profiles (Anbu). (b) Dm-Nw diagram observed by Parsivel disdrometers at Anbu. Convective-stratiform separation line (Bringi et al., 2009) is indicated with a dashed black line. (c)-(e) Average vertical profiles of Z_{HH}, K_{DP}, and Z_{DR}, respectively. r ray highlights indicate possible locations of the melting layer based on a sounding.

Investigation of Tropical cyclone intensification during Marine Heatwaves

Hwan Young Choi [a,b], Myung-Sook Park [b], Hyeong-Seog Kim [a] and Seonju Lee[b]

[a] Ocean Science and Technology School, Korea Maritime and Ocean University, Busan, South Korea

[b] Korea Ocean Satellite Center, Korea Institute of Ocean Science & Technology, Busan, Republic of Korea

Corresponding author: Myung-Sook Park, mspark@kiost.ac.kr , Hyeong-Seog Kim, hyeongseog@kmou.ac.kr

Marine Heat Wave (MHW) is one of the oceanic extreme warming events, in which sea surface temperature (SST) is abnormally warm for prolonged weeks to months and spread over hundreds to thousands of kilometers. Recently there has been increasing interest in MHW due to its devastating effects on marine ecosystems and influence on regional weather systems. In addition, Tropical Cyclone (TC) is an extreme weather event with strong surface wind and intense precipitation over the warm ocean condition, which causes fatalities and socioeconomic damage. Under global warming, the MHW occurred frequently and as it lasts longer. Thus, future TC activities are more likely to undergo characteristics changes under the influence of MHW. We show the MHW impacts on the western Pacific and North Atlantic TCs by observation data from 1982-2019. Therefore, we divided TCs into two groups: TCs intensifying under the MHW (MHW TC) were 84, and others without the MHW (non-MHW TC) were 363. Compared to non-MHW TC and MHW TC, MHW TCs are rapidly intense from 3 days prior to the maximum intensity day in the TC life cycle and LMI wind speed is also stronger than 17.97knot. In addition, the MHW TC precipitation rate has increased about twice, due to increasing water vapor with extremely high SST. At the same time, MHW TC releases latent heat flux on the ocean and atmospheric boundary. Precipitation-rich conditions and a lot of LHF released increased the convection near the TC center these two factors boast the TC intensity. For more detail, we also examine the unusual ocean structure during the 2016-2017 western North Pacific marine heatwave developments. With MHW TC cases we invested in how the unique atmospheric and oceanic conditions consist of MHW, and it affects the TC intensification process. This study establishes the scientific connection between MHW events and tropical cyclones by examining the effect of MHW events on TC intensity.

Convective and Microphysical Characteristics of Extreme Precipitation over the Pearl River Delta at Monsoon Coast

Yali Luo[a], Shuting Yu[b], Yanyu Gao[c], Chong Wu[c], Mingxin Li[c], Dong Zheng[c], and Weixin Xu[d]

[a] *Nanjing University of Information Science & Technology (NUIST), Nanjing, China*

[b] *Ji'nan Meteorological Bureau, Ji'nan, China*

[c] *Chinese Academy of Meteorological Sciences, Beijing, China*

[d] *Sun Yat-Sen University, Zhuhai, China*

Corresponding author: Yali Luo, yali.luo@nuist.edu.cn

Extreme precipitation is an issue of worldwide concern, but its microphysics remain elusive. Using multisource data including 5-yr dual-polarization radar observations, convective and microphysical characteristics of extreme precipitation features (EPFs) over a densely populated monsoon coastal region in South China are investigated including the common features, the dependence on rainfall extremity, and the subseasonal variations.

Based on the 95th, 99th and 99.9th percentiles of 1-min rain rates observed by AWSs, the EPFs are classified into three groups with increasing rainfall extremity (ER1, ER2, ER3): 56,167 EPFs producing rain rates of 84 mm hr^{-1} – 126 mm hr^{-1}, 35,037 EPFs producing rain rates of 126 mm hr^{-1} – 186 mm hr^{-1}, and 21,527 EPFs producing rain rates of at least 186 mm hr^{-1}. The EPFs with maxHt_40dBZ above 9 km, between 6 and 9 km, below 6 km are then categorized into “intense”, “moderate”, and “weak” convection, respectively.

Common features are observed in the three categories of EPFs. Most EPFs (93%, 82%, 71% in ER1 to ER3) are meso-γ-scale convective elements embedded in non-linear shaped 20-dBZ precipitation regions, which include about three fourths of the meso-β-scale and one fourth of the meso-γ-scale. The EPFs have a wide range of convective intensity from “weak” to “intense” convection with active warm rain processes and a major portion of EPFs (about 60% to 80%) containing moderate-to-intense mixed-phase microphysical processes. Coalescence dominates the liquid-phase processes (accounting for about 70%) and the RSDs feature a mean size larger than the “maritime-like” and a mean population much higher than “continental-like” regime.

The convective and microphysical characteristics vary to some extent with the increasing rainfall extremity from ER1 to ER3. The fractions of intense and weak convective EPFs substantially increase (7.6%, 20.6%, 31.6%) and decrease (41.3%, 22.9%, 18.9), respectively, while those of the moderate convective EPFs remain about

50%. The more extreme rainfall is accompanied by enhanced mixed-phase processes, larger IWC and LWC, slight albeit statistically significant increases in the mean size and number concentration of raindrops, and slight decreases in the fraction of coalescence in the liquid-phase processes.

Each April-to-August is divided into the pre-monsoon period, active-monsoon period and post-monsoon period based on the SCS summer monsoon activity, while the days with a tropical cyclone (TC) centered within 300 km from the Guangzhou radar are classified as a separate period (i.e., the TC days). During the pre-monsoon period, precipitation systems are the largest in area but their EPFs are the least frequent and have the lowest raindrop concentration, likely due to the colder, drier environment with large vertical wind shear (VWS). Onset of the summer monsoon increases the frequency and convective intensity of EPFs, leading to an increase in raindrop size, consistent with the substantial increases of CAPE and moisture during the active-monsoon period. EPFs share similar convective intensity and RSD between the post-monsoon and active-monsoon periods, although the post-monsoon EPFs are slightly less frequent and have a smaller horizontal scale related to the reduced 0–6-km VWS. EPFs associated with TCs have the weakest convective intensity but the most active warm-rain processes with the RSD being closer to the maritime regime.

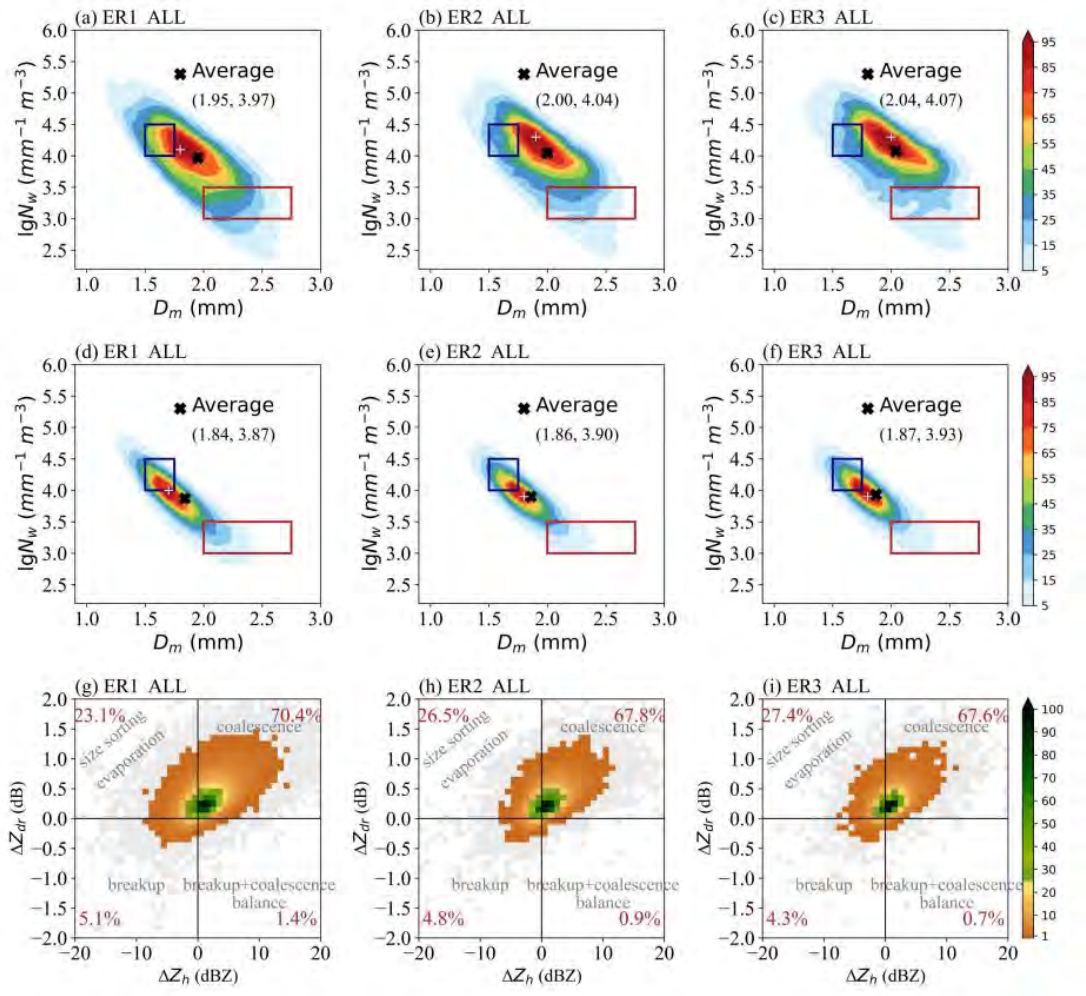

Figure 1. Normalized occurrence frequency (unit: %) of D_m and lgN_w at 1 km msl: (a-c) at the pixels with the 95th percentile of K_{dp}, and (d-f) their medians in individual EPFs. (g-i) Normalized occurrence frequency (unit: %) of the medians of ΔZ_h and ΔZ_{dr} from 3 to 1.5 km in the EPFs. Black "x" and white "+" in (a-f) represent the average and mode, respectively, while blue and red squares represent the maritime-like and continental-like clusters (Bringi et al., 2003). Red numbers in (g-i) denote the proportions in each quadrant.

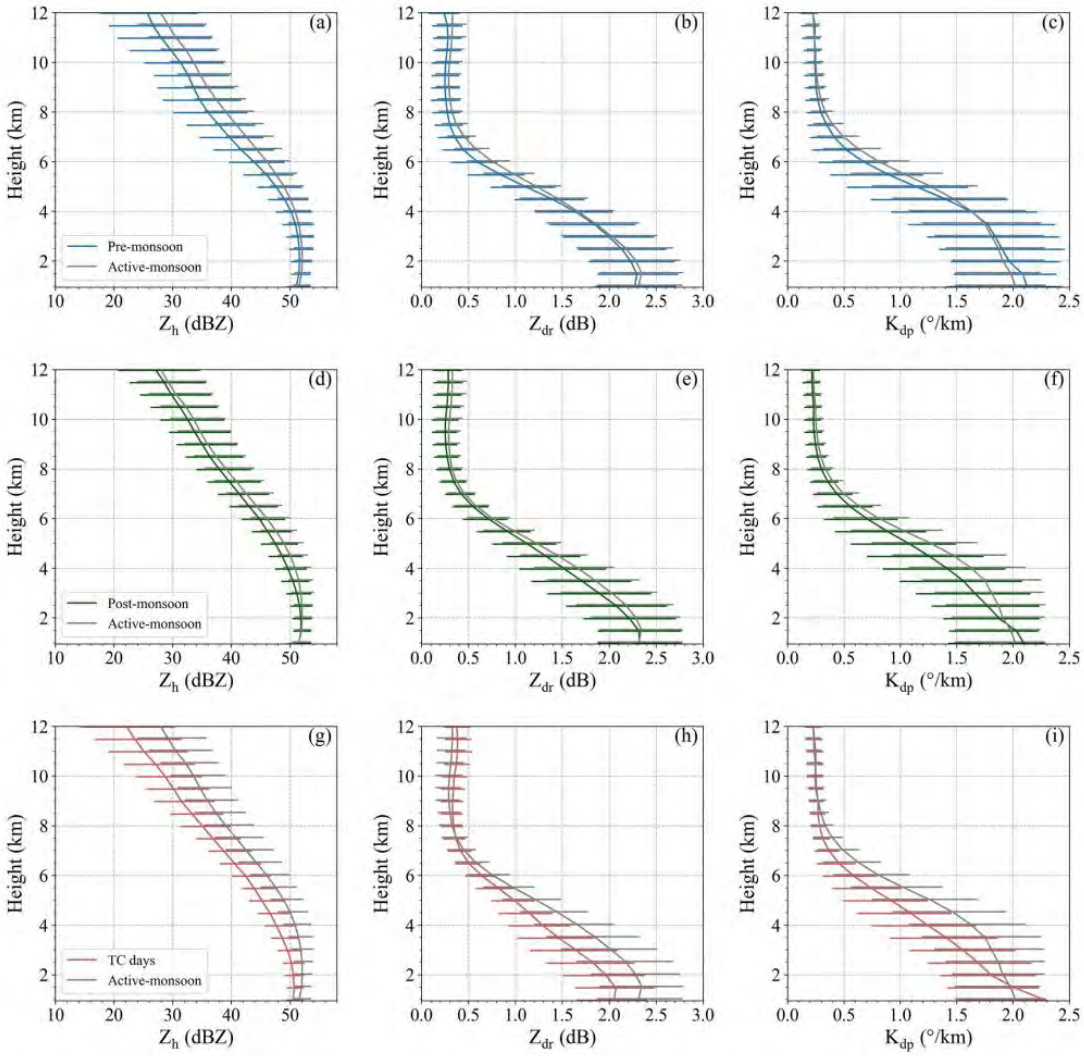

Figure 2. Average VP95 of Z_h (unit: dBZ), Z_{dr} (unit: dB) and K_{dp} (unit: °/km) during each of the four periods with the bars denoting the range from the 25th to 75th percentiles. Colors denote the periods as labeled.

Observation of initial stage of thunderstorm in South Taiwan

Radiant Rong-Guang Hsiu [a] and Ben Jong-Dao Jou [a, b]

[a] *Department of Atmospheric Sciences, National Taiwan University, Taipei, Taiwan*

[b] *Center for Weather Climate and Disaster Research, National Taiwan University, Taipei, Taiwan*

Abstract

Earlier studies indicate when subtropical high dominates Taiwan, the prevailing wind is southeasterly and convective storms frequently develop over the southwest plains. On 20th June 2008, during SoWMEX/TiMREX, a thunderstorm initiated and developed in Pingtung Plain. Clear-air signals within the boundary layer was observed by NCAR S-POL radar.

From Pingtung sounding, the inversion layer located near 800 hPa at 1100 LST and the mixed layer developed to 900 hPa. After 1100 LST, the surface wind changed to westerly possibly due to the enhanced differential heating between sea and land. Field photos and images from satellite observed the presence of cumulus clouds and the cumulus clouds thickened toward the foothill of the mountain in the east. After the passage of westerly wind, SPOL observed the cumulus clouds possessed Zhh 5~15 dBZ and ZDR ~ 0 dB, respectively. The westerly wind decelerated toward the foothill and increased speed convergence and favored upward lifting.

Deeper convective cell occurred near the foothill after 1300 LST. SPOL RHI showed Zhh was 20–30 dBZ below 2km altitude, and the maximum Zdr was ~4 dB. However, the 20 dBZ echo top still rose to approximately 4.5 km altitude and then decayed. It suggests there were several pulses of convective cell development. Until 1345 LST, the echo top of the developing cell bursted above the height of melting level and subsequently, the echo top continued to rise to approximately 15 km altitude. The detailed evolution of SPOL observations will be presented in the meeting.

Corresponding author: Dr. Ben Jong-Dao Jou, jouben43@gmail.com

The Variational Retrieved Raindrop Size Distribution by Moment-based Operators from Polarimetric Radar Measurements

Abstract

Drop size distribution (DSD) is one of the fundamental parameters for the microphysics process and it is difficult to directly observe the full weather system because of the limited area of the instrument. Using dual-polarimetric radar to retrieve DSD is useful to obtain the change of microphysical for the entire weather system. In general, the retrieved method is based on gamma distribution to reduce the degree of freedom and get the DSD parameter, such as shape parameter (μ), slope parameter (Λ), and intercept parameter (N0). However, the shape of DSD is incompatible with the gamma distribution if the specific microphysical processes are dominated. To avoid the model error of DSD, there is a new method with the moment-based operator to change the dual-polarimetric variables to the moments of DSD.

In this study, the OSSE experiment generated by the generalized gamma model (GG model) is tested to evaluate the different retrieved methods based on the variational method. Compare with the traditional operator, gamma model (μ, Λ, and N0), the moment-based operator for retrieved can reduce the error in each moment and avoid the error from the DSD shape hypothesis. Moreover, the different groups of moments (M2M3M4 and M3M4M6) have different sensitivity between lower moments and higher moments. The bias in high moments is less than the lower moment in each operator. In lower moments, the retrieved results are underestimated in different moment-based operators. Compare with different moment operators, the M2M3M4 can retrieve the results with less bias in lower moments. Changing the operators to moment based is significant to reduce the error from the model hypothesis and obtain accurate results for different moments to observe the microphysics process in the weather system.

An End-to-end Deep Learning Approach for Analyzing Tropical Cyclone 2-D Surface Winds Utilizing Satellite Data

Yung-Yun CHENG and Buo-Fu CHEN

Center for Weather and Climate Disaster Research,

National Taiwan University, Taipei, Taiwan

Corresponding author: Buo-Fu CHEN, bfchen777@gmail.com

Although tropical cyclone (TC) forecasts can fairly well capture the TC track and primary rainfall distribution, limited skills are found in forecasting TC structural changes and asymmetric gusty winds. The barrier to further understanding TC structural change is due mainly to the lack of observation, and it is difficult to have systematic 2-D wind analyses. Here, we developed a deep learning model — Deep Learning 2-D Structure Analysis Model for Tropical Cyclones (DSAT-2D) — to produce TC wind analysis in high-temporal-spatial resolutions based on generative adversarial networks (GAN). We use IR1 satellite observation and ERA5 reanalysis data as the model input for the DSAT-2D. The ASCAT surface wind data were collected and used as the label data. Note, however, that the ASACT analysis tends to underestimate winds greater than 15 m/s. Thus, we proposed several methods to fix this issue before training the model. Furthermore, other innovative designs in the DSAT-2D model include: (i) we regrid all data in a polar coordinate to better handle the TC tangential and radial features, and (ii) we also set the target of the DSAT-2D model as the TC radial wind and tangential wind.

Experiment results demonstrate that the DSAT-2D model can capture the TC asymmetric wind structure while possessing the capability of increasing the maximum estimation frequency from approximately 12 hours (e.g., ASCAT data) to less than one hour. The DSAT-2D model may help understand the TC asymmetric wind evolution and improve TC forecasts. Future applications of assimilating this value-added information into the numerical weather prediction model will also be discussed.

Response experiments of heavy rainfall events to global warming

Yasutaka Wakazuki and Kasumi Kobayashi

Graduate School of Science and Engineering, Ibaraki University, Mito, Japan

Corresponding author: Yasutaka Wakazuki, ywakazki@gmail.com

Abstract

In recent years, many hydrological disasters related to heavy rainfall have been caused in Japan by Baiu frontal precipitation systems and typhoons. Many studies point out that serious rainfall events have increased in recent years, and heavy rains and floods are predicted to intensify and become more frequent in the future climate. Here, we have an important question whether the degrees of precipitation enhancements for heavy rainfall events are mainly controlled only by the enhancement of water vapor or not. The degrees of precipitation enhancements should be investigated for various phenomena and locations. This study investigated how mesoscale heavy rainfall phenomena climatologically change by applying high-resolution simulations with a non-hydrostatic cloud-resolving atmospheric model and the pseudo-global-warming method. Three types of events were extracted for the investigation: Narrow range quasi-stationary meso-β-scale rainband event at Northern Kyushu in July 2017, wide range rainband event in Western Japan in July 2018, and Typhoon Hagibis in 2019. In addition, we applied the atmospheric water budget analyses to understand factors for precipitation to be enhanced.

To estimate the precipitation enhancement for the events, climatological increments of air temperature and water vapor, calculated from the d4PDF data set, were applied and added to the initial and lateral boundary conditions in the pseudo-global-warming experiments. Two types of climatological increments in mean temperatures since the Industrial Revolution was assumed to be 2 and 4 °C, corresponding to temperature increases around 2040 and 2100 based on the RCP8.5 scenario. In addition to the regular future climate experiments (stabilization increment experiments), neutral increment experiments were performed, in which the air temperature increase is uniform for all vertical levels.

The atmospheric model simulations with the grid spacing of 1 km reproduced precipitations well. In the future climate experiments, precipitation increased in all 2- and 4-°C stabilized and neutral experiments (Table 1). In particular, a significant increase in rainfall was observed in the 4-°C neutral experiment (not shown). The atmospheric water budget analyses derived that water vapor increase affected precipitation enhancement for all cases. In addition, dynamic effects related to the

intensification of convections resulted in increased precipitation that exceeded the CC effect (enhancement of water vapor). In the case of Typhoon Hagibis, the convergent-enhancement impact on the mountain slopes on the upwind side significantly contributed to the enhancement of precipitation (Fig. 1). In the case of the Baiu frontal rainband on the Northern Kyushu, the occurrence enhancement of line-shaped rainbands largely contributed to the enhancement of rainfall, especially on the upwind side of the precipitation system. In the case of the Baiu frontal wide-range rainband, precipitation was almost the same as the enhancement of the water vapor. In contrast, the local intensification of the convective effect appeared on the upwind side of the rainfall area.

Table 1: Increase rate of precipitation [(Future – Present) / Present]

Case	Experiment	Total precipiation	Period (R>10mm/h)
Case III (Typhoon Hagibis) (48 hours)	+2℃	+9 %	+9 %
	+4℃	+29 %	+22 %
Case I (96 hours)	+2℃	+8 %	+12 %
	+4℃	+26 %	+34 %
Case II (18 hours)	+2℃	+14 %	+18 %
	+4℃	+44 %	+51 %

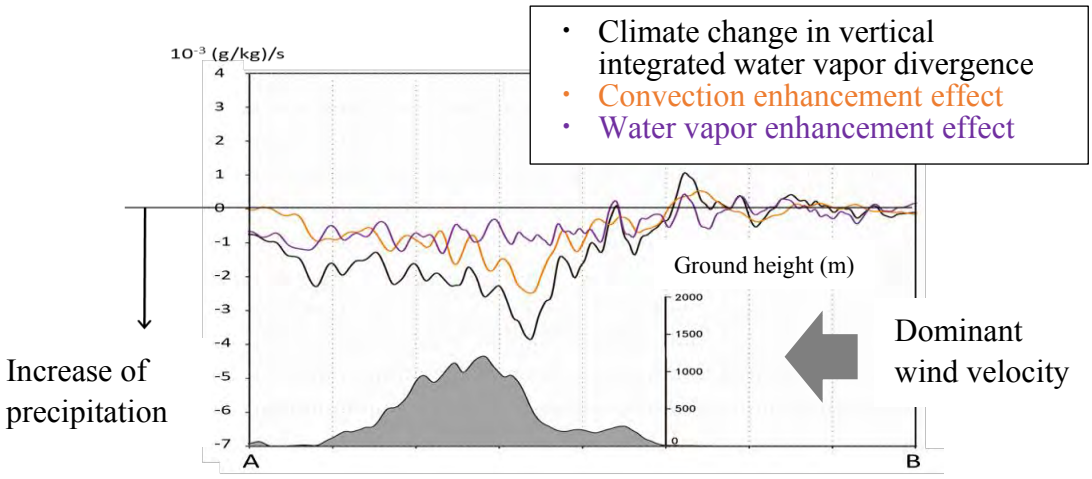

Fig.1: Atmospheric water budget analysis results along the dominant wind velocity for the case of Typhoon Hagibis. Climate change of precipitation is roughly explained by climate change of vertically integrated water vapor convergence, which is decomposed by the combination between the convection enhancement effect and the water vapor enhancement effect. The result shows that the precipitation was enhanced mainly by the convection enhancement effect on the upwind side of the high mountain.

Finding the missing constants on each horizontal layer in thermodynamic retrieval using multiple-Doppler-radar synthesized winds

Yu-Chieng Liou and Yung-Lin Teng

Dept. of Atmospheric Sciences, National Central University, Taoyuan, Taiwan

Corresponding author: Yu-Chieng Liou, tyliou@atm.ncu.edu.tw

ABSTRACT

It has been long recognized that when performing thermodynamic retrieval using wind fields synthesized by multiple Doppler radars, unknown constants with the form of the horizontal average of the pressure and temperature perturbations exist on each horizontal level in the retrieved thermodynamic fields, causing ambiguity in the retrieved vertical structure. In this research the Equation of State (EoS) is implemented as an additional constraint so that the horizontal average of the pressure and temperature perturbations on each level can be explicitly estimated and removed from the retrieved three-dimensional thermodynamic fields. The only in-situ independent observations needed to perform the correction is the pressure and temperature measurements taken at a single ground station. Experiments in this research were conducted under the Observation System Simulation Experiment (OSSE) framework to demonstrate the validity of the new approach. Problems and possible solutions associated with using real data sets and potential future extended applications of this new method are discussed.

Impact study of lower-atmospheric wind and thermodynamic profiles on convective weather forecasts over the CONUS

Junkyung Kay [a], Tammy Weckwerth[a], Glen Romine[a], Yue (Michael) Ying[b], and Dave Turner[c]

[a] *NCAR, Boulder, CO, USA*

[b] *NERSC, Bergen, Norway*

[c] *NOAA, Boulder, CO, USA*

Corresponding author: Junkyung Kay, junkyung@ucar.edu

The lack of sufficient observations in the lower atmosphere may lead to poor forecast performances. A combination of autonomous remote sensing instruments including the Atmospheric Emitted Radiance Interferometer (AERI), the water vapor MicroPulse Differential absorption lidar (MPD), and the Doppler wind lidar (DWL) can be utilized to fulfill these observational gaps in the lower atmosphere. The first field campaign of a network of remote sensing instruments, called the MPD Network Demonstration Project, combined the observational capabilities of the MPDs, AERIs, and DWLs at five sites at the DOE Atmospheric Radiation Measurement (ARM) Southern Great Plains (SGP) field site from 22 April – 19 July 2019. During the field campaign, temperature and water vapor profiles from the AERI, water vapor profiles from the MPD, and wind profiles from the DWL were collected to supplement the existing weather radar, wind profilers, and surface station data. This presentation will provide results of assimilating the wind and thermodynamic profiles from the field campaign. The impacts of AERI, MPD, and DWL are evaluated for a mesoscale convective precipitation on 14 June 2019. The Advanced Research version of the Weather Research and Forecasting model (WRF-ARW) and the Data Assimilation Research Testbed (DART) data assimilation system are used to conduct data assimilation experiments. The preliminary results suggest that data assimilation of the combined AERI, MPD, and DWL profiles resulted in an improvement in the analysis and forecast of an elevated moist layer and its variability, which led to more accurate prediction skill in precipitation. A comprehensive evaluation will be further performed to analyze the complementary aspects of the AERI, MPD, and DWL profiles.

Developing a rainfall threshold for a landslide early warning system in a data-scarce environment: a prototype from the Kulon Progo Region in Yogyakarta, Indonesia

Danang Eko Nuryanto[a], Guruh Samodra[b], Erwin Eko Wahyudi[c], Nanang Susyanto[d], Muhammad Auzan[c], Andi Dharmawan[c], Danang Sri Hadmoko[b], and Donaldi Sukma Permana[a]

[a] *Agency for Meteorology, Climatology, and Geophysics (BMKG), Jakarta, Indonesia*

[b] *Department of Environmental Geography, Faculty of Geography Universitas Gadjah Mada, Yogyakarta, Indonesia*

[c] *Department of Computer Science and Electronics, Faculty of Mathematics and Natural Sciences Universitas Gadjah Mada, Yogyakarta, Indonesia*

[d] *Department of Mathematics, Faculty of Mathematics and Natural Sciences Universitas Gadjah Mada, Yogyakarta, Indonesia*

Corresponding author: Danang Eko Nuryanto, danang.eko@bmkg.go.id

Abstract

Rainfall induced landslides pose a significant threat to communities living in mountainous areas in Indonesia, one of the most landslide-affected countries in the world. Due to its steep topography, volcanic soils and very high population density, Java Island is the most affected region. Landslide risk is often mitigated by slope stabilization and drainage methods in sites where landslides have taken place, and by reducing exposure of structures through proper land use planning. However, in densely populated areas, such as Java, landslide risk is best mitigated through reducing the population exposure by means of Landslide Early Warning Systems (LEWS). Landslide early warning is much more complicated compared to other types of natural hazards, as landslide initiation locations are difficult to predict, both in space and time, there are many different landslide types that have their own characteristics, and also landslide damage is most often caused by the runout, which requires even more parameters. The main purpose of this study is to describe the development of a geographical LEWS WebGIS prototype in a scarce data environment using comprehensive landslide inventory data, rainfall satellite data, and rainfall data forecasts. Based on the landslide inventory and IMERG rainfall data, the rainfall threshold for landslide occurrence was computed using the cumulated event rainfall (E) and the length of the event (D). The deployment of the landslide threshold on rainfall data forecasting was used to predict the chance of spatiotemporal landslides in the future. Landslide inventory data was divided into 647 landslides (January 2018 to July

2021) for rainfall threshold establishment and 137 landslides (September 2021 to March 2022). The development of LEWS WebGIS prototype based on rainfall threshold for landslide occurrence provides new possibilities to better awareness and better communication strategies and warning to landslide hazard in a scarce data environment.

Keywords: Kulon Progo region, landslide early warning system, rainfall threshold

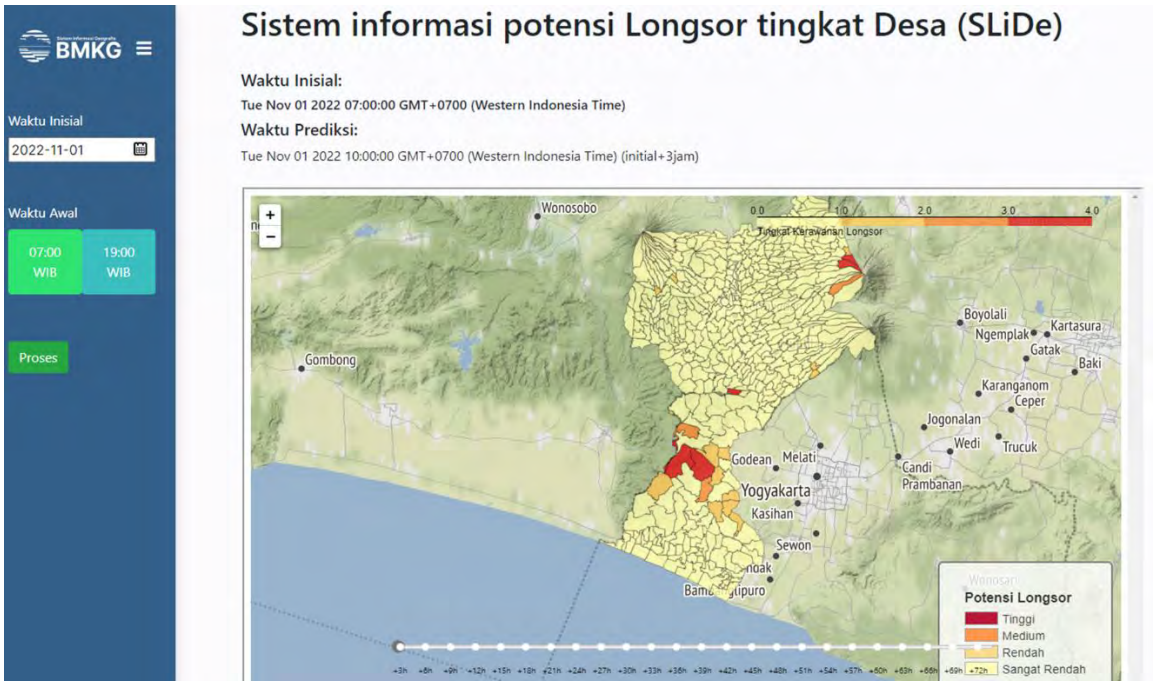

Figure 1. A prototype of webGIS based geographic LEWS in Kulon Progo Region

High-resolution retrievals of surface precipitation and hydrometeor profiles from the GPM Microwave Imager

Simon Pfreundschuh[a], Paula J. Brown [a], Christian D. Kummerow[a,] Clément Guilloteau[b]

[a] Colorado State University, *Fort Collins, Colorado, USA*

[b] University of California, Irvine, *Irvine, California, USA*

Corresponding author: Simon Pfreundschuh, s.pfreundschuh@gmail.com

The Global Precipitation Measurement (GPM) satellite mission constitutes the state-of-the-art of global, space-borne precipitation measurements. The GPM satellite, the core observatory of the mission, carries the dual-frequency precipitation radar (DPR) and a passive microwave imager, the GPM Microwave Imager (GMI). While DPR provides high-resolution retrievals of precipitation and hydrometeor profiles at a resolution of 5 km, its spatial coverage is limited to a swath width of 250 km.

We have developed GPROF-NN HR, a novel, neural-network-based retrieval algorithm that aims to extend the high-resolution profiling capabilities of DPR to the considerable wider swath of GMI. GPROF-NN HR significantly improves upon existing GMI retrievals in terms of accuracy and ability to resolve the spatial variability of precipitation. Validation of the retrieval against several years of ground-based measurements over CONUS and the tropical Pacific has shown that its accuracy at 5 km resolution is on-par with that of the combined GMI/DPR retrievals. The principal advantage of the GPROF-NN HR retrieval is that its swath width is more than three times that of DPR-based retrievals, thus enabling the retrieval to provide a more comprehensive view of specific weather events. An example of retrieved profiles of rain water content (RWC) and snow water content (SWC) in Hurricane Ida is shown in Fig. 1. The clearly visible rain bands demonstrate the retrieval's ability to resolve spatial structure of the Hurricane.

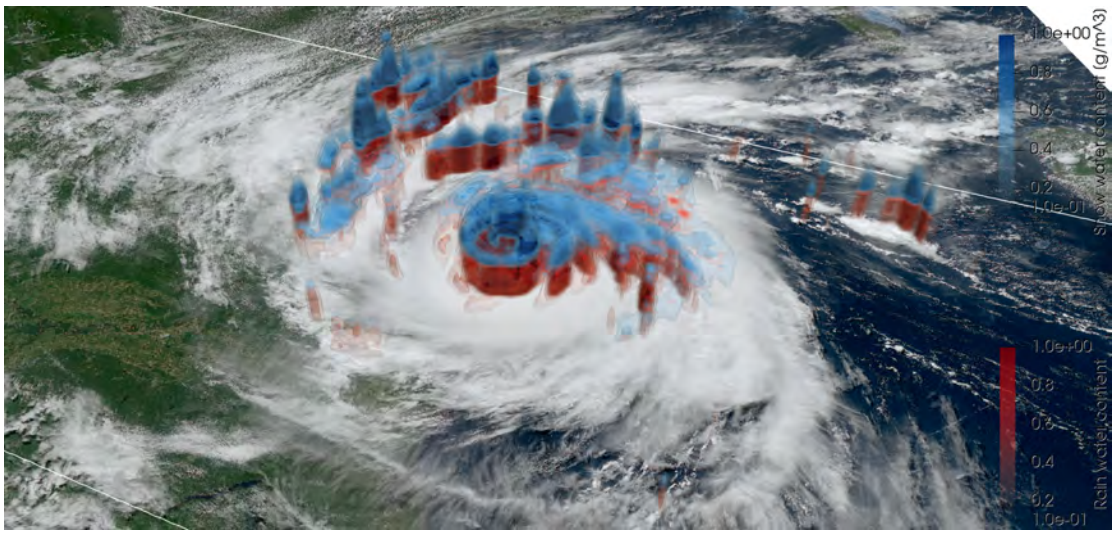

Figure 1: Rain water content (red iso-surfaces) and snow water content (blue iso-surfaces) in Hurricane Ida on 2021-08-29 15:14 UTC.

We have made GPROF-NN HR available as a Python-based, easy-to-use command line application, which only requires GMI L1C files as input, thus enabling interested researchers to run the retrieval for specific cases they may be interested in. Compared to currently operational DPR retrievals, GPROF-NN HR significantly increases the availability of high-resolution, quasi-global (60 S – 60 N) precipitation and hydrometeor-profile retrievals. We therefore expect GPROF-NN to be a powerful tool for studying hydrometeors in mesoscale convective systems.

Validating GOES Radar Estimation via Machine Learning to Inform NWP (GREMLIN) product over CONUS

Yoonjin Lee [a] and Kyle Hilburn [a]

[a] *Cooperative Institute for Research in the Atmosphere (CIRA)/Colorado State University (CSU), Fort Collins, CO, USA*

Corresponding author: Yoonjin Lee, yoonjin.lee@colostate.edu

Ground-based radar data is useful for observing severe weather and initializing convection for short-term forecasts. However, not many regions over the globe have dense ground-based radar networks, which are only available over land. To fill this observation gap, Geostationary Operational Environmental Satellites (GOES) Radar Estimation via Machine Learning to Inform NWP (GREMLIN) provides synthetic radar reflectivity from geostationary satellites. GREMLIN is a U-Net based model that generates composite reflectivity using GOES-16 Advanced Baseline Imager (ABI) and Geostationary Lightning Mapper (GLM) data. GREMLIN not only shows good skill compared to Multi-Radar/Multi-Sensor System (MRMS), one of ground-based radar products, but GREMLIN also shows improvements in precipitation forecasts when used during convective initialization. Since GREMLIN's performance has only been evaluated over a testing dataset that is within a similar climate and precipitation regime as in the training dataset, this study expands the evaluation to the entire contiguous United States (CONUS) and the entire annual cycle. Validation metrics such as root-mean square difference (RMSD) and bias as well as categorical verification metrics such as probability of detection (POD), false alarm ratio (FAR), critical success index (CSI), and frequency bias index (FBI) are calculated over CONUS by season, day of year, and time of day, and their regional and temporal variations are examined. GREMLIN generally shows low RMSD in spring, summer, and fall, but it has relatively high RMSD in winter due to cold surfaces frequently mistaken as precipitating clouds. Some of these errors in winter can be removed by applying the GOES ABI level 2 clear sky mask product. In summer when GREMLIN has the highest accuracy, diurnal patterns of RMSD in different longitude regions follow diurnal patterns of precipitation occurrence, while other seasons do not have such patterns. Categorical statistics at two thresholds of 5 dBZ and 30 dBZ are used to evaluate POD, FAR, CSI, and FBI. GREMLIN's accuracy is the best over the mid to eastern United States where it has been trained. However, over the northeastern part, CSI for the 30 dBZ threshold is very low due to low POD caused by different brightness temperature distributions and low frequency of lightning. On the other hand, Florida has relatively high FAR due to high frequency of lightning. In some regions, such as Texas and Washington, low GREMLIN accuracy is shown, but this is due to spurious echoes in MRMS.

Leveraging the Power of Machine Learning for Excessive Rainfall Forecasting

Aaron J. Hill [a], and Russ S. Schumacher [a]

[a] *Department of Atmospheric Science, Colorado State University, Fort Collins, Colorado, USA*

Corresponding author: Aaron Hill, aaron.hill@colostate.edu

Postprocessing numerical weather prediction output has gained considerable popularity in recent years as machine learning (ML) has emerged as an efficient and viable tool in generating explicit forecasts of weather hazards. As an example, the Colorado State University Machine Learning Probabilities (CSU-MLP) prediction system was developed to provide probabilistic first-guess forecasts of excessive rainfall to aid operational forecasters at the Weather Prediction Center (WPC). The CSU-MLP system uses Random Forests (RFs), reforecasts of the Global Ensemble Forecast System (GEFS/R), and multiple observational datasets of excessive rainfall to produce daily probabilistic forecasts extending out to 8 days in support of WPC operations and their experimental products. The system has shown positive skill out to day 6 regardless of the observational dataset used to train the RF models and there has been considerable interest garnered from the National Weather Service in using these products in operations. This presentation will provide a brief overview of the CSU-MLP system, including performance metrics, and highlight how we are using explainable artificial intelligence techniques to decipher what the RFs are learning surrounding the complex prediction task of extreme rainfall.

Deep Convection of IOP 2 case during TAHOPE 2022

Ming-Jen Yang[1], Jyong-En Miao[1], Ming-Dean Cheng[2], Ching-Yuang Huang[3], Pay-Liam Lin[3], Po-Hsiung Lin[1], Cheng-Shang Lee[1], Chung-Chieh Wang[4], Ching-Hwang Liu[5], Pao-Liang Chang[2], Jou-Ping Hou[6], Shu-Chih Yang[3], Kao-Shen Chung[3], Wei-Yu Chang[3], Ping-Fang Lin[2]

[1]National Taiwan University, [2]Central Weather Bureau, [3]National Central University, [4]National Taiwan Normal University, [5]Chinese Culture University, [6]National Defense University

Corresponding author: Ming-Jen Yang, mingjen@as.ntu.edu.tw

ABSTRACT

"Taiwan-Area Heavy rain Observation and Prediction Experiment" (TAHOPE) 2022 was conducted from 25 May to 10 August 2022 to study Mei-Yu fronts, mesoscale convective systems (MCSs), typhoons, and afternoon thunderstorms near Taiwan and Yonaguni, Japan. The intense observation dataset collected during TAHOPE 2022 includes the data from NCAR S-Pol radar, CSU SEA-Pol radar, Micro-Pulse DIAL (MPD), NCU TEAM-R radar, CWB operational radars, extra-release sounding, wind profiler, and surface observations. There are totally eleven IOPs and eight special observation periods (SOPs) conducted during the 2022 field phase. The SOP indicates a severe weather event which was miss-forecasted during the field campaign. The weather features observed during eleven IOPs include MCS (IOP 1, 2, and 3), quasi-stationary Mei-Yu front (IOP 3), prefrontal southwesterly flow (IOP 4), afternoon thunderstorm (IOP 2, 5, 8, and 11), and tropical depression/typhoon (IOP 6, 7, 8, 9, and 10). Among all IOP cases, the IOP 2 case with afternoon thunderstorm activity is selected to highlight the kinematic and microphysical characteristics of deep convective storms over northeastern Taiwan.

Dual-polarimetric parameters from S-POL radar, including horizontal reflectivity, differential reflectivity (Z_{DR}), specific differential phase (K_{DP}), and correlation coefficient, are used to examine the kinematic and microphysical process for IOP 2 event on 31 May 2022. Two convection episodes were observed. For the first episode, convective precipitation was accompanied by strong and upright updrafts (with peak intensity near 10 m s^{-1}) and deep convergence zone (with the depth of 4 km). For the second episode, the convection was accompanied with weak and slantwise updrafts (with peak intensity < 4 m s^{-1}), and deep easterly flow with dry-air intrusion enhanced evaporation and weakened the convective storms.

During the first episode, both Z_{DR} and K_{DP} columns were identified as deep convection occurred. The dominant warm-rain processes were collision-coalescence and hydrometeor size-sorting, and riming process was active when both the vertical and horizontal extents of graupel and hail particles were enlarged. During the second episode, the convective storm exhibited a distinct multicell structure with cells at various stages of maturity. Both convective and stratiform regions showed significant evaporation (riming) at lower (upper) levels. Riming with Hallett-Mossop splintering was identified in the convection region, and melting (diffusion) was dominant at the middle (upper) levels in the stratiform region.

Moist Flow Regime Transition and Heavy Orographic Rainfall Formation Mechanisms During Super Typhoon Netpartak's Passage over Taiwan's Central Mountain Range

S. M. Shajedul karim, and Yuh-Lang Lin
North Carolina A&T State University

Super Typhoon Nepartak was the third most intense tropical cyclone worldwide in 2016, which made landfall on 8 July in Taitung County, Taiwan. It was a very severe and deadly storm that made landfall in Taiwan in the last decade. As Nepartak moved towards and passed over Taiwan's Central Mountain Range (CMR), heavy orographic rainfall occurred along its movement, with the amount of rainfall increasing as it approached landfall. This study aims to investigate the moist flow regime transition and formation and enhancement mechanisms of orographic rainfall during the passage of Nepartak over the CMR, using both real case and idealized case (2D and 3D) Weather Research and Forecasting (WRF) simulations. In particular, we differentiate the contribution of different forcing to the formation of orographic rainfall, such as orographic lifting, the release of instabilities, and the enhancement of a pre-existing system. Our results show that the moist flow regime transition significantly influenced the formation of orographic rainfall. The study also found that upslope rainfall over Yu-Shan Mountain was mainly produced by orographic lifting, while heavy orographic rain production over Tai-Tung resulted from a low-CAPE and high-wind environment. Our study provides valuable insights into the orographic impacts on precipitation during the passage of a tropical cyclone over an isolated, 3D mountain range.

The role of free-tropospheric moisture convergence for rainfall events in western Japan

Hiroki Tsuji [a] and Y. N. Takayabu[a]

[a] *Atmosphere and Ocean Research Institute (AORI), The University of Tokyo, Kashiwa, Chiba, Japan*

Corresponding author: Hiroki Tsuji, h-tsuji@aori.u-tokyo.ac.jp

The role of free-tropospheric moisture convergence for rainfall events in western Japan is statistically investigated using 15 years of the Japan Meteorological Agency's mesoscale gridded analysis (MSM) data. Rainfall events are defined by peaks of area-averaged precipitation around Kyushu Island located in western Japan. The time evolution of each term in the water vapor budget equation shows an increase in the free-tropospheric (900–300 hPa) integrated water vapor flux convergence (IVFC) before rainfall events with increasing precipitable water tendency, contributing to atmosphere moistening. In contrast, the boundary-layer (1000–900 hPa) IVFC shows little change until just before the rainfall events. This preceding moistening is favorable for organizing mesoscale convective systems (MCSs) with slantwise ascending deep inflow layers that produce a large amount of precipitation. The moist absolutely unstable layer (MAUL) is frequently observed around the precipitation peaks, which is especially notable for larger precipitation peaks. These results indicate that the free-tropospheric IVFC contributes to heavy rainfall in western Japan by providing environments favorable for formation and maintenance of organized MCSs.

We further analyze a rainfall event over Kyushu in July 2020 focusing on the mechanism moistening the free troposphere. An increase in moisture associated with the free-tropospheric IVFC is also analyzed in this event. A synoptic scale upper-tropospheric trough transports free-tropospheric moisture from the South China Sea to Kyushu via southern China. The free-tropospheric moisture converges in a sub-synoptic (about 2000 km) scale cloud system developed in front of the trough, providing a moist environment before the rainfall event. A mesoscale depression below the trough developed over central China enhances the free-tropospheric moisture transport. Cyclonic circulations associated with the mesoscale depression and the sub-synoptic scale cloud system enhance the baroclinicity around Kyushu. Under such an environment, an MCS develops with intense precipitation areas causing the rainfall event (Fig. 1a). The vertical cross-section of an intense precipitation area shows structures consistent with the organized precipitation systems with deep inflow layers and MAUL (Fig. 1b). These results suggest a hierarchy structure for the extreme rainfall that the organized precipitation system develops under the moist environment prepared by the large-scale free-tropospheric moisture flux convergence associated with the upper-tropospheric trough, the sub-synoptic scale cloud system and the mesoscale depression.

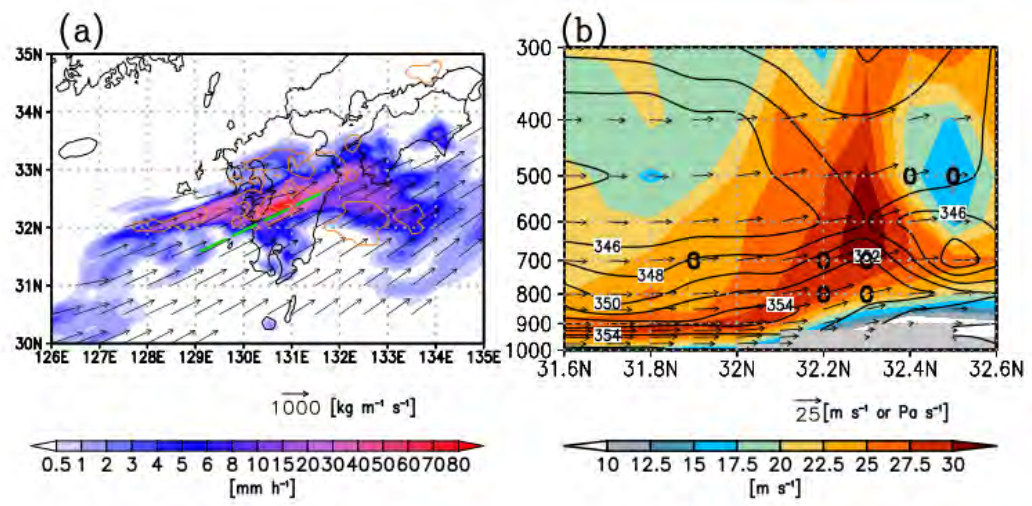

Fig. 1: (a) Precipitation distribution (color, mm h^{-1}) and vertically (1000–300 hPa) integrated water vapor flux (vector, kg m^{-1} s^{-1}, shown only over 1000 kg m^{-1} s^{-1}) obtained from the MSM data at the rainfall peak time. Orange contours designate areas where MAUL conditions are satisfied at least 2 vertical levels between 500 and 800 hPa. (b) A vertical cross-section of a wind velocity along the cross-section (color, m s^{-1}), wind vectors (m s^{-1} for horizontal direction and Pa s^{-1} for vertical direction), and equivalent potential temperature (black contour, K) along the green dashed lines in Fig. 1a. The black circles indicate grids that fulfill the MAUL condition.

References

Tsuji, H. et al., 2021, *Geophys. Res. Lett.*, doi:10.1029/2021GL095030

Tsuji, H. and Y. N. Takayabu 2023, *J. Meteor. Soc. Japan*, under review.

A High Resolution Tropical Mesoscale Convective System Reanalysis (TMeCSR)

Man-Yau Chan[a], Xingchao Chen[b], and Ruby Leung[c]

[a] *National Center for Atmospheric Research, Boulder, Colorado, USA*

[b] *Department of Meteorology and Atmospheric Science, The Pennsylvania State University, State College, Pennsylvania, USA*

[c] *Atmospheric Science and Global Change, Pacific Northwest National Laboratory, Richland, Washington, USA*

Corresponding author: Man-Yau Chan, manyau@ucar.edu

Abstract

The advent of reanalysis data products has dramatically accelerated progress in our understanding, modelling and prediction of Earth system phenomena. However, in the context of tropical mesoscale convective systems (TMCSs) over the Pacific warm pool and East Asia, the benefits of reanalysis products are largely restricted to providing environmental information on TMCSs. This restriction is a result of the coarse spatial resolutions of existing reanalysis products – it is difficult to explicitly resolve TMCSs with coarse-resolution numerical weather models. Furthermore, in-situ observations over the region are too sparse and infrequent to explicitly resolve the mesoscale structures within TMCSs, and remote-sensed satellite observations are underutilized in many reanalysis products. The creation of a high-resolution TMCS-resolving reanalysis dataset that effectively utilizes both in-situ and remote observations thus has the potential to accelerate research into these socioeconomically important systems.

In this talk, I will present on the creation and validation of a high-resolution Tropical Mesoscale Convective Systems Reanalysis (TMeCSR) community dataset over a region frequented by TMCSs. This dataset spans the Indian Ocean, the Pacific warm pool, tropical continental Asia, and the Western Pacific, and has captured more than 1200 TMCS events. The TMeCSR is created by assimilating in-situ observations and frequently available high-resolution satellite data (infrared radiances and atmospheric motion vectors) into an ensemble of MCS-resolving Weather Research and Forecasting (WRF) simulations (9-km grid spacing). This assimilation is achieved using the state-of-the-art Pennsylvania State University Ensemble Kalman Filter (PSU-EnKF) system. All the standard WRF model output variables, as well as latent and radiative heating rates, are publicly accessible at an hourly frequency and 9-km horizontal resolution for June, July and August of 2017. Uncertainty estimates of this dataset are also publicly available. Finally, the TMeCSR outperforms the gold standard ECMWF Reanalysis version 5 (ERA5) at resolving TMCSs and the diurnal rainfall cycle of the equatorial Maritime Continent. The TMeCSR is thus a veritable trove of publicly available and observation-constrained gridded TMCS data that will likely benefit TMCS research for years to come.

(329 words)

Role of diurnal gravity waves in MCS initiation and Tropical Cyclogenesis over the Bay of Bengal

Xingchao Chen[a] and Chin-Hsuan Peng[a]

[a] *Department of Meteorology and Atmospheric Science and Center for Advanced Data Assimilation and Predictability Techniques, The Pennsylvania State University, University Park, Pennsylvania*

Corresponding author: Xingchao Chen, xzc55@psu.edu

Previous observational studies have indicated that mesoscale convective systems (MCSs) are responsible for the majority of summer precipitation over the Bay of Bengal (BoB), yet their initiation and organization remain poorly understood. Using 20 years of satellite observations and MCS tracking, we found that the majority of MCSs responsible for summer precipitation over the BoB are initiated from the coastal or open ocean regions, rather than inland areas. Diurnal MCSs frequently initiated near the coastlines are due to land-sea breezes, while early morning MCSs initiated over the open ocean are strongly influenced by diurnal radiative forcings. Our findings also highlight clear propagating signals of diurnal MCS initiation from the west and north coastlines of the BoB towards the central BoB region. Reanalysis data indicates a strong association between the offshore propagating signal and diurnal wind and temperature perturbations. Using a linear model, we found that the offshore propagating MCS initiation signal is generated by diurnal gravity waves emitted from coastal regions, which are in turn caused by diurnal variations in the land-sea sensible-heat difference and the latent heating of coastal convective systems. The diurnal gravity waves can be strongly influenced by the background monsoonal flow and vertical wind shear. Additionally, we found that the diurnal gravity waves may also play a crucial role in modulating tropical cyclogenesis over the BoB. Using a novel high-resolution regional reanalysis, we demonstrated that the diurnal gravity waves radiated from inland afternoon convection modulated the diurnal MCSs that preceded the formation of tropical cyclone (TC) Mora (2017) by modulating the offshore stability and relative humidity.

Initial Moisture Impacts on Tropical Cyclogenesis Forecasts as Seen through All-Sky Radiance-Based Ensemble Data Assimilation Experiments

Christopher M. Hartman [a,b] and Xingchao Chen [a,b]

[a] *Department of Meteorology and Atmospheric Science, The Pennsylvania State University, University Park, PA, USA*

[b] *Center for Advanced Data Assimilation and Predictability Techniques (ADAPT), The Pennsylvania State University, University Park, PA, USA*

Corresponding author: Christopher M. Hartman, cxh416@psu.edu

In this study, we use an ensemble-based data assimilation system to demonstrate the sensitivity of the tropical cyclogenesis forecasts of Hurricane Irma (2017) to the initial moisture content within its precursor disturbance. To this end, we use the Pennsylvania State University ensemble Kalman filter (PSU WRF-EnKF) system to perform cycling experiments that either assimilate or withhold all-sky infrared radiances observed by the upper-tropospheric water vapor channel of the Meteosat-10 SEVIRI instrument and all-sky microwave radiances observed by the NASA Global Precipitation Measurement (GPM) mission constellation of satellites. Both experiments (with and without all-sky radiances) assimilated all conventional observations from the Global Telecommunications System (GTS). Deterministic and ensemble forecasts are initialized from the analyses of these experiments two days prior to the formation of Irma.

Results indicate that deterministic forecasts initialized from the experiment that withheld all-sky radiances feature a premature genesis by at least 24 hours due to an overestimation of the spatial coverage of deep convection within the pre-Irma disturbance. This overestimation led to the earlier spin-up of a low-level meso-β-scale vortex that became Hurricane Irma. The assimilation of all-sky radiances reduced the initial moisture content and cloud coverage of the pre-Irma disturbance relative to the experiment that did not. This led to a more realistic representation of the convective evolution in deterministic forecasts and a more accurate genesis timing. In terms of the ensemble forecasts, ensemble sensitivity analysis reveals statistically significant correlation between the initial moisture within 300 km of the center of the pre-Irma disturbance and the intensity two days later. By modifying the initial moisture content at different vertical levels within a control ensemble member, we explore in more detail the impacts of initial moisture on the convective evolution and genesis forecast of Irma. In summary, analysis of deterministic and ensemble forecasts reveals that assimilation of all-sky radiances leads to a more realistic forecast of the genesis timing of Irma through a modulation of the initial moisture content within the pre-Irma disturbance.

Monsoon Tail Rainband in the Western North Pacific and Tropical Cyclogenesis

Chaehyeon Chelsea Nam [a,b], Michael M. Bell [a], and Brenda Dolan[a]

[a] Colorado *State University, Fort Collins, CO, USA*

[b] *Kyungpook National University, Daegu, South Korea*

Corresponding author: C. Chelsea Nam, ccnam@colostate.edu

During the Propagation of Intra-Seasonal Tropical OscillatioNs (PISTON) field campaign, which was conducted in the summer of 2018 and 2019 over the western North Pacific (WNP), we observed that most of the TCs have an elongated rainband in their southwestern (SW) quadrant. During PISTON, we called the rainband in the SW quadrant of the TC the "monsoon tail," assuming that the low-level convergence of monsoon southwesterlies and the TC-induced cyclonic circulation produced the particularly vigorous convection in the SW quadrant. A great example was Typhoon Jebi. As Jebi was moving northwestward, the monsoon tail rainband became detached from the main TC circulation, but the widespread convection persisted for a couple of days afterward. The widespread convective area had a closed low-level circulation observed by satellites and monitored for potential TC development, as Invest 98W by the Joint Typhoon Warning Center (JTWC). Invest 98W dissipated before it reached TC intensity.

Although Invest 98W did not undergo tropical cyclogenesis, our observation of monsoon tail rainband during PISTON and, in particular, Invest 98W case prompted several scientific questions:

- How common is it for TCs in the WNP to have a monsoon tail rainband?
- How does the monsoon tail rainband sustain itself after it is detached from the TC?
- How likely is it for the monsoon tail rainband to lead to subsequent TC genesis?

This study answers the above three science questions through climatological analysis and case studies of the monsoon tail rainbands of Typhoons Jebi (2018) and Lingling (2019) that were observed during PISTON. Our results show that the monsoon tail rainband is a common feature for TCs in the WNP due to the climatological northeasterly VWS. Variations in the convective activity are shown to be related to the strength of the low-level and upper-level monsoonal flow on synoptic and seasonal timescales, with VWS having the highest correlation to cold cloud tops in the southwest quadrant. Some monsoon tail rainbands sustain convective organization even after separating from pre-existing TCs. However, despite the enhanced convective activity, the persistent VWS that produced the rainbands was an overriding negative factor that inhibits genesis.